A Crystallographic Study of a Series of Nitrobenzoic Acid Co-crystals and Molecular salts

Matthew Scheepers

Supervisor: Prof. A. Lemmerer

A Dissertation submitted to the Faculty of Science, University of the Witwatersrand, Johannesburg, in fulfilment of the requirements for the degree of Master of Science.

2018, Johannesburg

DECLARATION

I declare that this Dissertation is my own, unaided work. It is being submitted for the Degree of Master of Science at the University of the Witwatersrand, Johannesburg. It has not been submitted before for any degree or examination at any other University.

_____

____**____day of_____in__2018__

Abstract

Co-crystals are structures in which two or more neutral components are present in the same crystal structure. This differs in comparison to salts, where ionically charged species exist within the structure. Co-crystals and salts are deployed frequently within the pharmaceutical industries as a means to improve the physical properties of active pharmaceutical ingredient(s) (API) with unsuitable physical properties. Nitrobenzoic acids are present in many important pharmaceutical ingredients, and have been reported in the literature to frequently form many co-crystals and salts. This study focuses on four particular nitrobenzoic acids: 2-chloro-4-nitrobenzoic acid, 2-chloro-5-nitrobenzoic acids, 3,5-dinitrobenzoic acid and 4-nitrobenzoic acid with the goal of determining the suitability of these compounds in co-crystal/salt formation. These compounds did form co-crystals/salts by using suitable co-formers, which did include several drugs such as flufenamic acid and theophylline (drugs which have been reported in the literature has having poor physical properties). These co-crystals and molecular salts had their structures determined using single crystal X-ray diffraction (SC-XRD), and thermal properties such as melting points determined using differential scanning calorimetry (DSC). The melting points of the co-crystals/salts reported here are indeed different to the respective co-formers, which indicates that new physical properties have arisen in comparison to the respective co-formers.

List of Tables

List of Figures

Contents

1. Introduction

1.1 Why Study Crystals?

The advancement of technology has been led by the development of new and improved materials. For example, early civilizations that used iron were able to dominate over other civilizations that did not, simply because iron made better weapons than bronze. Many materials are made up of crystalline material, which are solids with long range periodic order. They can be described by a repeating unit called the unit cell, which can be used to create a representation of the structure of the crystal. The properties of a solid depend on the arrangement of atoms or molecules. For example diamond and graphite are both allotropes of carbon. However, diamond is hard and strong while graphite is soft and brittle. This can be attributed due to the difference in their crystal structure. Therefore, if one can determine the structure of a material, they can use that structure to rationalise some of the resulting properties of that material.

1.2 Pharmaceutical Drugs

The scientific approach to the treatment, cure and prevention of diseases is led by the use and development of various pharmaceutical drugs ranging from common aspirin all the way to chemotherapy drugs used to treat various cancers. Large pharmaceutical companies have earned over billions of dollars worldwide by the large scale production and marketing of these drugs [1]. The markets for these drugs are highly competitive, where it is possible that several drugs treating the same conditions are possible. In this case, drugs which are more effective with minimal side effects and lower production will out-compete other rival drugs.

However, the development of new drugs with improved bioactivity and reduced unwanted side effects remains a challenge. After a viable drug molecule is “discovered”, it may be modified chemically to improve its bioactivity while reducing the undesirable side effects (usually achieved by modifying functional groups, removing stereogenic centres etc.). Then it needs to go through clinical trials in order to gain FDA approval, after which it will be marketed and will compete with rival drugs. This process can take several years, with the possibility that the final product may be hindered due to poor physical properties, or perform poorly on the market, or even completely rejected for human use [2].

Two possible solutions to these problems are present. One can modify the API by adding or changing existing functional groups. The manipulation of existing functional groups such as adding more polar groups to make the API more soluble in water can lead to the development of undesired physiological side effects, or even preventing the API from reaching the intended target (and will require doing extensive clinical trials). The other possible solution is crystal engineering, which is based on the principles of supramolecular chemistry. Here the drug molecular structure remains intact (avoid doing clinical trials again), and is improved by altering its crystal structure with hopes of improving its physiochemical properties.

1.3. Crystal Engineering

1.3.1 Introduction

Crystal Engineering involves the pre-meditated design and control of the formation of molecular networks from neutral molecules and/or salts. Crystal engineering differs from crystal prediction. Crystal prediction deals with predicting the three-dimensional crystal structure, together with the particular properties and structural features of a molecule(s) (such as determining space-groups, lattice parameters

etc.). Crystal engineering, on the other hand, deals with changing the aspects of well-studied existing molecules (such as determining new phases etc.) [3].The goal of crystal engineering is to improve or even completely change the properties of the solid-state, especially with regard to desired compounds with poor physical properties.

1.3.2 The Study of Intermolecular Interactions

The prediction of the physical properties based on the inspection of the molecular structure is near impossible. Many of the physical properties of compounds arise due the intermolecular interactions as well as the spatial arrangements of molecules in the solid form. The assembly of molecules to form large and complex networks that make up various solids is not random. Molecular recognition is the aspect where certain intermolecular interactions are favoured and co-ordination of molecules occurs due to these interactions. Interactions such as hydrogen bonding, $\pi\cdots\pi$, metal co-ordination (chelation), Van der Waals and electrostatic interactions often dictate the overall geometry and direction molecules form in the network. For example, DNA consists of two nucleotide strands held together by hydrogen bonds. It was the recognition that the nucleobases can only bond with its counterpart (eg. adenine with thymine, guanine with cytosine) that eventually led to elucidation of the overall structure determination of DNA and hence its function. The understanding of the possible interactions can allow one to gain insight into how molecules form their respective crystal structures and hence predict/explain the resulting physical properties.

1.3.3. Hydrogen Bonding

The hydrogen bond is one of the most important intermolecular interactions to consider in the design of molecular crystals. The IUPAC definition for the hydrogen bond is as follows:

> The hydrogen bond is an attractive interaction between a hydrogen atom from a molecule or a molecular fragment X–H in which X is more electronegative than H, and an atom or a group of atoms in the same or a different molecule, in which there is evidence of bond formation. [4]

If the hydrogen bond is represented as X-H$\cdots$A, X-H is defined as the hydrogen bond donor and A as the hydrogen bond acceptor. More than one hydrogen bond acceptor is possible: bifurcated hydrogen bond arrangements consist of two hydrogen bond acceptors while trifurcated hydrogen bond arrangements consist of three hydrogen bond acceptors [5]. Trifurcated hydrogen bond arrangements are rarely observed in crystal structures. The bond energies of hydrogen bonds, typically between 10-65 kJ mol^{-1}, are significantly higher than those of the Van der Waals (<8 kJ mol^{-1}) [6]. Hydrogen bond lengths (X-H$\cdots$A) can vary between 2.45 – 3.35 Å [7], while hydrogen bond angles are typically close to 180°. In order for a hydrogen bond to form, the hydrogen bond donor must approach the hydrogen bond acceptor at some distance *d*. In order for the hydrogen bond to stabilize, the attractive forces must overcome the repulsive forces so that the overall potential energy of the system is minimized. Fig. 1.2.3 shows a schematic representation of the hydrogen bond potential, where a region of the graph shows the minimum potential energy that is needed to be obtained in order to form a stable hydrogen bond.

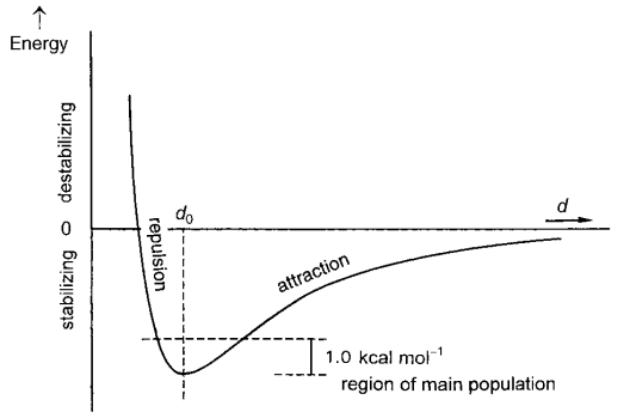

Fig. 1.3.1 Schematic representation of the hydrogen bond potential. The minimum potential energy is at a distance d_0. Figure obtained from [6].

The hydrogen bond is a directional force in molecular crystals. This significance is that a formal notation based on Graph Sets can be used to describe the arrangement of the molecule based on the hydrogen bonds present. The patterns in which hydrogen bonding forms between neighbouring molecules may be described as chains (*C*), Rings (*R*), Discrete (*D*) or Self (*S*) [8]. These patterns are defined according to the number of hydrogen bond donors, acceptors and the number of atoms involved in making up the motif. The reasoning for using such definitions is that hydrogen bonding can be reduced from a complex pattern to that of a simple descriptive one, such that the resulting properties from such bonding can be explained with eases, and to predict such complex patterns.

1.3.4 Use of Synthons

Large complex structures can often be understood by breaking down the structures into various, smaller parts. Proteins for example, are essentially large macromolecules that could be described more easily by breaking them down in their primary, secondary, tertiary and quaternary structures. A similar approach to molecular crystals could also be applied. Crystal structures involving organic molecules can often be constructed by using supermolecules. In comparison to "regular" molecules, If atoms form covalent bonds between each other to form molecules, then molecules form intermolecular bonds to form 'supermolecules' [9], with the molecule being the unit of matter of interest.

Supramolecular synthons can be defined as "structural units within supermolecules which can be formed and/or assembled by known or conceivable synthetic operations involving intermolecular interactions" [10]. A large number of synthons are known to exist across a wide spectrum of different compounds that share similar functional groups. For example the carboxylic acid functional group is well known for forming a dimer (Fig. 1.2.1) within many crystal structures which feature a carboxylic acid. It is possible to use these types of interactions in order to predict and describe the type of crystal structures that can form.

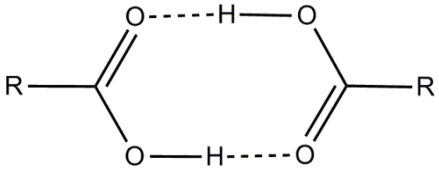

Fig. 1.3.2 The carboxylic acid dimer with graph set $R_2^2(8)$.

In addition to the carboxylic acid motif in Fig 1.2.1, several different synthons can be used to predict the potential formation of co-crystals such as the ones in Fig.1.2.2 below.

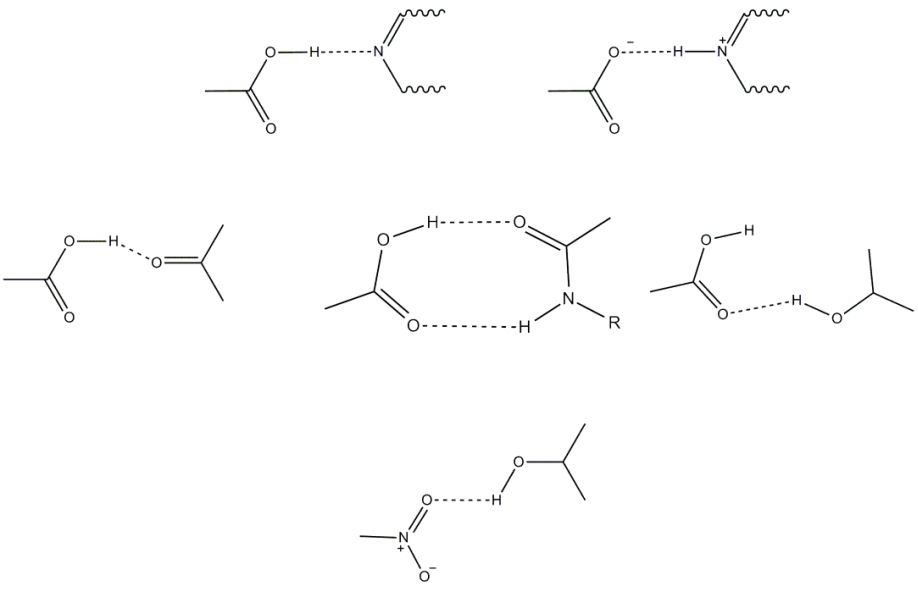

Fig 1.3.3 Several different plausible synthons used to predict whether co-crystal/molecular salt formation is possible for this work.

1.3.5 The Crystallization Process

How does one synthesize crystals? What exactly is crystallization? What factors favour one crystal form over the other? The exact process of crystallization remains a mystery. However, several theories can be put forward to try and explain these processes. Although many chemical processes depend on the kinetics or thermodynamics involved, crystallization is usually kinetically controlled [11]. This can be explained by using the Curtin-Hammett principle, which states that the kinetically favoured product would likely form first since the activation barrier would be much lower than the otherwise thermodynamically favoured product. It is possible that the kinetic form may be thermodynamically unstable, and may convert eventually into the thermodynamically favoured form. In such case polymorphism is possible.

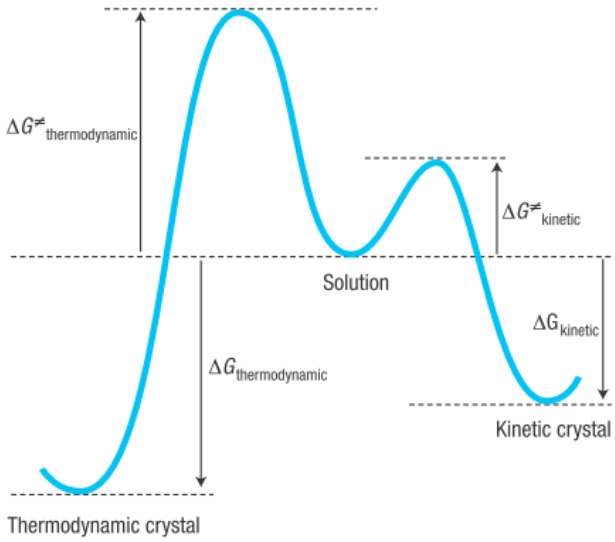

Fig. 1.3.5 the energy diagram illustrating the Curtin-Hammett principle in terms of the crystallization process. In this case the crystal formed will be the kinetic form due to the lower activation barrier than the thermodynamic form. Image obtained from [11].

Crystals are typically grown from solution. The exact mechanism by which crystals grow out of solution is not exactly clear, but several theories could give a reasonable explanation for the phenomena. Typical methods for growing crystals by solution are to dissolve the solute such that it reaches supersaturation. At supersaturation, the solid phase start forming in a process called nucleation [12], where atoms or molecules congregate together to form a nucleus. Once the nucleus exceeds the critical size it becomes a crystal. Crystal growth occurs by the addition of more atoms or molecules into the crystal. The atoms or molecules add such that the symmetry of the crystal form is preserved. Factors such as the

1.4 Multi-component Complexes (co-crystals and salts)

Multi-component complexes such as co-crystals and molecular salts are systems designed to contain more than one component in the solid state, and are a rapidly growing area of interest in modern chemistry. Co-crystals are the combination of two or more neutral molecules that make up the supramolecular complex [13]. This distinguishes them from salts where a proton transfer has occurred, leading to the formation of an ionic bond. In addition co-crystals are further distinguished from hydrates and solvates in the sense that all the co-formers involved must be solid at ambient conditions.

Co-crystals and salts are becoming increasingly more important due to the different physical properties that can arise. For example, flufenamic acid is a drug reported to have poor water solubility. A co-crystal of flufenamic acid with 2-chloro-4-nitrobenzoic acid was determined to have a solubility of 5 times that of the pure flufenamic acid [14]. This obvious improvement of the drug proves that there is much potential from the research and development of co-crystals within the pharmaceutical industry.

1.4.1 pK_a and the ΔpK_a Rule.

Many organic molecules are acids and bases because they consist of functional groups which can donate or accept protons in solution. However, these protons do not always dissociate/associate with organic molecules and a mixture of non-ionised and ionised forms exist in equilibria. For the general case of the acid HA, the dissociation of a proton can be represented as the following:

$$HA \rightleftharpoons H^+ + A^-$$

For which the acid dissociation constant K_a can be represented as:

$$K_a = \frac{[H^+][A^-]}{[HA]}$$

The definition of the pK_a is as follows:

$$pK_a = -\log K_a$$

The definition of pK_a is useful for comparing the extent of which protons will associate or dissociate with different molecular species in solution. For the case of a base, the conjugate acid is considered. Stronger acids will have a small or negative pK_a, while stronger bases will have a much larger pK_a. The *p*H of the solution will change according to the acid or base, which can be expressed by the Henderson Hasselbalch equation below:

$$pH = pK_a + \log\frac{[A^-]}{[HA]}$$

This equation indicates that for a weak acid or base, a mixture of both the acid and its conjugate acid exist in solution, and the proportion of which is affected by the *p*H of the solution.

The pK_a's of some molecules (including some used in this dissertation) are reported in Table 1.3.1.

Table 1.4.1 pK_a's of some compounds, including some of the co-formers used for this work (in water at 25 °C).

Co-former	pK_a of co-former
4-aminopyridine	9.26
imdazole	7.18
2-amino-3-hydroxypyridine	5.15
2-amino-5-bromopyridine	2.73
2-aminopyridine	6.67
3-aminopyridine	6.16
Pyridoxine	9.23
3-cyanopyridine	1.78
2-acetylpyridine	3.00
theophyline	8.60
Pyridine	5.23

Despite how useful the definition of the pK_a is for comparing the strength of different acids and bases, there are limitations. First, the pK_a reported in many cases use water as the solvent. This presents a problem since different solvents have different effects on the solute. For example, according to a paper by Rossini *et al*. [15], which examines both experimental and theoretical pK_a's of various compounds in different solvents, the pK_a of pyridine in DMSO is 3.50, which makes it more acidic than in water. Consideration of solvent to predict the acidity or basicity of a compound is problematic due to limited experimental data. Temperature also needs to be considered when using and comparing pK_a's. Most pK_a's are often reported at 25 °C. Usually the pK_a does not change drastically within a few degrees. However, the formation of a co-crystal or salt may require heating; in this case the change in the pK_a may change more drastically. This relationship can be expressed in terms of the van't Hoff equation below:

$$\frac{d}{dT}\ln K = \frac{\Delta H^o}{RT^2}$$

Where K is the equilibrium constant, R is the universal gas constant and ΔH^o is the standard enthalpy. Generally heating increases the K_a, which decreases the pK_a. Thus, when considering the pK_a of a molecule, the solvent and temperature would need to be accounted for, as these factors will change the pK_a, and thus the behaviour of a molecule in solution.

It is possible to use the pK_a of a molecule to try and predict whether a co-crystal or salt can form. An almost "rule of thumb" relating to pK_a exists [16]. Accordingly one looks at the value of ΔpK_a = pK_a (conjugate acid of base) – pK_a (acid). If ΔpKa is less than zero a co-crystal should be synthesised, whereas a value greater than 2-3 should lead to a salt. Values between 0-3 can predict either case and are dependent on the crystal system in question.

An example of where the pK_a rule has been used is the work by Lemmerer *et al*. [17]. In this work a series of co-crystals and salts consisting of 2-chloro-4-nitrobenzoic acid (2c4n) with pyridines with varying pK_a's was synthesised. The ΔpK_a of each crystal system along with other co-crystals and salts containing 2c4n and similar compounds reported in the CSD was calculated. The results show that most of the salts

formed when the ΔpK_a was greater than three and most of the co-crystals formed when the ΔpK_a was less than zero. Results between zero and three varied. The conclusion of the study shows that the ΔpK_a rule seems to work rather well.

1.5 Hypothesis and Aims

The major aim for this work is to synthesise and characterise a series of co-crystals and salts involving various nitrobenzoic acids. The nitrobenzoic acids chosen are 4-nitrobenzoic acid (4nba), 2-chloro-4-nitrobenzoic acid (2c4n), 2-chloro-5-nitrobenzoic acid (2c5n) and 3,5-dinitrobenzoic acid (dnba). These molecules were chosen primarily due to the fact that several co-crystals and salts have already been reported in the literature (see relevant chapters for examples), which therefore should allow new co-crystals and salts to easily form. Single crystal and powder X-ray crystal structures collected will confirm if co-crystals were synthesised successfully. SCXRD will be used to determine the atomic co-ordinates (and any other information such as disorder) of the atoms in the unit cell. PXRD will be used exclusively to confirm that the single crystals obtained represent the overall bulk. DSC will be used to determine any phase changes (including melting) that may occur as well as the associated temperature at which it occurs as well as the enthalpy involved.

There are various methods for choosing suitable co-formers to form co-crystal and salts. One method is to use the previously mentioned pK_a rule, while the other is to focus on the formation of various hydrogen bond interactions. Both will be employed. Considering the carboxylic acid group will more likely be involved in hydrogen bond interactions and/or donate its proton, the co-former of choice should interact with the carboxylic acid. Such compounds include the following:

- Pyridines. The nitrogen can either accept a transfer of the acidic hydrogen from the nitrobenzoic acid or act as a hydrogen bond acceptor. Pyridine derivatives could involve additional hydrogen bond donors such as aminopyridines or acceptors such as the carbonitrilepyridines. In which case, if possible, a series of pyridine derivative should be synthesised such as for example, 2-amino, 3-amino, and 4-aminopyridine etc.
- Other carboxylic acids and/or amines/amides: It is plausible that a hydrogen bond pair could exist between other carboxylic acids (forming either the ring or chain motif) or even with amines/amides. The co-formers of choice here will be more diverse but should include only "simple" small molecules (or molecules with not too many significant functional groups).

The nitro group is a possible hydrogen bond acceptor. In contrast to the carboxylic acid, including co-formers which have various possible hydrogen bond donors could potentially form a hydrogen bond pair with the nitro group. Hydrogen or halogen bonding to the nitro group can occur via an interaction with either both oxygens (both symmetric and asymmetric) or co-ordinate only to one [18]. Therefore, it is important to still consider the nitro group even though the carboxylic acid group will more likely be involved in important hydrogen bonding patterns.

The co-formers used for this investigation is tabulated in Table 1.4 below.

Table 1.5 The nitrobenzoic acids and co-formers used in this study.

Name	Abbreviation(s) used	Note(s)	Scheme
4-Nitrobenzoic acid/ 4-Nitrobenzoate	4nbaH (neutral form) 4nba(-) (ionised form)		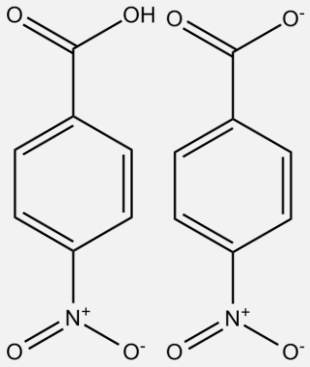
2-Chloro-4-nitrobenzoic acid/ 2-Chloro-4-nitrobenzoate	2c4nH (neutral form) 2c4n(-) (ionised form)		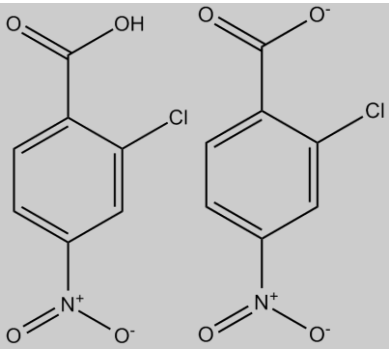
2-Chloro-5-nitrobenzoic acid/ 2-Chloro-5-nitrobenzoate	2c5nH (neutral form) 2c5n(-) (ionised form)		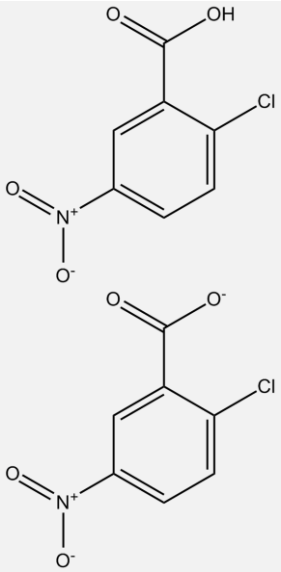
3,5-Dinitrobenzoic acid/ 3,5-Dinitrobenzoate	dnbaH (neutral form) dnba(-) (ionised form)		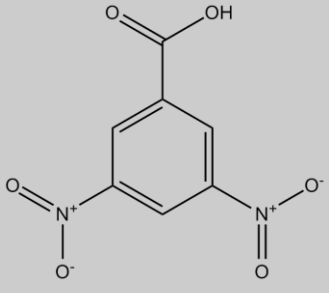

			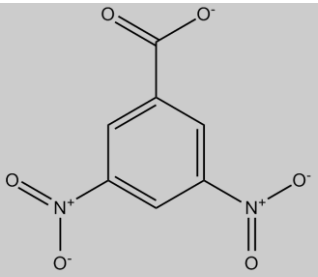
2-Aminopyridinium	2apH		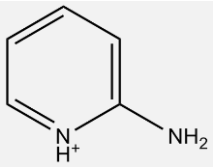
3-Aminopyridinium	3apH		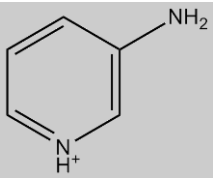
4-Aminopyridinium	4apH		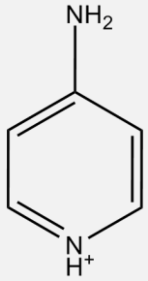
2-Amino-5-bromopyridinium	2a5BrpH		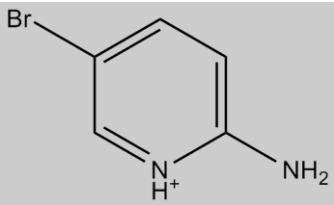
Pyridoxinium	pyd	Known as vitamin B6	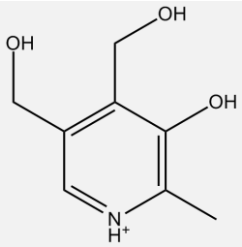
2-Acetylpyridine	2OAcP		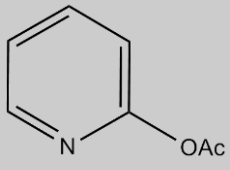
2-Amino-3-hydroxypyridinium	2a3hpH		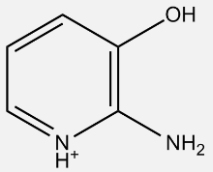

3-Cyanopyridine	3cnp		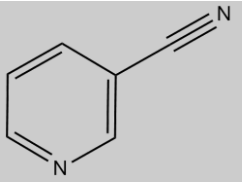
Urea	-		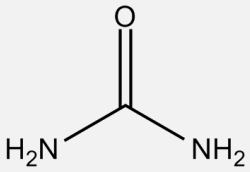
Thiourea	-		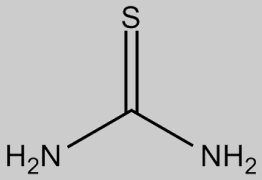
Flufenamic Acid	fa	Member of the non-steroidal anti-inflammatory drugs (NSAIDS).	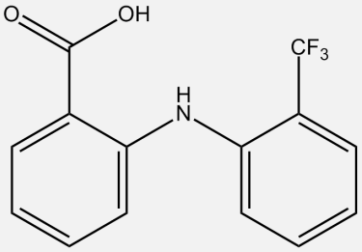
Dimethylaminobenzophenone	dmabp		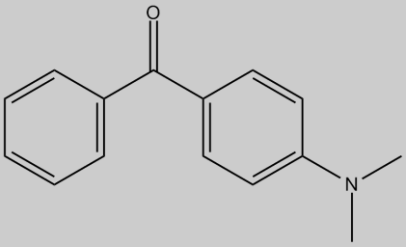
Theophylline	thp	Drug used to treat respiratory diseases.	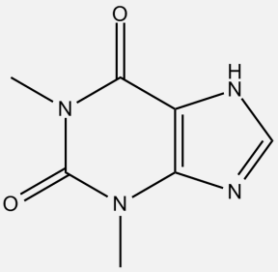
(trans)-Cinnamic Acid	Cinnamic Acid		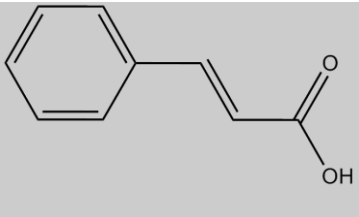
Imidazole	imd		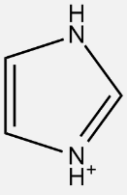

2. Methods and Materials

2.1 Crystal Synthesis

All reagents used for synthesis and characterization were of analytical grade, purchased from Sigma-Aldrich, unless otherwise stated. Reagents were used as received, without further purification.

0.100 g of the respective nitrobenzoic acid was dissolved in a hot solution with an equimolar amount of the respective co-former in a suitable solvent. This solution was stirred until no solid remained. This solution was covered loosely and the solvent was left to evaporate over several days at room temperature until single crystals of suitable size were grown. The masses used and the solvent of choice that was used to synthesise each co-crystal/molecular salt is listed in Table 2.1.

Table 2.1 The masses and solvents used to synthesise the various co-crystals and molecular salts.

Nitrobenzoic Acid	**Molar Weight of nitrobenzoic acid /g mol^{-1}**	**Co-Former**	**Molar Weight of co-former / g mol^{-1}**	**Mass Used /g**	**Solevnt system used**
4-Nitrobenzoic acid	167.1189	Cinnamic Acid	148.159	0.089	Ethanol
4-Nitrobenzoic acid	167.1189	Imidazole	68.077	0.041	Ethanol
4-Nitrobenzoic acid	167.1189	2-Amino-3-hydorxypyridine	110.110	0.066	Ethanol
4-Nitrobenzoic acid	167.1189	4-Aminopyridine	94.117	0.056	Ethanol
4-Nitrobenzoic acid	167.1189	2-Amino-5-bromopyridine	173.013	0.104	Ethanol
2-Chloro-4-nitrobenzoic acid	201.560	2-Aminopyridine	94.117	0.047	Ethanol
2-Chloro-4-nitrobenzoic acid	201.560	3-Aminopyridine	94.117	0.047	Ethanol
2-Chloro-4-nitrobenzoic acid	201.560	Pyridoxine	169.180	0.084	Ethanol
2-Chloro-4-nitrobenzoic acid	201.560	Flufenamic acid	281.230	0.140	Ethyl acetate
2-Chloro-4-nitrobenzoic acid	201.560	Urea	60.060	0.030	Ethyl acetate
2-Chloro-5-nitrobenzoic acid	201.560	3-Cyanopyridine	104.109	0.052	Ethanol
2-Chloro-5-nitrobenzoic acid	201.560	4-Aminopyridine	94.117	0.047	Ethanol
2-Chloro-5-nitrobenzoic	201.560	Pyridoxine	169.180	0.084	Ethanol

acid					
2-Chloro-5-nitrobenzoic acid	201.560	Urea	60.060	0.030	Ethyl acetate
3,5-Dinitrobenzoic acid	212.118	2-Acetylpyridine	Liquid used in excess		Ethanol
3,5-Dinitrobenzoic acid	212.118	3-Aminopyridine	94.117	0.044	Ethanol
3,5-Dinitrobenzoic acid	212.118	3-Cyanopyridine	104.109	0.049	Ethanol
3,5-Dinitrobenzoic acid	212.118	Diethylaminobenzophenone	225.290	0.106	Methanol
3,5-Dinitrobenzoic acid	212.118	Flufenamic acid	281.230	0.133	Ethanol:Water (1:1 vol)/acetic acid
3,5-Dinitrobenzoic acid	212.118	Pyridoxine	169.180	0.080	Ethanol
3,5-Dinitrobenzoic acid	212.118	Theophylline Monohydrate	198.179	0.093	Ethyl acetate
3,5-Dinitrobenzoic acid	212.118	Thiourea	76.120	0.036	Ethyl acetate

2.2 Characterization Techniques and Instrumentation

2.2.1 Crystal data and X-ray structural analysis

The Bruker D8 VENTURE PHOTON CMOS area detector diffractometer, equipped with a graphite monochromated Mo $K\alpha_1$ sealed tube (50 kV, 30 mA), was used to collect all the intensity data. Crystal structures were determined at 173 K and to achieve satisfactory thermal ellipsoids. The program *SAINT+*, vers. 6.02 [19] was used to integrate the data and the program *SADABS*[20] was used to make empirical absorption corrections. Space group assignments were made using *XPREP* [20] on all compounds. In all cases, the structures were solved in the *WinGX* Suite of programs [21] by direct methods using *SHELXS-97* [20] and refined using full-matrix least-squares/difference Fourier techniques on F^2 using *SHELXL-97*. [20] All non-hydrogen atoms were refined anisotropically. Thereafter, all hydrogen atoms attached to N or O atoms, except where otherwise stated, were located in the difference Fourier map and their coordinates refined freely with isotropic parameters 1.5 times those of the 'heavy' atoms to which they are attached. All C-H hydrogen atoms were placed at idealized positions and refined as riding atoms with isotropic parameters 1.2 times those of the 'heavy' atoms to which they are attached. Diagrams and publication material were generated using *ORTEP-3*, [21] and *Mercury* [22].

2.2.2. Differential Scanning Calorimetry (DSC)

Differential scanning calorimetry data (Table 1) were collected using a Mettler Toledo 822^e with aluminium pans under ambient conditions. Exothermic events were shown as peaks. Co-crystals were heated and cooled to determine melting points as well as any additional phase transitions. The temperature and energy calibrations were performed using pure indium (purity 99.99%, m.p 156.6°C, heat of fusion: 28.45 $J.g^{-1}$).

2.2.3. Thermal gravimetric analysis (TGA)

A TGA curve was determined for the molecular salt of $dnba^{(-)}$-3apH to determine whether the salt underwent a possible dehydration (see Thermal analysis for further information). The TGA was performed on TA SDT Q600 on samples with mass ranging from 5-10 mg. These samples were heated from 25 to 800 at 10 °C/min

2.2.4 Powder X-ray Diffraction

Powder X-ray diffraction data for all compounds were measured at 293 K on a Bruker D2 Phaser diffractometer which employs a sealed tube Co X-ray source (λ = 1.78896 Å), operating at 30 kV and 10 mA, and LynxEye PSD detector in Bragg-Brentano geometry. Powder X-ray diffraction confirmed that the single crystal structures were representative of the bulk material (See Appendix).

2.3 Cambridge Structure Database

The Cambridge Structural Database (CSD) was used to determine which co-formers would be suitable for co-crystal experiments. Searches for each of the nitrobenzoic acids included both the neutral and ionized forms and were restricted to crystal structure containing two or more "molecules" per unit cell, as well as only restricting organic systems with 3D co-ordinates determined.

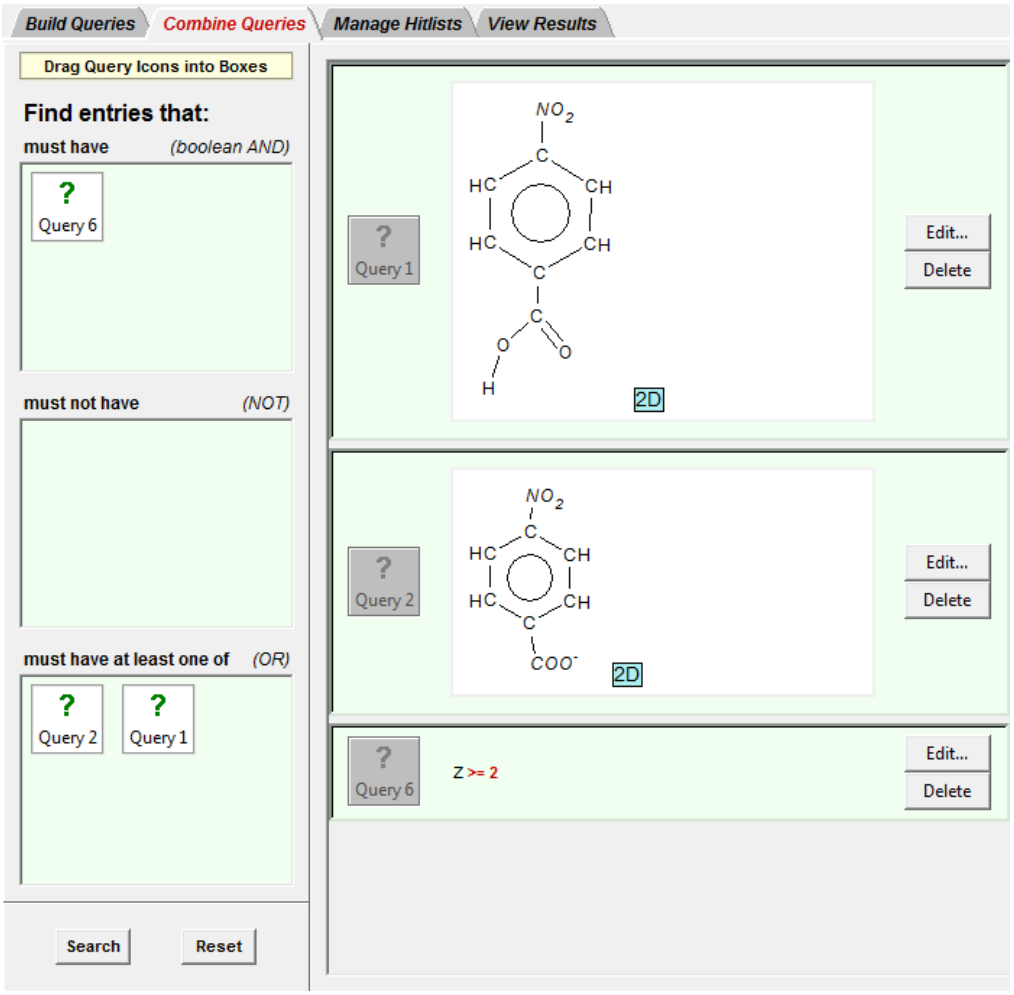

Fig 2.3 Example of queries combined to determine the number of co-crystals and molecular salts deposited on the CSD.

3. The Co-crystals and Salts of 4-Nitrobenzoic Acid

3.1 Introduction

4-Nitrobenzoic acid (4nba) is a relatively simple benzoic acid, consisting of the carboxyl group in a para position to the nitro group. 4nba is mostly used as a reagent in various syntheses and as a co-former for various APIs, although there is a possible application to use 4nba as an agent to identify *Tuberculosis Myobacterium* complexes in laboratories [23].

3.2 CSD Results

Several co-crystals/molecular salts with 4nba exist and have been published in the CSD [24]. A total of 170 results of co-crystals and molecular salts are present, of which 65 are co-crystals and 105 molecular salts. This indicates a high potential of forming a new co-crystal/molecular salt with 4nba. In Table 3.2 is a list of some more notable examples of co-crystals and molecular salts of 4nba in the literature. These examples have been chosen because they either contain similar functional groups or they form co-crystals/salts with important drugs.

Table 3.2 Some examples of the co-crystal/molecular salts that have formed with 4nba that has been reported in the literature

Ref Code/Reference	Co-former	Co-crystal/molecular Salt	Notable Features
ACUDIO / [25]	Isoniazid	Co-crystal	drug used to treat lung infections
XONQEY / [26]	2-amino-6-chloropyridine	Co-crystal	pyridine derivative
AFUJIW / [27]	2-Amino-4-phenyl-1,3-thiazol-3-ium	Molecular Salt	nitrogen containing heterocycle with amino group which acts as a base.
AJAKEB [28]	Isonicotinamide	Co-crystal	GRAS compound and pyridine derivative
DAQZIF01 / [29]	4,4'-bipyridine	Co-crystal	pyridine derivative
JEJNES / [29]	p-Methoxyanilinium	Molecular Salt	compound containing amino group acting as a base.
LIGZUX01 [30]	2-Hydroxyethylammonium	Molecular Salt	compound containing amino group acting as a base.
MOZPUN [31]	2,3-Diaminopyridinium	Molecular Salt	pyridine derivative
ODAZID01 [29]	2-aminopyridinium	Molecular Salt	pyridine derivative
PAVKUU [32]	4-Amino-N-(4,6-dimethylpyrimidin-2-yl)benzenesulfonamide (sulfadiazine)	Co-crystal	sulfadiazine is used as an anti-bacterial.

3.3. Co-crystals and Molecular Salts

One co-crystal and 4 molecular salts were synthesised, which are presented below. Fig. 3.3 shows the ortep diagrams of each case. PXRD patterns of each co-crystal/molecular salt were measured and are available in the Appendix (Figs. A1 – A5) together with the calculated pattern, which confirms the single crystal represent the bulk material in each case.

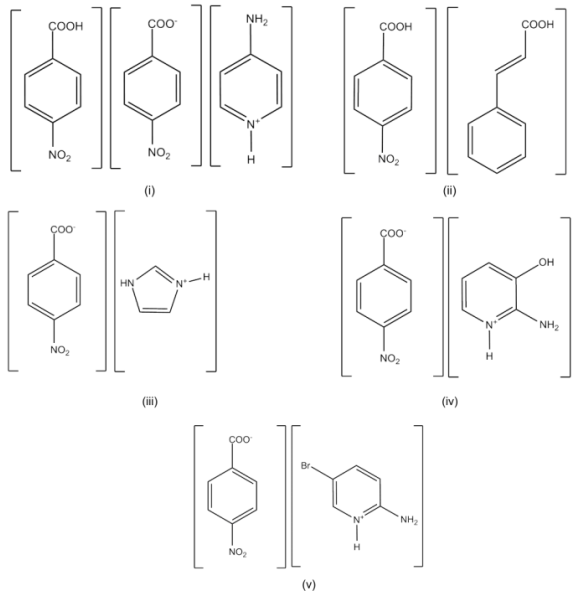

Scheme 3 Chemical structures of (i) 4nbaH + 4nba$^{(-)}$ + 4apH, (ii) 4nbaH + cinnamic acid, (iii) 4nba + imd,(iv) 4nba + 2a3hpH and (v) 4nba$^{(-)}$ + 2a5BrpH.

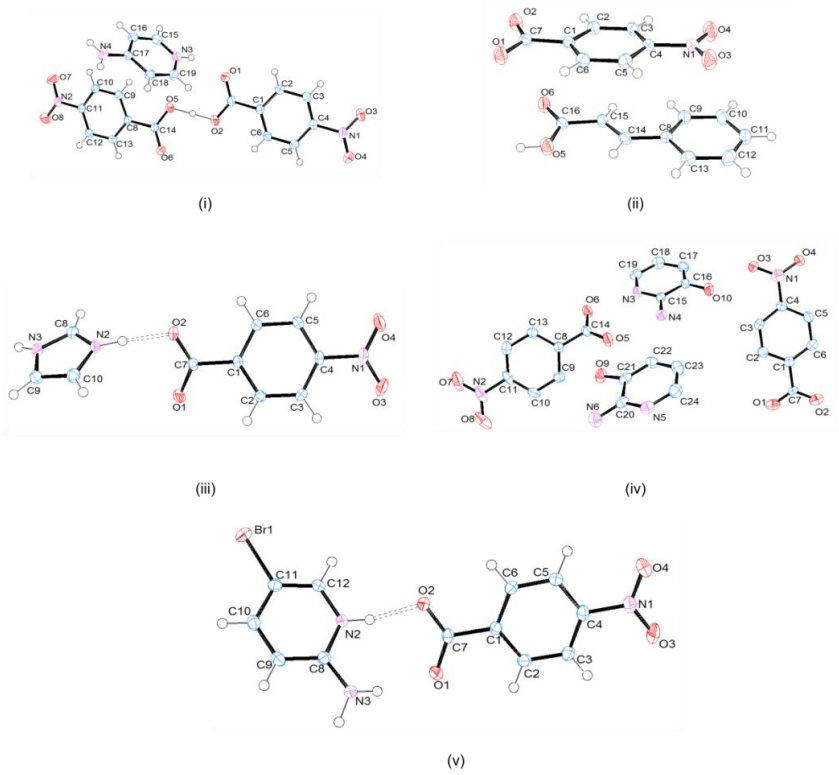

Fig.3.3 Ortep diagrams showing the numbering scheme of the asymmetric units for (i) 4nbaH + 4nba(-) + 4apH, (ii) 4nbaH + cinnamic acid, (iii) 4nba + imd,(iv) 4nba + 2a3hpH (with hydrogens omitted to allow clarity for numbering scheme of non-hydrogen atoms) and (v) 4nba$^{(-)}$ + 2a5BrpH.

Table 3.3 Crystal data and structure refinement for 4nba co-crystal and molecular salts

	4nba + Cinnamic Acid	**4nba + 2-amino-3-hydroxypyridine**	**4nba + Imidazole**	**4nba + 4-aminopyridine**	**2c5n + 2A5BP**
Empirical formula	$C_{16}H_{13}NO_6$	$C_{12}H_{11}N_3O_5$	$C_{10}H_9N_3O_4$	$C_{9.5}H_8N_2O_4$	$C_{12}H_{10}N_3O_4Br$
Formula weight	315.27	277.24	235.20	214.18	340.14
Temperature/K	173	173	173	173	173.15
Crystal system	monoclinic	monoclinic	triclinic	triclinic	monoclinic
Space group	$P2_1/n$	Cc	P-1	P-1	$P2_1/c$
a/Å	7.2514(3)	26.5972(8)	5.9441(2)	6.46250(10)	8.0104(2)
b/Å	7.5327(4)	7.8020(2)	7.3841(3)	6.92370(10)	6.30200(10)
c/Å	26.2982(13)	12.7184(3)	11.8182(5)	20.9788(4)	24.6372(5)
α/°	90	90	103.036(2)	85.2710(10)	90
β/°	91.666(2)	110.349(2)	100.414(2)	87.8970(10)	90.3160(10)
γ/°	90	90	90.994(2)	86.0550(10)	90
Volume/$Å^3$	1435.87(12)	2474.50(12)	496.11(3)	932.82(3)	1243.70(4)
Z	4	8	2	4	4
$\rho_{calc}g/cm^3$	1.458	1.488	1.574	1.525	1.817
μ/mm^{-1}	0.113	0.118	0.125	0.122	3.323
F(000)	656.0	1152.0	244.0	444.0	680
Crystal size/mm^3	0.394 × 0.128 × 0.052	0.458 × 0.258 × 0.122	0.536 × 0.214 × 0.092	0.519 × 0.382 × 0.136	0.447 × 0.442 × 0.324
Radiation	MoKα (λ = 0.71073)	MoKα (λ = 0.71073)	MoKα (λ = 0.71073)	MoKα (λ = 0.71073)	MoKα (λ = 0.71073)
2Θ range for data collection/°	5.786 to 62.214	5.47 to 56.58	5.674 to 55.994	1.948 to 56.632	3.306 to 55.998
Index ranges	$-10 \le h \le 10$, $-10 \le k \le 10$, $-38 \le l \le 38$	$-35 \le h \le 33$, $-9 \le k \le 10$, $-16 \le l \le 16$	$-7 \le h \le 7$, $-9 \le k \le 9$, $-15 \le l \le 15$	$-8 \le h \le 8$, $-9 \le k \le 9$, $-27 \le l \le 27$	$-10 \le h \le 10$, $-8 \le k \le 8$, $-32 \le l \le 32$
Reflections collected	39448	11608	14977	22283	14560
Independent reflections	4606 [R_{int} = 0.0835, R_{sigma} = 0.0588]	5417 [R_{int} = 0.0378, R_{sigma} = 0.0572]	2391 [R_{int} = 0.0334, R_{sigma} = 0.0222]	4628 [R_{int} = 0.0405, R_{sigma} = 0.0250]	2109 [R_{int} = 0.0417, R_{sigma} = 0.0375]
Data/restraints/parameters	4606/0/213	5417/2/380	2391/0/154	4628/0/284	2109/0/181
Goodness-of-fit on F^2	1.056	1.010	1.060	1.043	1.062
Final R indexes [I>=2σ (I)]	R_1 = 0.0753, wR_2 = 0.1486	R_1 = 0.0500, wR_2 = 0.1121	R_1 = 0.0379, wR_2 = 0.1000	R_1 = 0.0374, wR_2 = 0.0977	R_1 = 0.0291, wR_2 = 0.0896
Final R indexes [all data]	R_1 = 0.1233, wR_2 = 0.1672	R_1 = 0.0782, wR_2 = 0.1271	R_1 = 0.0449, wR_2 = 0.1050	R_1 = 0.0473, wR_2 = 0.1059	R_1 = 0.0362, wR_2 = 0.0907
Largest diff. peak/hole / e $Å^{-3}$	0.50/-0.34	0.26/-0.33	0.41/-0.25	0.24/-0.30	0.42/-0.56

3.3.1. 4nba$^{(-)}$ + 4-aminopyridinium

A molecular complex of 4-aminopyridine and 4nba was synthesised and crystallised as colourless needles. The asymmetric unit consists of one molecules of each 4nbaH, 4nba$^{(-)}$ and 4apH. The crystal structure consists of 2-dimensional layers of 4nbaH and 4nba$^{(-)}$ cross-linked with 4apH. The 4apH forms hydrogen bonds with both 4nbaH and 4nba$^{(-)}$ molecules at the carboxyl/carboxylate groups using the pyridinium and amino groups via N-H···O type interactions. A proton exchange occurs between both 4nbaH and 4nba$^{(-)}$. This is reflected in the Fourier maps of the electron density, where the hydrogen appears in the middle between the two 4nba molecules, indicating some degree of proton transfer exists with the structure, which this phenomenon has been reported previously [33]. This crystal structure has been reported before by Quah *et al*. [34]. However, in their structure the hydrogen at the carboxylic/carboxylate complex was positioned geometrically, which ignores the proton exchange that occurs between the two molecules. Therefore the structure obtained for this work should be a better representative for the real crystal structure of the 4nba$^{(-)}$-4-aminopyridinium salt.

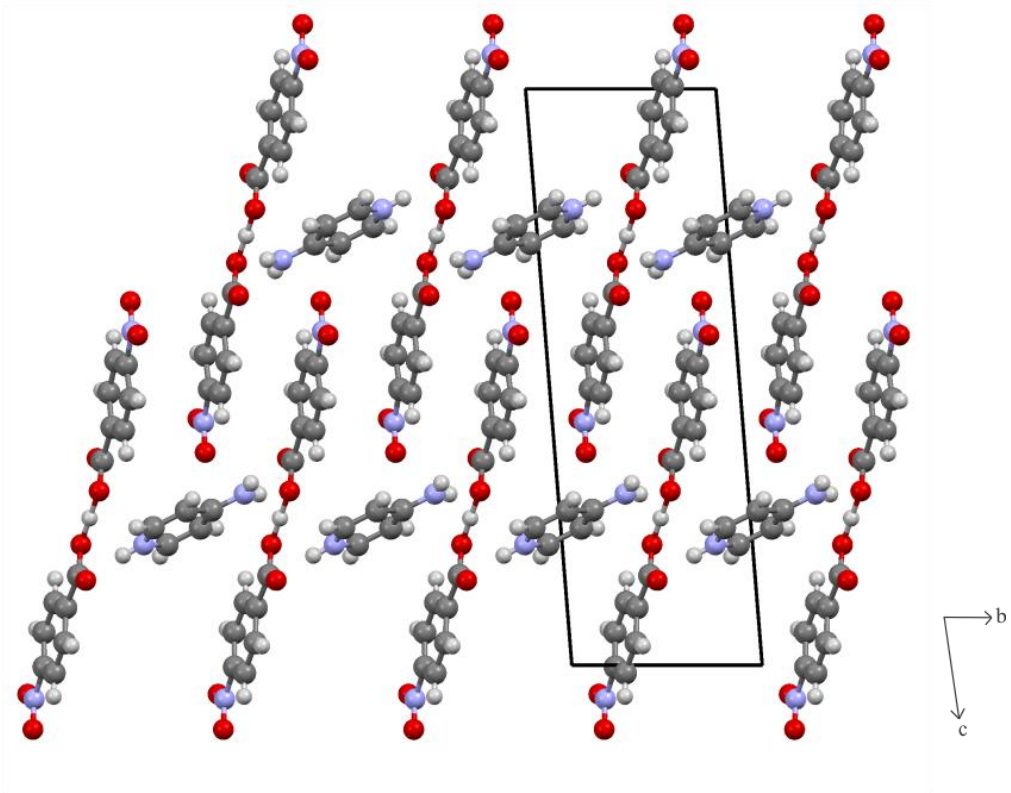

Fig 3.3.1 The packing of the 4nba-4AP molecular complex viewed down the a-axis, showing the layers of 4nba that are cross-linked together by 4AP molecules.

Table 3.3.1 Hydrogen bond table of 4nba$^{(-)}$ + 4apH

D-H···A	d(D-H)	d(H···A)	d(D···A)	<(DHA)
N3-H3A···O1	0.873(17)	1.989(17)	2.7813(13)	150(1)
N4-H4B···O5 (i)	0.889(16)	2.124(17)	3.0120(14)	176(1)
N4-H4A···O6 (ii)	0.862(18)	2.077(18)	2.8800(13)	155(2)

(i) x,y-1,z; (ii) x+1,y-1,z

3.3.2. 4nbaH + Cinnamic Acid

A co-crystal of 4nbaH and cinnamic acid was synthesised and was crystallised as colourless plate crystals. The structure consists of a 1:1 mole ratio of both 4nba and cinnamic acid in the asymmetric unit, and occupies the $P2_1/n$ space group. Hydrogen atoms attached to the carboxylic acids, atoms O1 and O5 respectively, were placed geometrically to the respective oxygen atoms. Molecules of 4nba and cinnamic acid do not interact with each other via hydrogen bonds. Identical molecules hydrogen bond to each other via the carboxyl group with a graph set of $R_2^2(8)$.

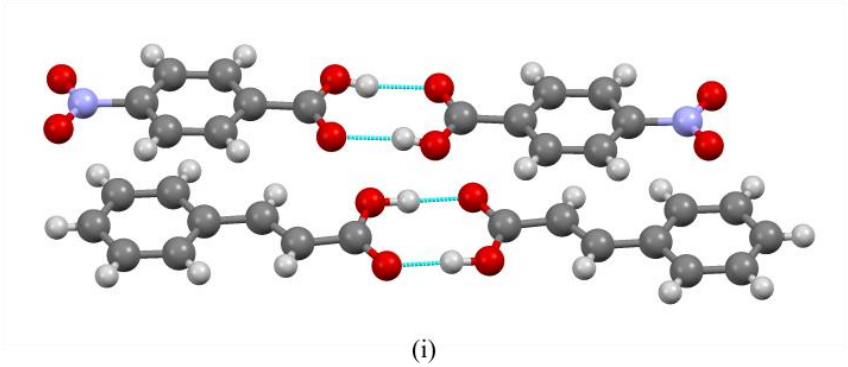

(i)

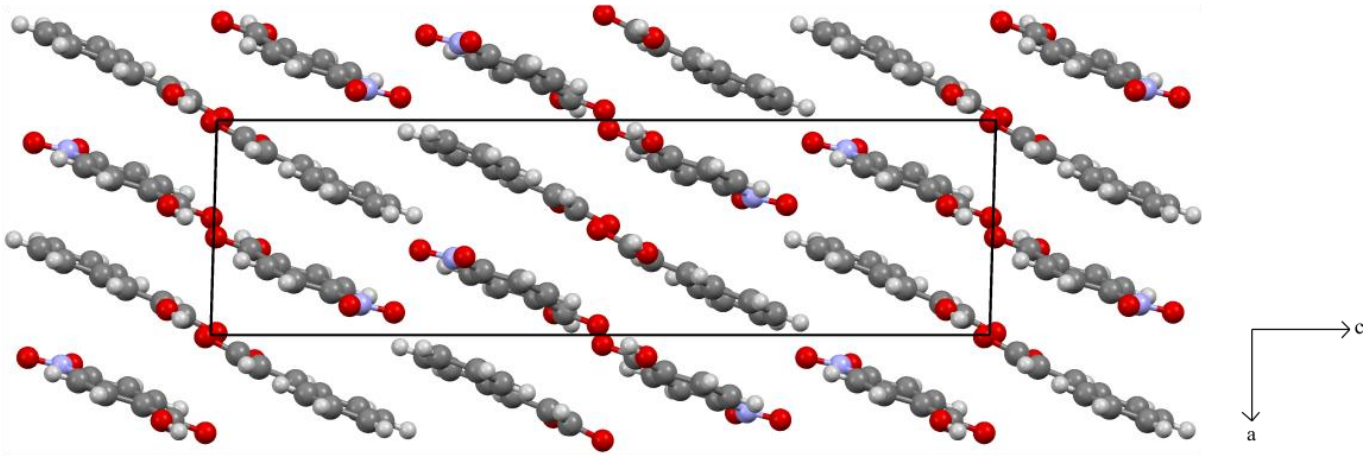

(ii)

Fig 3.3.2 The crystal structure of the 4nba-cinnamic acid co-crystal showing (i) the dimers forming the $R_2^2(8)$ hydrogen bonding motif and (ii) packing of molecules in this crystal structure.

Table 3.3.2 Hydrogen bond table of 4nba + Cinnamic Acid

D-H···A	d(D-H)	d(H···A)	d(D···A)	<(DHA)
O1-H1···O2 (i)	0.82	1.82	2.6228(19)	167
O5-H5···O6 (ii)	0.82	1.80	2.618(2)	172

(i) -x,-y,-z+1; (ii) -x+1,-y,-z+1

3.3.3. 4nba$^{(-)}$ + Imidazolium

A molecular salt of 4nba and imidazole was synthesised and crystallised as white blocks. Two molecules of each 4nba and imidazole forms a ring with a graph set of $R_2^2(16)$ with the imidazole rings form a link between the two carboxylate groups. The 4nba and imidazole molecules pack in a zig-zag manner with respect to each other.

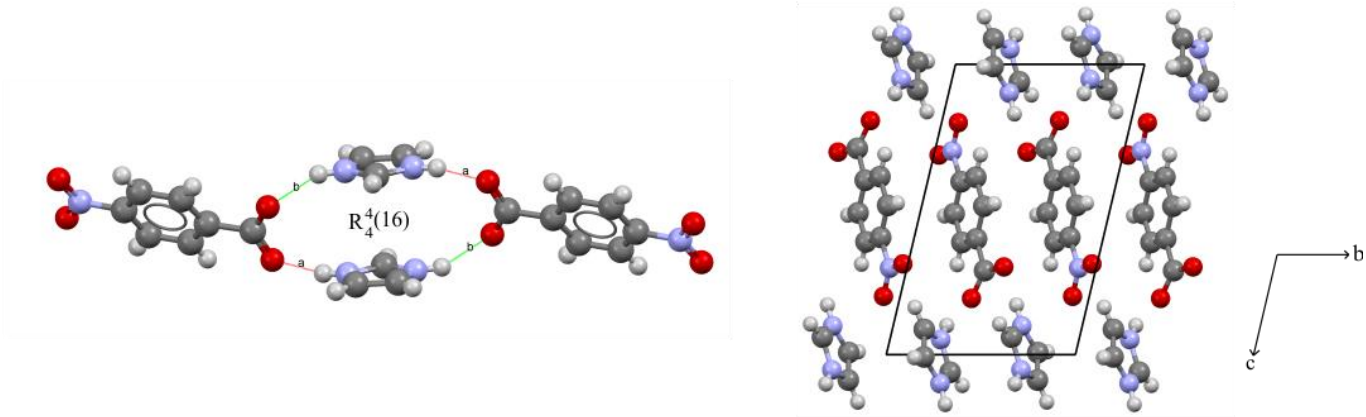

Fig. 3.3.3 Crystal structure of the 4nba-imidazole molecular salt showing (i) the tetramer formed via hydrogen bonds and (ii) the packing viewed down the *a*-axis.

Table 3.3.3 Hydrogen bond table for 4nba + Imidazole

D-H···A	d(D-H)	d(H···A)	d(D···A)	<(DHA)
N(2)-H(2A)...O(2)	0.917(18)	1.723(19)	2.6383(12)	176(16)
N(3)-H(3A)...O(1)(i)	0.900(18)	1.854(18)	2.7301(13)	164(16)

(i) -x,-y+1,-z+2

3.3.4. 4nba(-) + 2-amino-3-hydroxypyridinium

Needle crystals of a molecular salt of 2a3hpH and 4nba$^{(-)}$ was synthesised and crystallised as dark brown prisms. Two molecules of 2a3hpH and 4nba$^{(-)}$ each exist within the asymmetric unit, with both 4nba molecules having a proton transferred to the 2a3hpH molecules. Several hydrogen bonding motifs exist within this salt. The carboxylate from 4nba$^{(-)}$ forms the ring motif $R_2^2(8)$ with the amino and pyridinium of the 2a3hpH molecule. The nitro group of the 4nba$^{(-)}$ also forms a similar motif with the amino and pyridinium. In addition the hydroxyl and amino group (the hydrogen not involved in said ring motif) forms discrete hydrogen bonds to the carboxylate group.

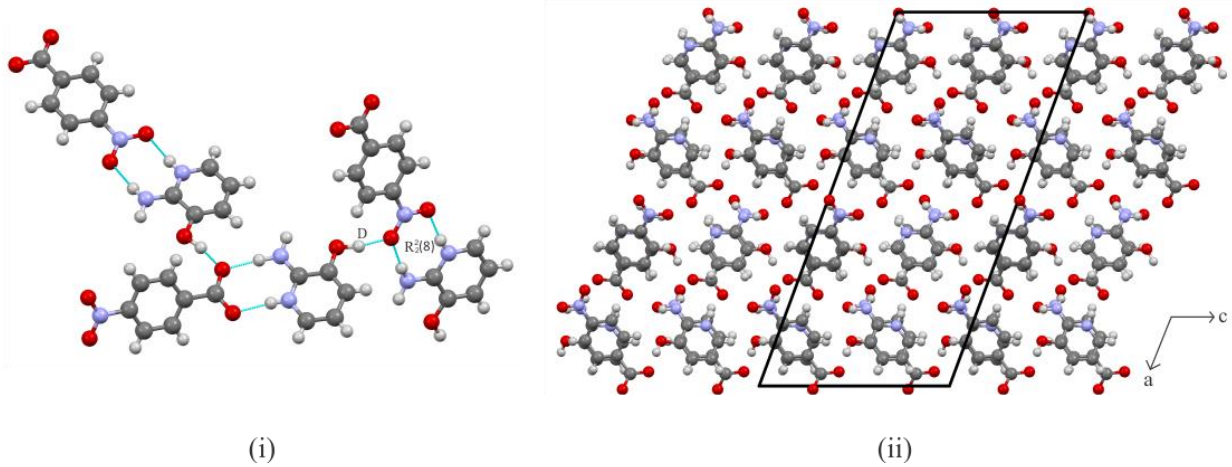

Fig 3.3.4 The crystal structure of the 4nba$^{(-)}$-2a3op molecular salt showing (i) the hydrogen bonding present and (ii) the packing of the molecules.

Table 3.3.4 Hydrogen bond table for molecular salt of 4nba + 2A3HP

D-H···A	d(D-H)	d(H···A)	d(D···A)	<(DHA)
N3-H3A···O6	0.91(4)	1.80(4)	2.707(4)	175(4)
N5-H5A···O4 (i)	0.89(4)	1.84(4)	2.705(4)	167(4)
N4-H4A···O5	0.93(5)	1.89(5)	2.821(4)	175(4)
N4-H4B···O6 (ii)	0.88(4)	2.22(4)	3.045(4)	157(4)
N6-H6A···O4(iii)	0.95(4)	2.55(4)	3.419(4)	152(3)
N6-H6B···O3 (i)	0.91(5)	1.91(5)	2.809(4)	173(4)
O9-H9A ···O5	1.03(5)	1.55(5)	2.576(4)	170(5)
O10-H10A···O3	0.99(5)	1.61(5)	2.590(3)	166(4)

(i) x-1/2,-y+3/2,z-1/2; (ii) x,-y+1,z+1/2; (iii) x-1/2,y+1/2,z-1

3.3.5 4nba(-) + 2-amino-5-bromopyridinium

4nba$^{(-)}$ formed a molecular salt with 2a5Brp and crystallised as yellow blocks. The molecular salt crystallises in the $P2_1/c$ space group with the asymmetric unit consisting of one molecule of each 4nba(-) and 2a5Brp. A proton transfer occurred between the carboxylate 4nba$^{(-)}$ and the pyridinium 2a5Brp. These two molecules form a dimer through the ring formed between the carboxylate hydrogen bonding to the one of the hydrogens on the amino group and the transferred proton. This dimer is connected to other neighbouring dimers through a hydrogen bond formed from the one hydrogen of the amino not involved in said ring to an oxygen atom of the carboxylate of a neighbouring 4nba$^{(-)}$ molecule. This forms a one-dimensional column which stack together to form a layered structure.

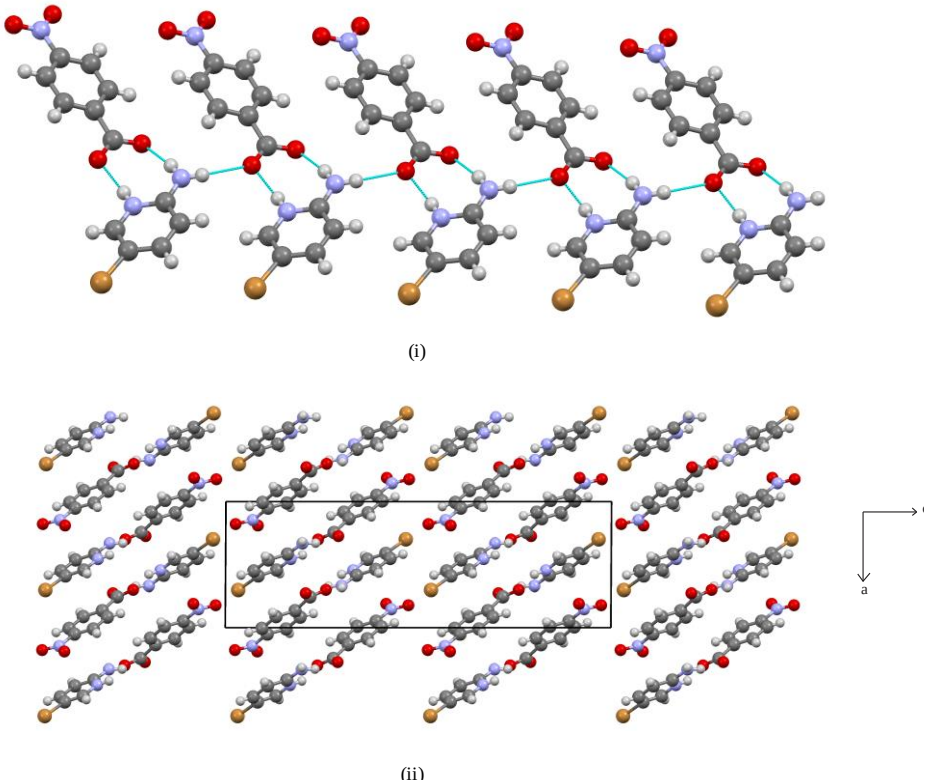

Fig 3.3.5 The crystal structure of the 4nba(-)- 2a5Brp molecular salt showing (i) the 1D columns formed by the various hydrogen bonding motifs and (ii) the packing diagram of the 4nba(-)-2a5Brp.

Table 3.3.5 Hydrogen bond table for the molecular salt of 4nba-2a5Brp

D-H···A	d(D-H)	d(H···A)	d(D···A)	<(DHA)
N2-H2A···O2	0.88	1.78	2.608(3)	155
N3-H2A···O1	0.91(4)	1.98(4)	2.836(3)	158(4)
N3-H2B···O2 (i)	1.00(3)	2.16(3)	3.072(3)	151(3)

(i) x,y-1,z

4. The Co-crystals and Salts of 2-chloro-4-nitrobenzoic acid and 2-chloro-5-nitrobenzoic acids

4.1 Introduction

2-chloro-4-nitrobenzoic acid (2c4n) and 2-chloro-5-nitrobenzoic acid (2c5n), like 4nba, are relatively simple molecules with the addition of a chlorine atom, which can serve as a potential weak hydrogen bond acceptor. These molecules can be used as potential anti-viral agents against HIV by boosting the immunity's response to the retrovirus [35]. 2c4n has been described in the literature as being polymorphic with two forms [36], while the CSD shows 2c5n containing only one form [24].

4.2 CSD Results

Several co-crystals and salts of 2c4n and 2c5n have been reported in the CSD with various co-formers [24], which indicate that the potential of forming novel co-crystals and salts is high. The CSD includes a total of 53 entries of co-crystals and salts involving 2c4n, which includes 29 co-crystals and 24 salts. 2c5n on the other hand consists of 8 co-crystals and salts, with 4-co-crystals and 4 salts.

Table 4.2.1 Examples of CSD search results for co-crystals and salts of 2c4n

Ref Code	Co-former(s)	Co-Crystal/Salt	Notes
LATLEZ / [37]	Isonicotinohydrazide	Co-crystal	important TB drug
JUHLIJ / [17]	2-chloropyridin-3-ol	Co-crystal	pyridine forming a co-crystal
REMKOJ / [38]	Imidazolium	Salt	nitrogen containing heterocycle
ZEKYIA / [39]	2-aminobenzoic acid	Co-crystal	benzoic acid forming a co-crystal with ring motif
HUHRAD / [40]	1,2,3-benzotriazole	Co-crystal	nitrogen containing heterocycle
HUHREH / [41]	Benzimidazolium	Salt	bicyclic compound with nitrogen acting as base
AFEDIY / [42]	4-Aminopyridinium	Salt	pyridinium salt
MAHWUO / [43]	3-Cyanopyridine	Co-crystal	same base used for 2c5n co-crystal
REHSEE / [44]	2-ethoxybenzamide	Co-crystal	heterocyclic compound acting as a base
DUHKIC / [45]	3-hydroxyanilinium	Salt	anilinium derivative with amino group acting as proton acceptor

Table 4.2.2 Examples of CSD search results for co-crystals and salts of 2c5n

Ref Code	Co-former(s)	Co-Crystal/Salt	Notes
AJIWIA / [46]	quinoline	Co-crystal	Bicyclic compound acting as a hydrogen bond acceptor
HIHPEU / [47]	1,2-bis(4-pyridyl)ethane	Co-crystal	Heterocyclic compound acting as a hydrogen bond acceptor
HIHPIY / [47]	8-Hydroxy-2-methyl-quinolinium dihydrate	Salt/ Hydrate	Heterocyclic compound acting as a base
HIHPOE / [47]	2-Ammonio-benzimidazole	Salt	Heterocyclic compound acting as a base
MEVYAN / [48]	Morpholinium	Salt	Heterocyclic compound acting as a base
UHAQAV / [49]	4-benzoylpyridine	Co-crystal	Pyridine acting as a hydrogen bond acceptor

4.3 SC-XRD Results (2-chloro-4-nitrobenzoic acid)

Two co-crystals and three molecular salts involving 2c4nH and 2c4n$^{(-)}$ respectively were synthesised and their structures are described below. Scheme 4.3 shows the chemical structure of each crystal system and Fig. 4.3.1 shows the Ortep diagrams of the crystal structures. PXRD patterns of each co-crystal/molecular salt were measured and are available in the Appendix (Figs. A6 – A10) together with the calculated pattern, which confirms the single crystal represent the bulk material in each case.

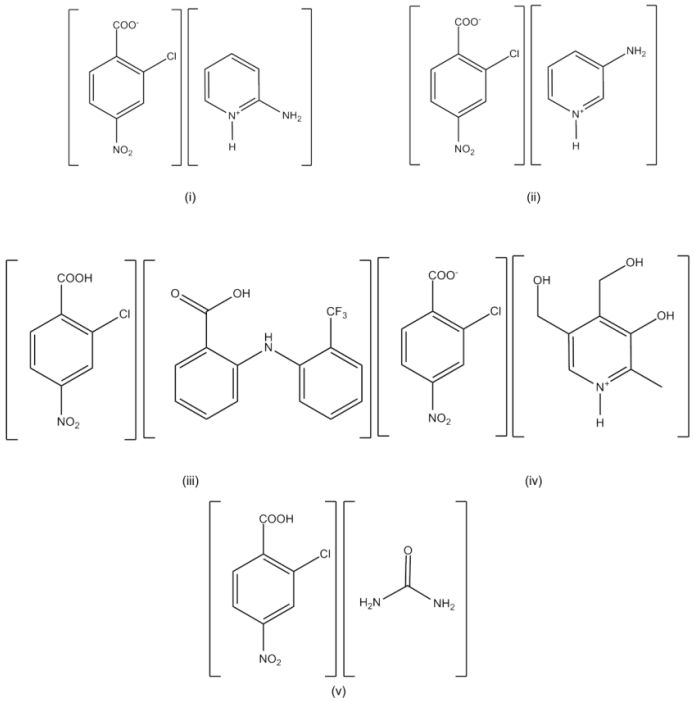

Scheme 4.3 Chemical structures of (i) 2c4n(-) + 2ap, (ii) 2c4n(-) + 3apH (iii) 2c4nH + fa, (iv) 2c4n(-) + pyd and (v) 2c4nH + urea

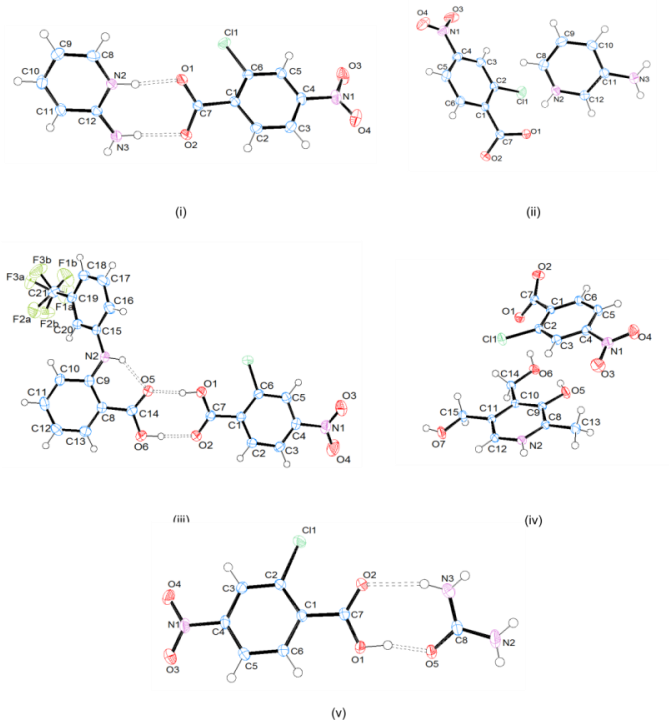

Fig. 4.3 Ortep diagrams showing the numbering scheme of the asymmetric units for (i) 2c4n(-) + 2ap, (ii) 2c4n(-) + 3apH (iii) 2c4nH + fa, (iv) 2c4n(-) + pyd and (v) 2c4nH + urea

Table 4.3 Crystal Structure Data for co-crystals and molecular salts of 2c4n

Identification code	**2c4n(-) + 2-aminopyridinium**	**2c4n(-) + 3aminopyridinium**	**2c4nH + flufenamic acid**	**2c4n(-) + pyridoxinium**
Empirical formula	$C_{12}H_{10}N_3O_4Cl$	$C_{12}H_{10}N_3O_4Cl$	$C_{21}H_{14}N_2O_6F_3Cl$	$C_{15}H_{15}N_2O_7Cl$
Formula weight	295.68	295.68	482.79	370.74
Temperature/K	173.15	173.15	173.15	296.15
Crystal system	triclinic	triclinic	monoclinic	monoclinic
Space group	P-1	P-1	$P2_1/c$	$P2_1/n$
a/Å	5.5746(3)	5.8116(2)	7.5293(2)	10.0439(4)
b/Å	10.5108(5)	10.7701(4)	31.9965(8)	15.3847(6)
c/Å	11.3341(6)	10.7983(5)	8.3852(2)	10.3831(4)
α/°	95.952(2)	79.1970(10)	90	90
β/°	103.834(2)	86.0390(10)	94.0650(10)	99.1320(10)
γ/°	93.121(2)	74.8790(10)	90	90
Volume/$Å^3$	639.20(6)	640.77(4)	2015.01(9)	1584.09(11)
Z	2	2	4	4
$\rho_{calc}g/cm^3$	1.536	1.532	1.591	1.555
μ/mm^{-1}	0.316	0.316	0.261	0.284
F(000)	304	304	984	768
Crystal size/mm^3	0.844 × 0.457 × 0.268	0.56 × 0.35 × 0.22	0.326 × 0.286 × 0.092	0.405 × 0.280 × 0.120
Radiation	MoKα$_1$ (λ = 0.71073 Å)	MoKα$_1$(λ = 0.71073 Å)	MoKα$_1$ (λ = 0.71073 Å)	MoKα (λ = 0.71073 Å)
2Θ range for data collection/°	7.554 to 55.996	7.264 to 55.992	2.546 to 56.478	5.874 to 56.7
Index ranges	$-7 \le h \le 7$, $-13 \le k \le 13$, $-14 \le l \le 14$	$-7 \le h \le 7$, $-14 \le k \le 14$, $-14 \le l \le 14$	$-10 \le h \le 7$, $-39 \le k \le 42$, $-11 \le l \le 10$	$-13 \le h \le 13$, $-20 \le k \le 20$, $-13 \le l \le 13$
Reflections collected	24627	22264	18155	39690
Independent reflections	3019 [R_{int} = 0.0194, R_{sigma} = 0.0103]	3051 [R_{int} = 0.0174, R_{sigma} = 0.0097]	4947 [R_{int} = 0.0457, R_{sigma} = 0.0408]	3956 [R_{int} = 0.0468, R_{sigma} = 0.0236]
Data/restraints/parameters	3019/0/181	3051/0/181	4947/147/338	3956/0/239
Goodness-of-fit on F^2	1.051	1.053	1.061	1.034
Final R indexes [I>=2σ (I)]	R_1 = 0.0302, wR_2 = 0.0832	R_1 = 0.0290, wR_2 = 0.0810	R_1 = 0.0442, wR_2 = 0.1025	R_1 = 0.0398, wR_2 = 0.1030
Final R indexes [all data]	R_1 = 0.0313, wR_2 = 0.0845	R_1 = 0.0306, wR_2 = 0.0824	R_1 = 0.0629, wR_2 = 0.1149	R_1 = 0.0524, wR_2 = 0.1114
Largest diff. peak/hole / e $Å^{-3}$	0.38/-0.28	0.34/-0.25	0.52/-0.39	1.19/-0.41

4.3.1 2c4n$^{(-)}$ + 2-aminopyridinium

Molecular salts of 2c4n$^{(-)}$ and 2apH was synthesised and crystallised as light yellow prisms. A proton transfer occurred between the carboxylate and the pyridinium. The resulting structure consists of several different hydrogen bond networks. The amino group along with the pyridinium proton of 2apH, hydrogen bonds to the carboxylate in several different graph set motifs. These include the pyridinium's proton and one of the amino group's hydrogen to each oxygen part of the carboxylate groups with ring motif $R_2^2(8)$, both hydrogens of the amino group of the two 2apH molecules hydrogen bonding to one of the carboxylate oxygen with ring motif $R_4^2(8)$ and finally a $R_4^4(16)$ system where two molecule of each 2c4n and 2AP are involved using one of the amino group's hydrogen and the pyridinium's proton on each molecule to hydrogen bond to one carboxyl of each 2c4nH molecule. This structure has been previously reported by Oruganti *et al*. [50].

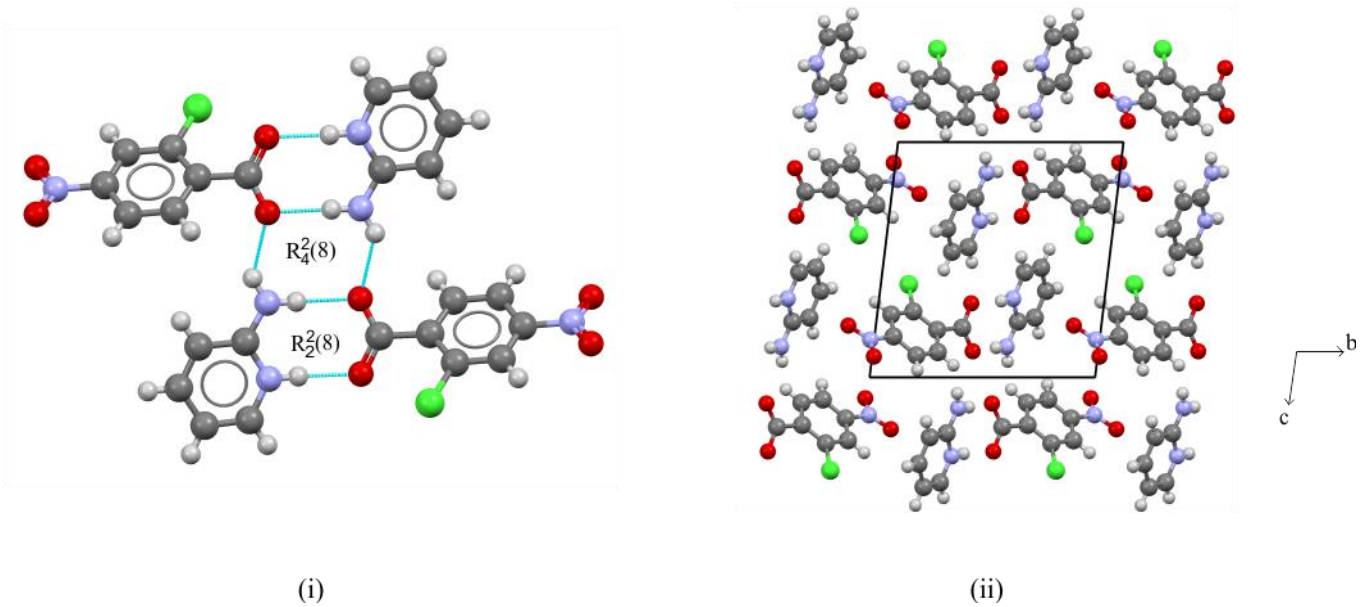

Fig 4.3.1 The crystal structure of the 2c4n$^{(-)}$-2apH molecular salt showing (i) the hydrogen bonding motif of the 2c4n(-) - 2apH tetramer and (ii) the packing viewed along the *a*-axis.

Table 4.3.1: Hydrogen bond table for the molecular salt of 2c4n$^{(-)}$ and 2apH

D-H···A	d(D-H)	d(H...A)	d(D...A)	<(DHA)
N2-H2A···O1	0.912(17)	1.842(17)	2.7409(11)	168(2)
N3-H3A···O2	0.859(18)	1.942(18)	2.8012(12)	178(2)
N3-H3B···O2 (i)	0.871(18)	2.092(18)	2.8152(12)	140(2)

(i) -x,-y+1,-z

4.3.2 2c4n$^{(-)}$ + 3-aminopyridinium

2c4n$^{(-)}$ formed a molecular salt with 3apH and crystallised as colourless blocks. The molecular salt crystallises in the *P*-1 space group with the asymmetric unit consisting of one molecule of each 2c4n$^{(-)}$ and 3apH where the proton has transferred between the 2c4n$^{(-)}$ and 3apH molecules. These molecules form a tetramer with the amino groups hydrogen bonding to the carboxylate oxygen with N-H···O$^-$ bond distances averaging 2.1 Å. These tetramers form infinite columns which are connected to each other via weak Cl···Cl (3.273 Å) bond interactions.

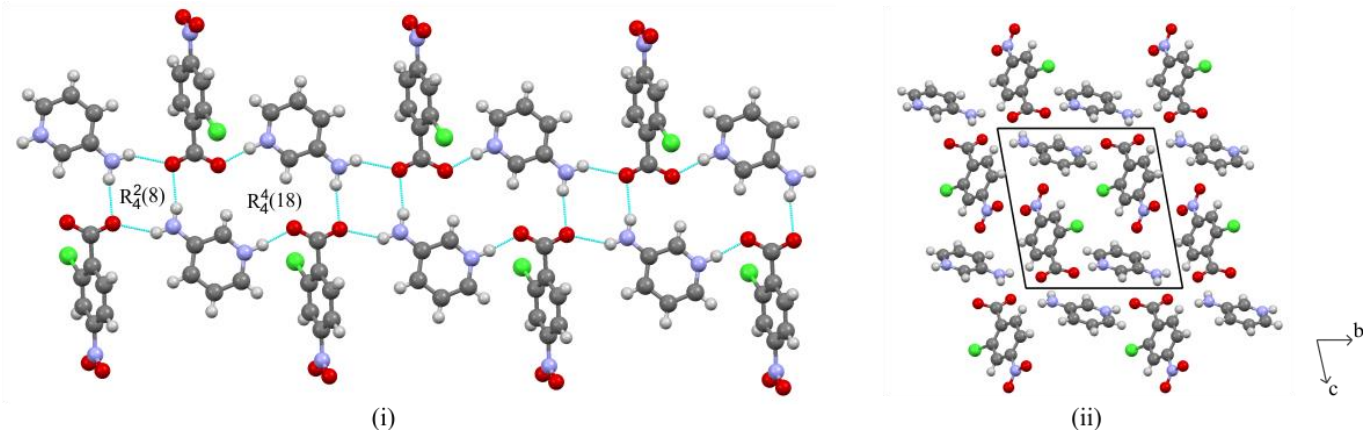

Fig. 4.3.2 The crystal structure of 2c4n$^{(-)}$-3apH showing (i) the 1D column of the 2c4n$^{(-)}$-3apH with the hydrogen bonding motifs and (ii) the packing diagram.

Table 4.3.2 Hydrogen bond table for the molecular salt of 2c4n$^{(-)}$-3AP

D-H Å A	d(D-H)	d(H···A)	d(D···A)	<(DHA)
N3-H3B···O2$^{(i)}$	0.868(17)	2.089(17)	2.9344(13)	165(2)
N3-H3A···O2$^{(ii)}$	0.846(18)	2.113(18)	2.8622(12)	147(2)
N2-H2···O1	0.918(19)	1.70(2)	2.6118(11)	174(2)

(i) -x+2,-y+1,-z; (ii) x,y-1,z

4.3.3 2c4n$^{(-)}$ + pyridoxinium

2c4n$^{(-)}$ formed a molecular salt with pyd and crystallised as slightly brown blocks. The molecular salt crystallises in the $P2_1/n$ group with the asymmetric unit consisting of one molecule of each 2c4n$^{(-)}$ and pyd where a proton transfer has occurred between the 2c4n and PYD molecules. 2c4n$^{(-)}$ and pyd form tetramers with a ring motif of $R_4^2(16)$. These tetramers ultimately pack in a layered structure with the layers connected to each other via hydrogen bonding between O1 of the carboxylate group and the hydroxyl group with a O-H···H distance of 1.840 Å.

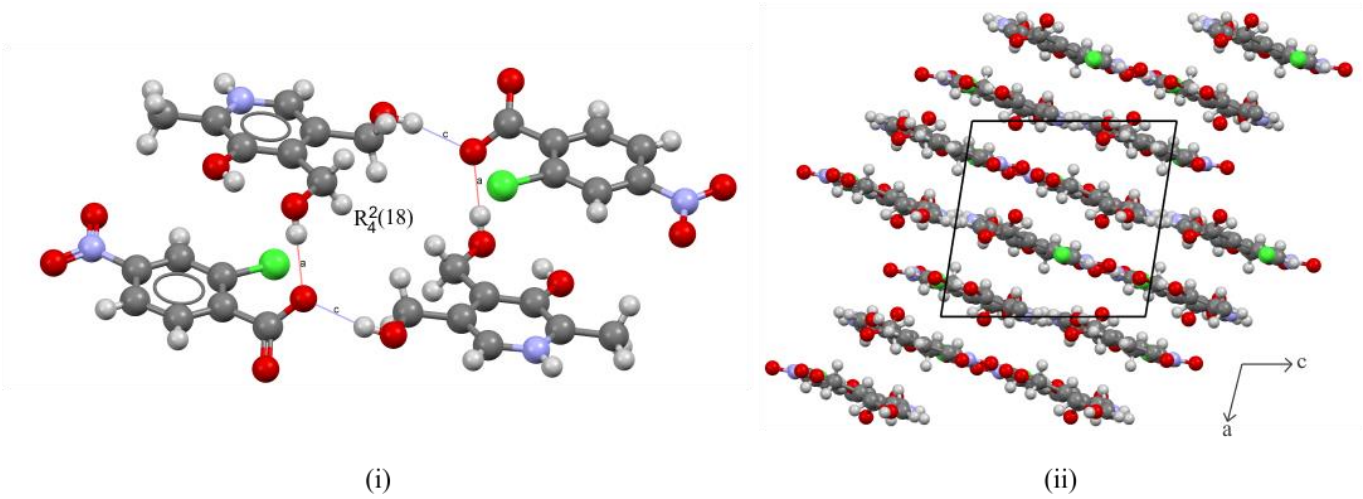

Fig 4.3.3 Crystal structure of the 2c4n$^{(-)}$-pyd molecular salt showing (i) the hydrogen between molecules in the tetramer and (ii) the layered structure linked together via hydrogen bonds.

Table 4.3.3 Hydrogen bond table for the molecular salt of 2c4n$^{(-)}$-pyd

D-H···A	d(D-H)	d(H···A)	d(D···A)	<(DHA)
N2-H2···O2$^{(i)}$	0.87(2)	1.82(2)	2.6735(17)	168(2)
O5-H5···O6	0.77(3)	1.86(3)	2.5739(17)	155(3)
O6-H6···O1	0.81(3)	1.84(3)	2.6450(18)	177(2)
O7-H7···O1$^{(ii)}$	0.85(3)	1.86(3)	2.7052(17)	171(2)

(i) x,y,z-1 (ii) -x+1,-y+2,-z+1

4.3.4 2c4nH + Flufenamic Acid

2c4nH formed a co-crystal with fa and crystallised as yellow blocks. The co-crystal crystallises in the $P2_1/c$ group with the asymmetric unit consisting of one molecule of each 2c4nH and fa. Rotational disorder is present with the trifluoro group on the fa molecules, with the three fluorine atoms modelled on two different conformations. Hydrogen bonding exists between the carboxylic acids of both 2c4n and FA which give the $R_2^2(8)$ ring dimer. The packing of the structure forms ribbon-like layers of 1-dimensional sheets of 2c4nH and fa. These sheets are connected to each other with weak C-H···F interactions between the fa rings containing the trifluoro group with distances of 2.625Å. This structure has been previously reported by Nechipadappu et al. [14].

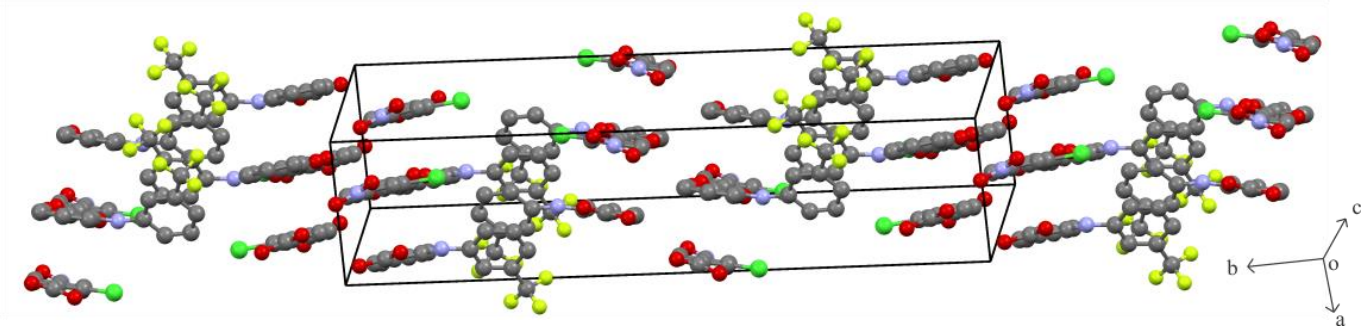

Fig 4.3.4 The crystal structure of 2c4n-FA co-crystal showing the ribbon-like layers of the 2c4n-FA co-crystal.

Table 4.3.4 Hydrogen bond table for the co-crystal 2c4n-FA

D-H···A	d(D-H)	d(H···A)	d(D···A)	<(DHA)
O1-H1···O5	0.91(3)	1.66(3)	2.5707(18)	174(3)
N2-H2···O5	0.87(2)	1.95(2)	2.6547(19)	137(2)
O6-H6···O2	0.96(3)	1.74(3)	2.6966(18)	173(3)

4.3.5 2c4nH + urea

2c4nH formed a co-crystal with urea and crystallised as colourless blocks. The co-crystal crystallises in the $P2_1/n$ group with the asymmetric unit consisting of one molecule of each 2c4nH and urea. The amide group and carboxyl group forms a ring with a graph set of $R_2^2(8)$, with the other amino group on urea free to form a hydrogen bond to the nitro group of 2c4nH. The overall packing consists of a series of different sets of columns which are cross-linked to each other via the second hydrogen on the amino group not involved in the carboxyl-amino ring formation to the carboxyl group.

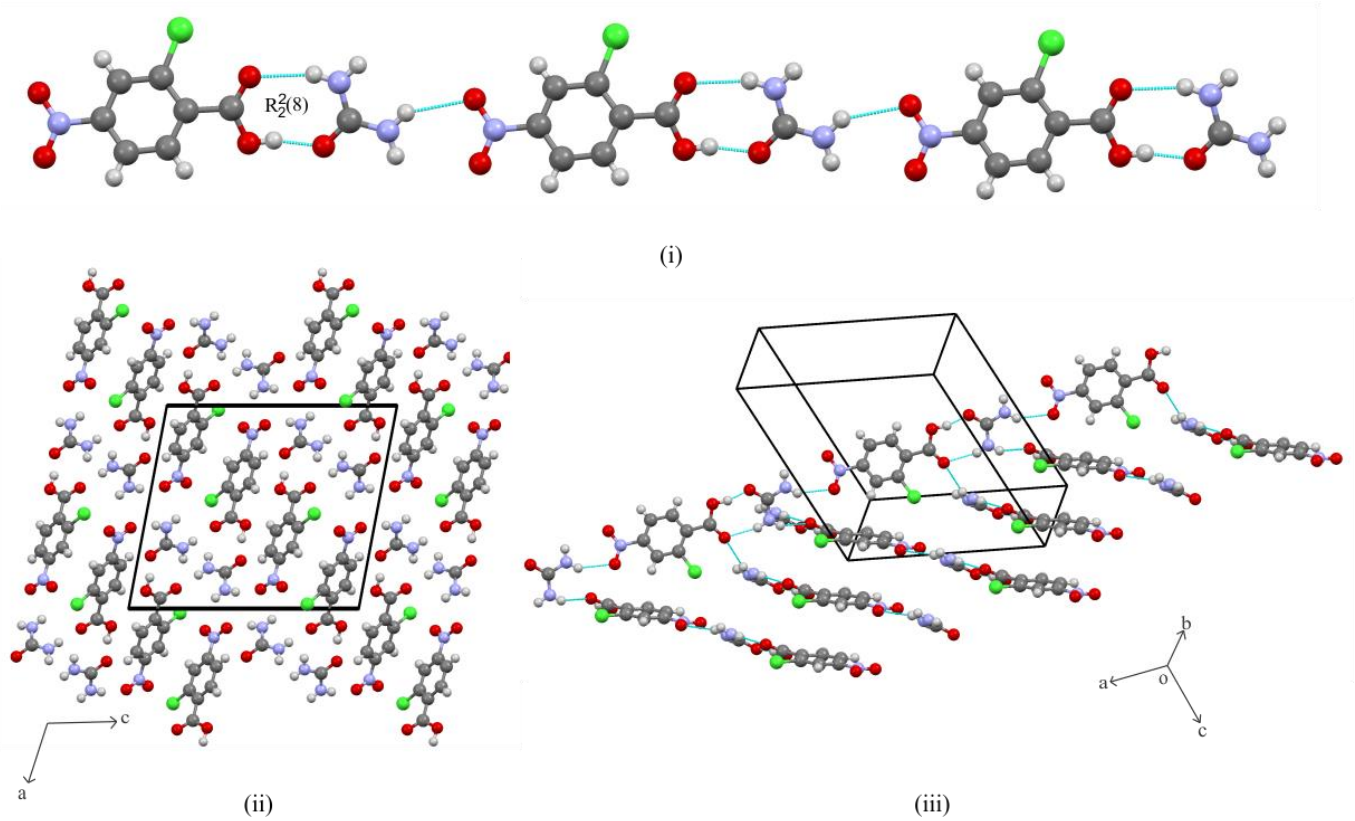

Fig 4.3.5 Crystal structure of the 2c4nH-urea co-crystal showing (i) one of the 1D columns with hydrogen bonding present, (ii) the packing scheme and (iii) one of the 1D columns which cross-links several other columns together.

Table 4.3.5 Hydrogen Bond table for the co-crystal of 2c4nH-urea

D-H···A	d(D-H)	d(H···A)	d(D···A)	<(DHA)
N3-H3A ···O2	0.86(2)	2.15(2)	2.9862(15)	164(2)
N3-H3B···O2 [(i)]	0.79(2)	2.29(2)	2.9634(15)	145(2)
N2-H2B···O4 [(ii)]	0.82(2)	2.35(2)	3.0554(15)	145(2)
N2-H2B···O2 [(i)]	0.82(2)	2.59(2)	3.1704(17)	129(2)
O1-H1···O5	0.97(2)	1.54(2)	2.4914(11)	166(2)

(i) -x+1/2,y+1/2,-z+3/2 (ii) x-1,y+1,z

4.4 SC-XRD Results (2-chloro-5-nitrobenzoic acid)

Two co-crystals and two molecular salts involving 2c5nH were synthesised and their structures are described below. Fig. 4.3.1 shows the Ortep diagrams of the crystal structures. PXRD patterns of each co-crystal/molecular salt were measured and are available in the Appendix (Figs. A11 – A14) together with the calculated pattern, which confirms the single crystal represent the bulk material in each case.

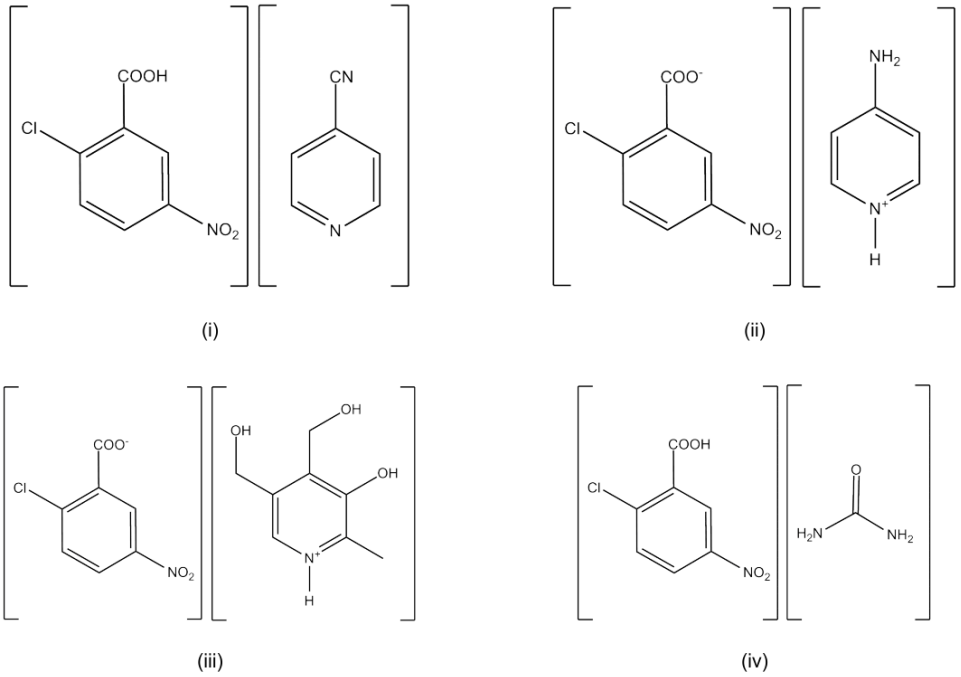

Scheme 4.4 Chemical diagram for (i) 2c5n(-) + 3cnpH, (ii) 2c5n(-) + 4apH, (iii) 2c5nH + urea and (iv), 2c5n(-) + pyd.

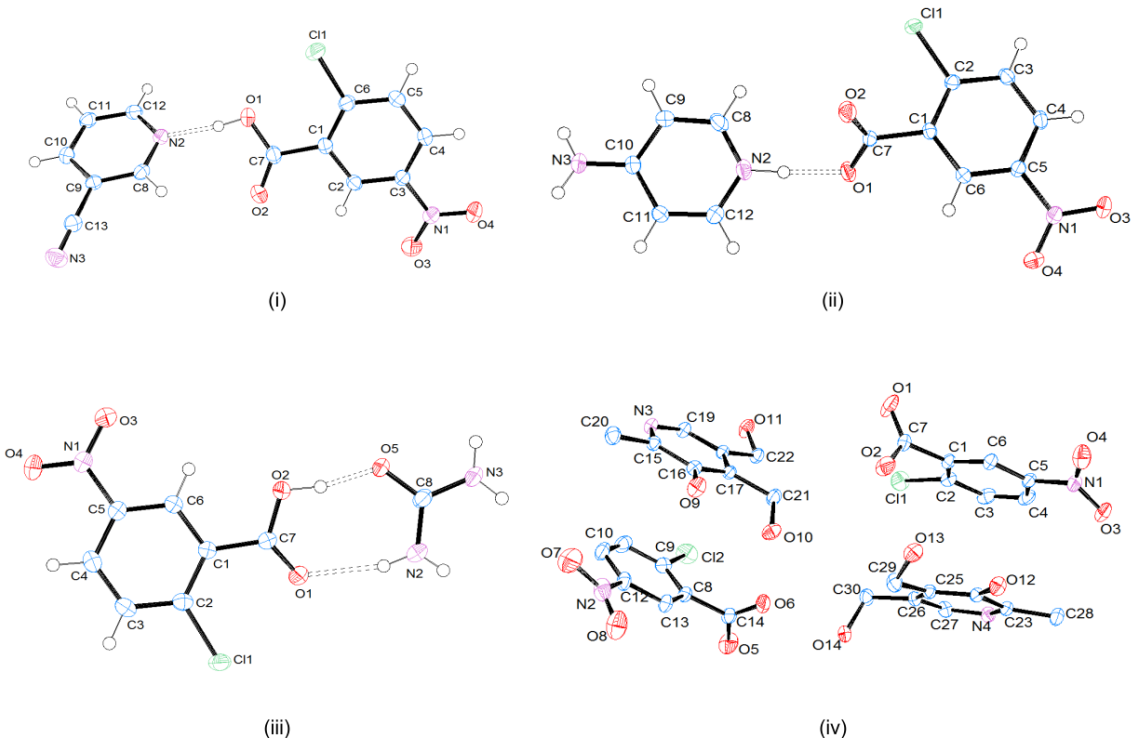

Fig. 4.4 Ortep diagrams showing the numbering scheme of the asymmetric units for (i) 2c5n(-) + 3cnpH, (ii) 2c5n(-) + 4apH, (iii) 2c5nH + urea and (iv), 2c5n(-) + pyd (with hydrogens omitted to allow clarity for numbering scheme of non-hydrogen atoms).

Table 4.4 Crystal Structure Data for co-crystals of 2c5n

Identification code	**2c5nH + 3cnp**	**2c5n(-) + 4apH**	**2c5n(-) + pyd**	**2c5nH + urea**
Empirical formula	$C_{13}H_8N_3O_4Cl$	$C_{12}H_{10}N_3O_4Cl$	$C_{13}H_{12}NO_8Cl$	$C_8H_8N_3O_5Cl$
Formula weight	305.67	295.68	185.37	261.62
Temperature/K	173.15	173.15	173.15	173.15
Crystal system	triclinic	monoclinic	triclinic	monoclinic
Space group	P-1	P21/n	P-1	P21/c
a/Å	7.5929(4)	12.5078(4)	6.9559(2)	10.4103(2)
b/Å	7.6584(4)	7.1490(2)	15.6259(4)	7.08260(10)
c/Å	13.0481(7)	13.9841(4)	15.6769(4)	15.0879(3)
α/°	79.277(2)	90	70.3060(10)	90
β/°	74.591(2)	95.8960(10)	85.9600(10)	104.9460(10)
γ/°	64.415(2)	90	87.0570(10)	90
Volume/Å3	657.52(6)	1243.82(6)	1599.61(7)	1074.83(3)
Z	2	4	8	4
ρcalcg/cm3	1.544	1.579	1.539	1.617
μ/mm-1	0.311	0.325	0.282	0.371
F(000)	312	608	768	536
Crystal size/mm3	0.936 × 0.528 × 0.432	0.246 × 0.325 × 0.148	0.555 × 0.426 × 0.142	0.512 × 0.321 × 0.258
Radiation	MoKα (λ = 0.71073)	MoKα (λ = 0.71073)	MoKα (λ = 0.71073)	MoKα (λ = 0.71073)
2Θ range for data collection/°	5.918 to 55.994	5.858 to 55.976	4.52 to 68.576	4.05 to 55.998
Index ranges	$-10 \le h \le 10$, $-10 \le k \le 10$, $-17 \le l \le 17$	$-16 \le h \le 16$, $-9 \le k \le 9$, $-17 \le l \le 18$	$-10 \le h \le 10$, $-24 \le k \le 24$, $-24 \le l \le 24$	$-13 \le h \le 13$, $-9 \le k \le 9$, $-19 \le l \le 19$
Reflections collected	22941	33735	48142	31268
Independent reflections	3123 [Rint = 0.0283, Rsigma = 0.0167]	2977 [Rint = 0.0200, Rsigma = 0.0090]	13209 [Rint = 0.0504, Rsigma = 0.0396]	2589 [Rint = 0.0470, Rsigma = 0.0178]
Data/restraints/parameters	3123/0/191	2977/0/181	13209/0/485	2589/0/155
Goodness-of-fit on F2	1.066	1.072	1.027	1.05
Final R indexes [I>=2σ (I)]	R1 = 0.0328, wR2 = 0.0883	R1 = 0.0291, wR2 = 0.0817	R1 = 0.0403, wR2 = 0.1091	R1 = 0.0298, wR2 = 0.0813
Final R indexes [all data]	R1 = 0.0347, wR2 = 0.0900	R1 = 0.0307, wR2 = 0.0832	R1 = 0.0514, wR2 = 0.1178	R1 = 0.0328, wR2 = 0.0853
Largest diff. peak/hole / e Å-3	0.30/-0.32	0.33/-0.30	0.67/-0.54	0.21/-0.35

4.4.1 2c5nH + 3-Cyanopyridine

2c5nH formed a co-crystal with 3cnp and crystallised as colourless blocks. This co-crystal forms in a triclinic system with space group of *P*-1 with the asymmetric unit consisting of one molecule of each 2c5nH and 3cnp. 2c5nH forms a discrete hydrogen bond between its carboxylic acid group to the pyridine of 3cnp. The overall structure packs in layers of 3cnp cross-linked by alternating layers of 2c5nH.

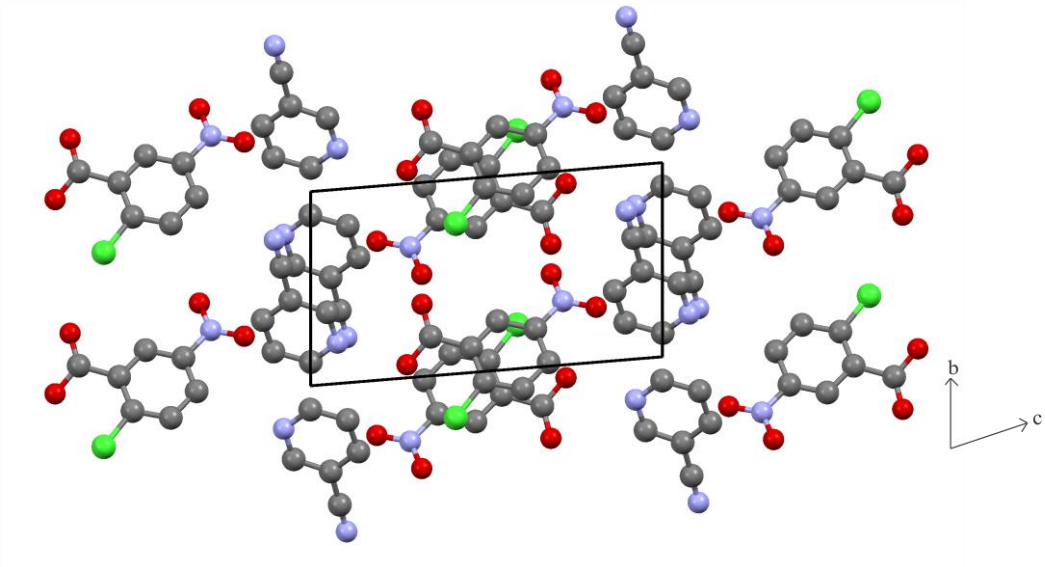

Fig. 4.4.1 Packing diagram of the 2c5nH-3cnp co-crystals with hydrogens omitted.

Table 4.4.1 Hydrogen bond table for the 2c5nH-3cnp co-crystal

D-H···A	d(D-H)	d(H···A)	d(D···A)	<(DHA)
O1-H1···N2	0.91(2)	1.72(2)	2.6271(13)	173(2)

4.4.2 2c5n$^{(-)}$ + 4-aminopyridinium

2c5n$^{(-)}$ formed a molecular salt with 4apH and crystallised as light yellow prisms. The molecular salt crystallises in the $P2_1/n$ group with the asymmetric unit consisting of one molecule of each 2c5n$^{(-)}$ and 4apH. A proton transfer occurred with 2c5n$^{(-)}$ donating its acidic proton to 4apH. 2c5n$^{(-)}$ and 4apH form 2D columns consisting of alternating molecules of 2c5n(-) and 4apH. Hydrogen bonding can be described using chains running from the pyridinium which is hydrogen bonding to the carboxylate group connected to an amino group of another 4apH molecule, with a graph set of $C_2^2(10)$.

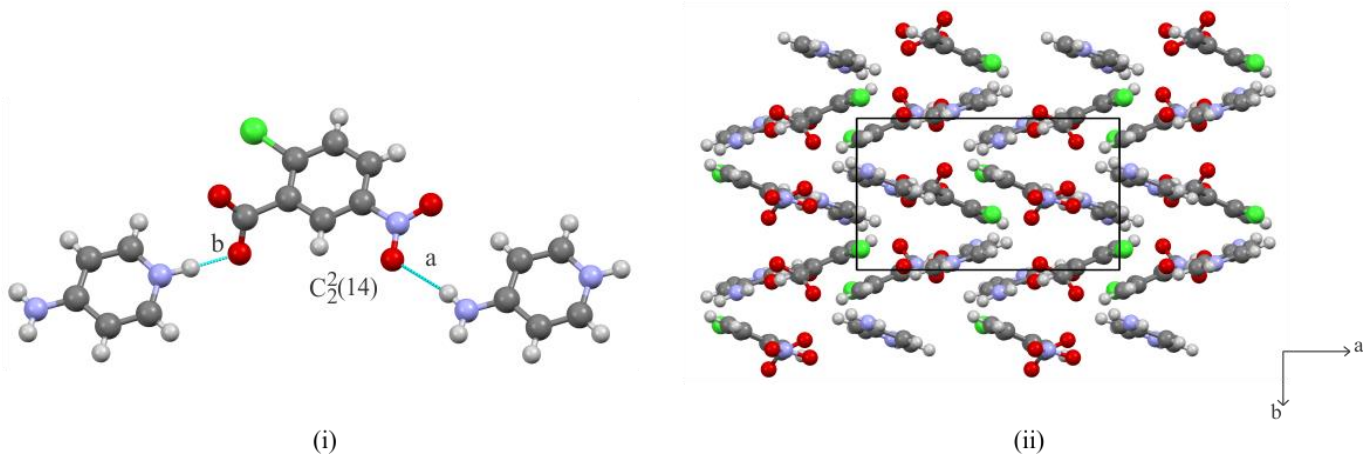

(i) (ii)

Fig. 4.4.2 The crystal structure of the molecular salt of 2c5n(-)-4apH showing (i) the chain formed due to the possible hydrogen bonds and (ii) the packing showing two different alternating layers in a zig-zag fashion.

Table 4.4.2 Hydrogen Bond table for the molecular salt of 2c5n(-)-4apH

D-H...A	d(D-H)	d(H···A)	d(D···A)	<(DHA)
N3-H3B···O(4) [(i)]	0.85(2)	2.24(2)	3.0785(14)	169(2)
N3-H3A···O2 [(ii)]	0.90(2)	2.08(2)	2.9730(14)	176(2)
N2-H2···O1	1.01(2)	1.64(2)	2.6443(13)	173(2)
N2-H2···O2	1.01(2)	2.64(2)	3.3010(13)	123(2)

(i) x,y,z+1; (ii) x+1/2,-y+3/2,z+1/2

4.4.3 2c5n$^{(-)}$ + pyridoxinium

2c5n$^{(-)}$ formed a molecular salt with pyd and crystallised as colourless blocks. The molecular salt crystallises in the *P*-1 group with the asymmetric unit consisting of two molecules of each 2c5n$^{(-)}$ and pyd. A proton transfer occurred between both 2c5n$^{(-)}$ molecules to both pyd molecules. Although several hydrogen bonding pairs exist within this structure, one of the most significant bonding motifs is a ring formation with graph set $R_4^4(20)$, consisting of a tetramer of two pairs of 2c5n(-) and pyd. This tetramer is formed by the pairing of 2c5n$^{(-)}$ and pyd via the one hydroxymethyl group hydrogen bonding to the carboxylate, with this pair bonding to another pair via the carboxylate-pyridinium interaction. The overall packing consists of stacking the 2c5n$^{(-)}$ and pyd molecules in rows with alternation between the two different molecules.

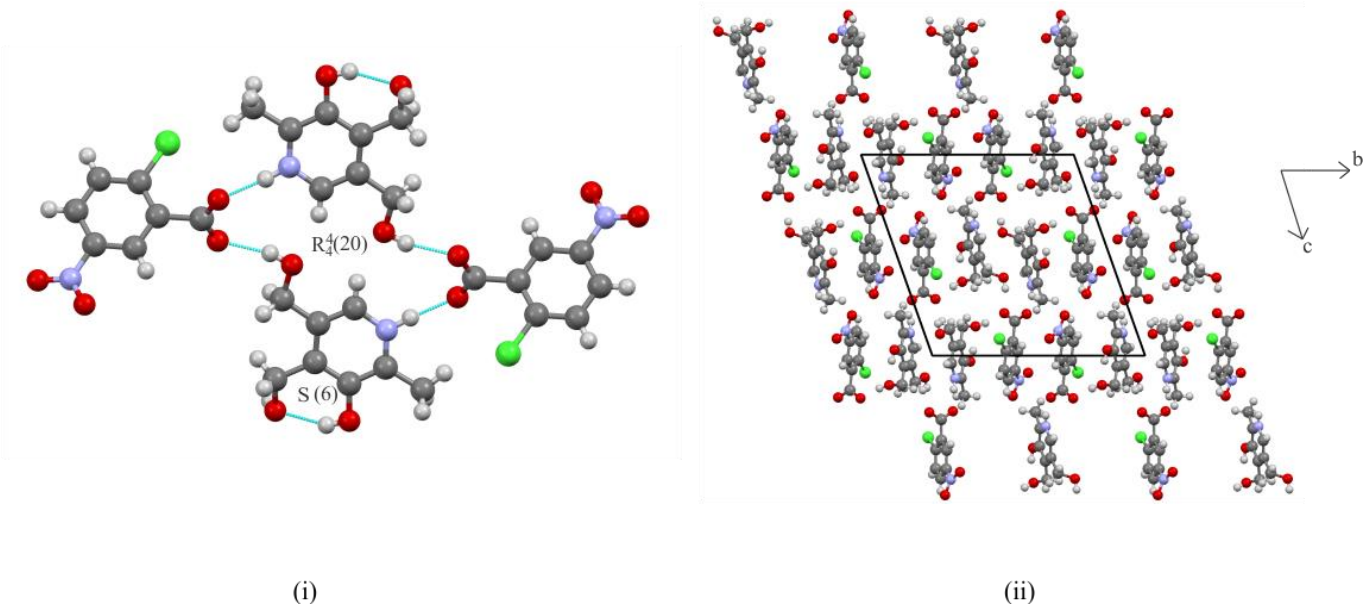

Fig. 4.4.3 Crystal structure of the molecular salt of 2c5n$^{(-)}$-pyd showing (i) the tetramer formed due to the various hydrogen bonding present and (ii) the packing.

Table 4.4.3 Hydrogen bond table for the molecular salt of 2c5n$^{(-)}$-pyd

D-H···A	d(D-H)	d(H···A)	d(D...A)	<(DHA)
N4-H4···O5 (i)	0.879(16)	1.875(16)	2.7061(11)	157(2)
O10-H10···O6	0.830(18)	1.802(18)	2.6246(11)	170(2)
O11-H11···O(2) (ii)	0.852(18)	1.850(18)	2.6842(10)	166(2)
O12-H12···Cl1 (iii)	0.896(19)	2.800(19)	3.3950(7)	125(2)
O12-H12···O13	0.896(19)	1.779(19)	2.6035(10)	152(2)
N3-H3···O1 (iv)	0.927(18)	1.770(18)	2.6947(11)	175(2)
O13-H13···O2	0.826(19)	1.826(19)	2.6471(11)	173(2)
O14-H14···O6	0.82(2)	1.82(2)	2.6363(11)	169(2)
O9-H9···Cl2(iii)	0.84(2)	2.89(2)	3.4541(8)	126(2)
O9-H9···O10	0.84(2)	1.84(2)	2.6199(11)	153(2)

(i) -x+2,-y+1,-z+1; (ii) x+1,y,z; (iii) x-1,y,z; (iv) -x+2,-y+2,-z

4.4.4 2c5n + urea

2c5nH formed a co-crystal with urea and crystallised as colourless blocks. The co-crystal crystallises in the $P2_1/n$ group with the asymmetric unit consisting of one molecule of each 2c5nH and urea. Hydrogen bond interactions of 2c5nH with urea are similar to those observed in the 2c4nH-urea co-crystal. A tetramer is present with a ring motif $R_4^4(24)$ consisting of two molecules of each 2c5nH and urea. This tetramer is formed by the interactions of the amino groups of urea mono-co-ordinated to one nitro and one of the oxygens of the carboxylic acid of each 2c5nH molecule. In addition, the amide-carboxylic acid heterosynthon is present, with the same ring motif $R_2^2(8)$. The overall packing shows 1D column packed in a zig-zag formation with respect to each other.

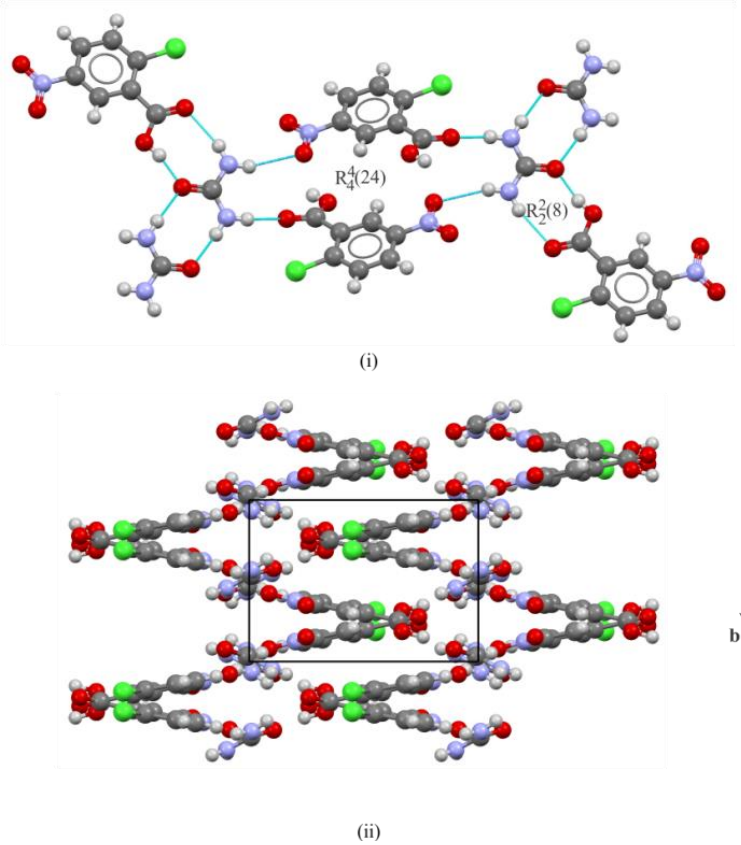

Fig. 4.4.4 The crystal structure of the co-crystal of 2c5nH-urea showing (i) the octamer formed due to the various hydrogen bonding present and (ii) the zig-zag packing.

Table 4.4.4 Hydrogen Bond Table for the co-crystal of 2c5nH-urea

D-H···A	d(D-H)	d(H···A)	d(D···A)	<(DHA)
N3-H3B···O(1) [(i)]	0.852(17)	2.083(18)	2.8945(13)	159(2)
N3-H3A···O(5) [(ii)]	0.846(17)	2.047(18)	2.8831(14)	170(2)
N2-H2A···O1	0.877(18)	2.123(18)	2.9773(15)	164(2)
O2-H2···O5	0.96(2)	1.54(3)	2.4855(12)	167(3)
N2-H2B···O3 [(iii)]	0.780(18)	2.487(18)	3.2108(15)	155(2)

(i) -x,y+1/2,-z+1/2; (ii) -x,-y+1,-z+1; (iii) x-1,-y+1/2,z-1/2

5. The Co-crystals of 3,5-Dinitrobenzoic Acid

5.1 Introduction

3,5-dinitrobenzoic acid (dnba) consists of two nitro groups as opposed to the one nitro group that have been studied as part of this dissertation so far. Dnba exists in two polymorphs (crystal structures consisting of the same molecules but existing in different packing schemes): a primitive monoclinic form with space group $P2_1/c$ and a base-centred monoclinic form with space group $C2/c$ [51].

5.2 CSD Results

Several co-crystals/molecular salts with dnba exist and have been published in the CSD [24]. A total of 277 results of co-crystals and molecular salts are present, of which 145 are co-crystals and 133 salts. This indicates a high potential of forming a new co-crystal/molecular salt with 4nba. In Table 5.2 is a list of some more notable examples of co-crystals and molecular salts of dnba in the literature.

Table 5.2 Examples of entries of dnba co-crystal/salts on the CSD.

Ref Code	Co-formers(s)	Co-crystal/salt	Notes
PUHROZ / [52]	3,5-Dimethylpyridine	Co-crystal	heterocycle acting as a hydrogen bond acceptor
WEBXAE / [53]	Pyridin-4-ylmethanaminium	Salt	pyridinium derivative acting as a base.
TEZREX / [54]	5-Chloro-2-hydroxyanilinium	Salt	anilinium derivative where amino group is acting as a base.
OQEFOH / [55]	4-amino-N-(3,4-dimethyl-1,2-oxazol-5-yl)benzenesulfonamide	Co-crystal	sulfamoxole, a sulfamide anti-bacterial
NEMSUT / [56]	phenylurea	Co-crystal	urea derivative.
LATSAC / [57]	piperidin-2-one	Co-crystal	heterocycle acting as a hydrogen bond acceptor
IXOZIG02 [58]	2-hydroxypyridinium	Salt	pyridinium derivative acting as a base.
HESXUY [59]	3-Ammoniobenzoic acid	Salt	benzoic acid with amine side group which acts as a base.
GINMOG [60]	2,6-Diamino-5-(2,4-diamino-6-oxo-1,6-dihydropyrimidin-5-ylmethyl)-4-oxopyrimidin-1-ium	Salt	complex heterocycle acting as a base.

5.3 Co-crystals and Molecular Salts of 3,5-Dinitrobenzoic Acid

Dnba formed three salts, four co-crystals and one solvate. The Ortep diagrams of each crystal structure are show below in Fig. 5.3. PXRD patterns of each co-crystal/molecular salt were measured and are available in the Appendix (Figs. A15 – A22) together with the calculated pattern, which confirms the single crystal represent the bulk material in each case.

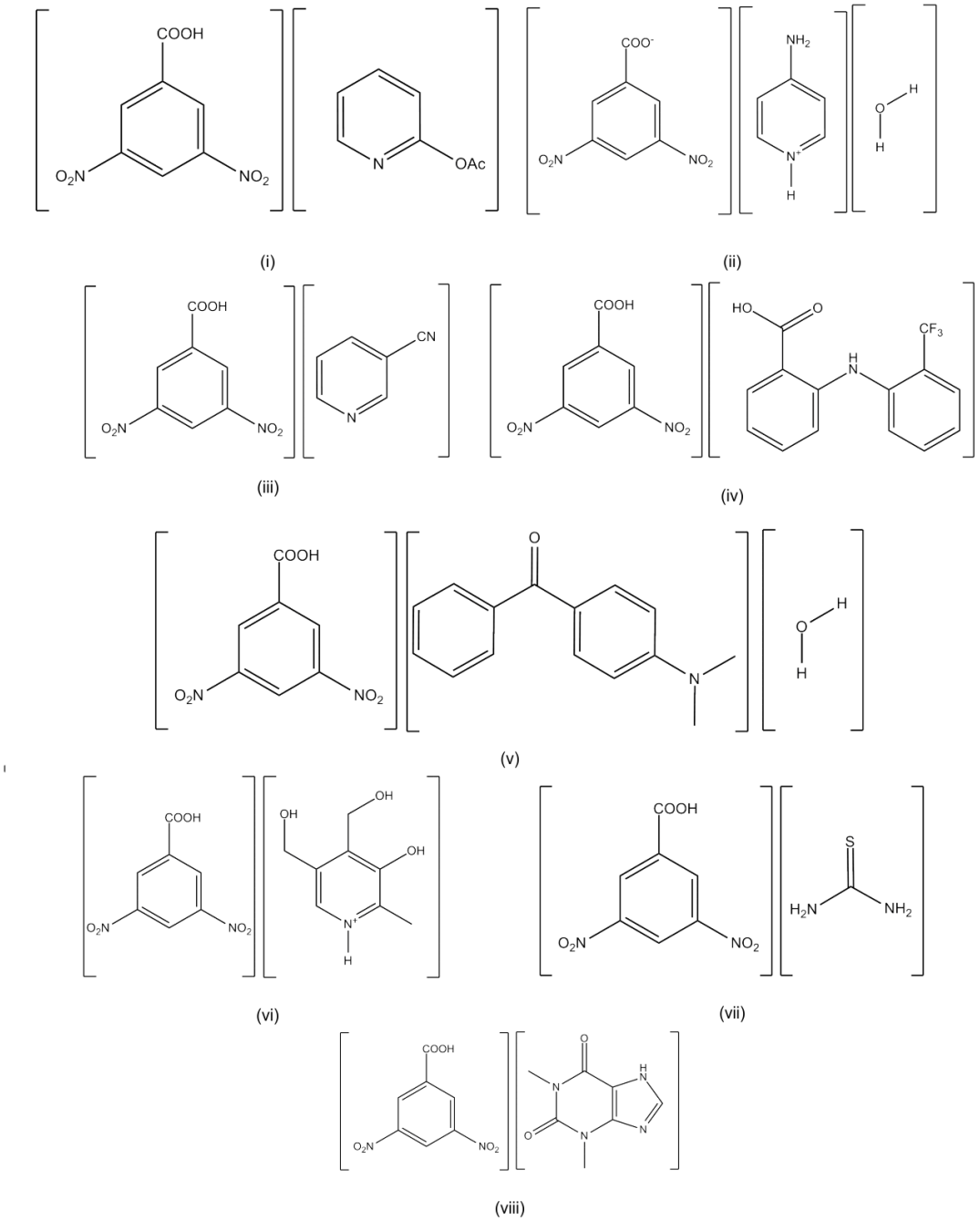

Scheme 5.3 Chemical diagrams for (i) dnbaH + 2OAcp, (ii) dnba(-) + 3apH + water, (iii) dnbaH + 3cnp, (iv) dnbaH + fa, (v) dnbaH + dmabp + water, (vi) dnba(-) + pyd, (vii) dnbaH + thiourea and (viii) dnbaH + thp.

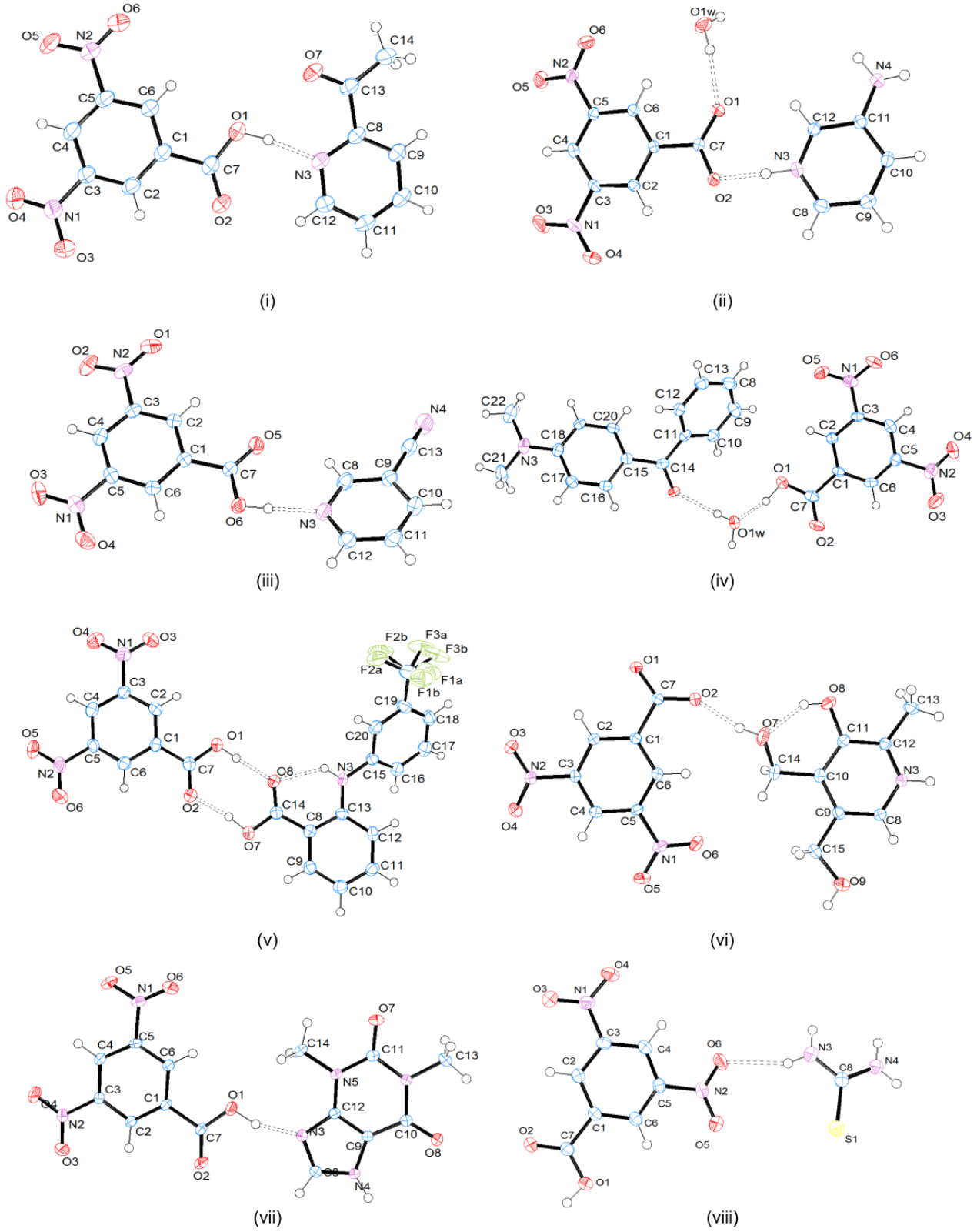

Fig. 5.3 Ortep diagrams showing the numbering scheme of the asymmetric units for (i) dnbaH + 2OAcp, (ii) dnba(-) + 3apH, (iii) dnbaH + 3cnp, (iv) dnbaH + dmabp, (v) dnbaH + fa, (vi) dnba(-) + pyd, (vii) dnbaH + thp and (viii) dnbaH + thiourea.

Table 5.3 Crystal data and structure refinement for co-crystals and molecular salts of dnba

Co-crystal/Salt	**dnbaH + 2OAcp**	**dnbaH + 3cnp**	**dnba(-) + 3apH**	**dnbaH + dmabp**
Empirical formula	$C_{14}H_{11}N_3O_7$	$C_{13}H_8N_4O_6$	$C_{12}H_{12}N_4O_7$	$C_{22}H_{21}N_3O_8$
Formula weight	333.26	316.23	324.26	455.42
Temperature/K	173	173.15	173.15	173.15
Crystal system	monoclinic	monoclinic	monoclinic	monoclinic
Space group	P21/n	P21/c	P21/c	P21/n
a/Å	8.9295(9)	6.1678(3)	8.7922(5)	10.086(3)
b/Å	13.9281(14)	9.2276(5)	7.0559(4)	21.253(6)
c/Å	11.8082(11)	24.0942(13)	22.2560(15)	10.341(3)
α/°	90	90	90	90
β/°	100.347(3)	96.703(2)	91.063(2)	101.293(14)
γ/°	90	90	90	90
Volume/$Å^3$	1444.7(2)	1361.92(12)	1380.46(14)	2173.6(11)
Z	4	4	4	4
ρcalcg/cm^3	1.532	1.542	1.56	1.392
μ/mm^{-1}	0.126	0.126	0.131	0.108
F(000)	688	648	672	952
Crystal size/mm^3	0.512 × 0.248 × 0.248	0.347 × 0.258 × 0.159	0.413 × 0.334 × 0.088	0.223 × 0.072 × 0.044
Radiation	MoKα (λ = 0.71073)	MoKα (λ = 0.71073)	MoKα (λ = 0.71073)	MoKα (λ = 0.71073)
2Θ range for data collection/°	4.566 to 56.922	6.652 to 55.984	5.852 to 56	5.554 to 46.596
Index ranges	-11 ≤ h ≤ 11, -18 ≤ k ≤ 18, -14 ≤ l ≤ 15	-8 ≤ h ≤ 8, -12 ≤ k ≤ 12, -31 ≤ l ≤ 31	-11 ≤ h ≤ 11, -9 ≤ k ≤ 9, -29 ≤ l ≤ 29	-8 ≤ h ≤ 11, -23 ≤ k ≤ 23, -11 ≤ l ≤ 8
Reflections collected	13893	27504	29639	6773
Independent reflections	3638 [Rint = 0.0717, Rsigma = 0.0614]	3286 [Rint = 0.0451, Rsigma = 0.0289]	3325 [Rint = 0.0398, Rsigma = 0.0220]	2901 [Rint = 0.0953, Rsigma = 0.1333]
Data/restraints/parameters	3638/0/222	3286/0/209	3325/0/224	2901/0/309
Goodness-of-fit on F2	1.022	1.037	1.035	0.984
Final R indexes [I>=2σ (I)]	R1 = 0.0553, wR2 = 0.1420	R1 = 0.0473, wR2 = 0.1032	R1 = 0.0417, wR2 = 0.1021	R1 = 0.0640, wR2 = 0.1110
Final R indexes [all data]	R1 = 0.0936, wR2 = 0.1678	R1 = 0.0679, wR2 = 0.1124	R1 = 0.0541, wR2 = 0.1089	R1 = 0.1343, wR2 = 0.1329
Largest diff. peak/hole / e $Å^{-3}$	0.29/-0.23	0.25/-0.25	0.39/-0.28	0.20/-0.25

Table 5.3 (cont.)

Co-crystal/salt	**dnbaH + fa**	**dnbaH + pyd**	**dnba + thp**	**dnbaH + Thiourea**
Empirical formula	$C_{21}H_{14}N_3O_8F_3$	$C_{15}H_{15}N_3O_9$	$C_{14}H_{12}N_6O_8$	$C_8H_8N_4O_6S$
Formula weight	493.35	381.3	392.3	288.24
Temperature/K	173.15	173.15	173.15	173.15
Crystal system	triclinic	monoclinic	monoclinic	monoclinic
Space group	P-1	P21/n	C2/c	P21/c
a/Å	7.6667(4)	9.2152(5)	18.7625(6)	13.0957(2)
b/Å	10.7718(5)	14.1356(7)	15.4699(6)	9.0162(2)
c/Å	13.4392(5)	12.5534(6)	12.6823(4)	9.8594(2)
α/°	70.846(2)	90	90	90
β/°	84.228(2)	104.378(2)	117.917(2)	92.6450(10)
γ/°	88.073(2)	90	90	90
Volume/$Å^3$	1043.11(8)	1584.02(14)	3252.7(2)	1162.89(4)
Z	2	4	8	4
ρcalcg/cm^3	1.571	1.599	1.602	1.646
μ/mm-1	0.139	0.135	0.134	0.31
F(000)	504	792	1616	592
Crystal size/mm^3	0.142 × 0.117 × 0.052	0.215 × 0.436 × 0.080	0.415 × 0.401 × 0.206	0.243 × 0.193 × 0.163
Radiation	MoKα (λ = 0.71073)	MoKα (λ = 0.71073)	MoKα (λ = 0.71073)	MoKα (λ = 0.71073)
2Θ range for data collection/°	3.222 to 50.998	6.296 to 55.984	5.266 to 55.998	3.114 to 55.994
Index ranges	$-9 \le h \le 9$, $-12 \le k \le 13$, $-16 \le l \le 16$	$-12 \le h \le 12$, $-18 \le k \le 18$, $-16 \le l \le 16$	$-24 \le h \le 24$, $-20 \le k \le 20$, $-16 \le l \le 16$	$-17 \le h \le 17$, $-11 \le k \le 11$, $-13 \le l \le 13$
Reflections collected	15916	36275	36969	17130
Independent reflections	3871 [Rint = 0.0746, Rsigma = 0.0776]	3814 [Rint = 0.0344, Rsigma = 0.0172]	3044 [Rint = 0.0357, Rsigma = 0.0219]	2797 [Rint = 0.0506, Rsigma = 0.0393]
Data/restraints/parameters	3871/51/353	3814/0/261	3044/0/256	2797/0/176
Goodness-of-fit on F2	1.098	1.061	1.061	1.014
Final R indexes [I>=2σ (I)]	R1 = 0.0660, wR2 = 0.1413	R1 = 0.0405, wR2 = 0.1108	R1 = 0.0427, wR2 = 0.1186	R1 = 0.0368, wR2 = 0.0819
Final R indexes [all data]	R1 = 0.1308, wR2 = 0.1636	R1 = 0.0521, wR2 = 0.1227	R1 = 0.0501, wR2 = 0.1247	R1 = 0.0616, wR2 = 0.0933
Largest diff. peak/hole / e $Å^{-3}$	0.25/-0.29	0.34/-0.28	0.25/-0.22	0.28/-0.24

5.3.1 DnbaH + 2-acetylpyridine

DnbaH formed a solvate with 2OAcp, forming colourless plates. The solvate crystallises in the $P2_1/n$ space group, with the asymmetric unit consisting of molecule of each dnbaH and 2OAcp. DnbaH forms a discrete hydrogen bond to pyridinium of 2OAcp with the carboxylic acid group, which can be observed in the ortep diagram. This dimer forms 2D sheets which stack together.

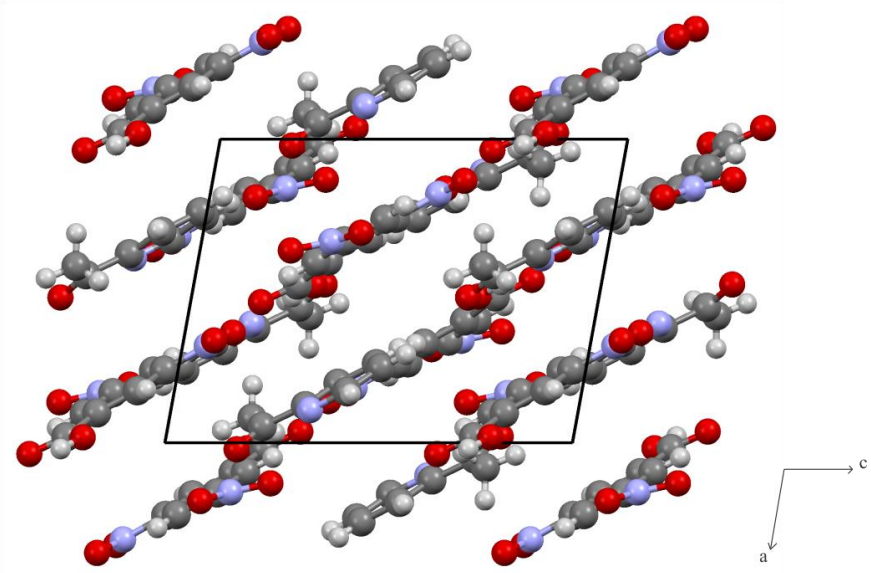

Fig. 5.3.1 The packing diagram of the dnbaH-2OAcp solvate

Table 5.3.1 Hydrogen bond table for the solvate of dnbaH-2OAcp

D-H···A	d(D-H)	d(H···A)	d(D···A)	<(DHA)
O1-H1···N3	0.98(3)	1.73(3)	2.707(2)	171(3)

5.3.2 DnbaH + 3-cyanopyridine

DnbaH formed a co-crystal with 3cnp, forming colourless needles. The co-crystal crystallises in the $P2_1/c$ space group, with the asymmetric unit consisting of molecule of each dnbaH and 3cnp. Dnba forms a discrete hydrogen bond to the pyridinium of 3cnp with the carboxylic acid group, which can be observed in the Ortep diagram. The 3cnp and dnba molecules form alternating columns of each molecule which then stack together with inversion of molecules along its column.

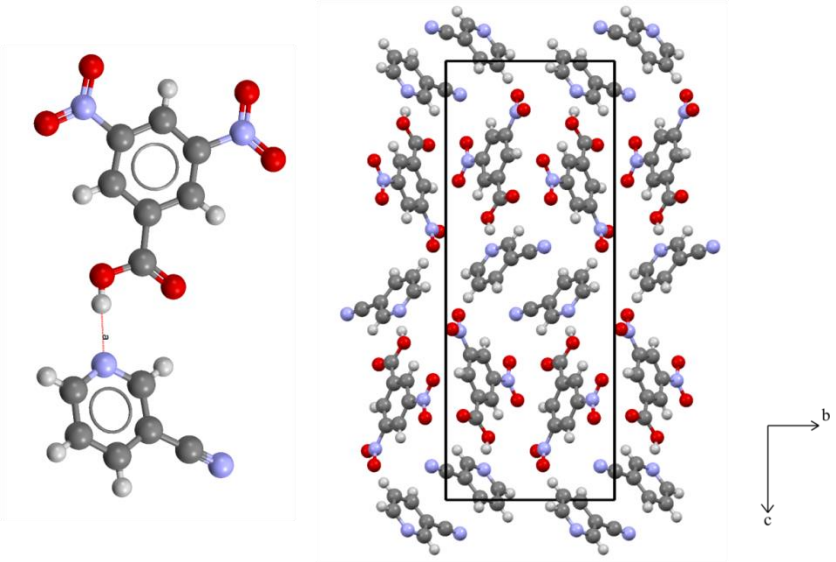

(i) (ii)

Fig 5.3.2 The crystal structure of the dnba-3cnp co-crystal showing (i) the discrete hydrogen bond and (ii) the slight zig-zag packing of the crystal structure.

Table 5.3.2 The Hydrogen bond table for the dnba-3cnp co-crystal.

D-H···A	d(D-H)	d(H···A)	d(D···A)	<(DHA)
O6-H6···N3	0.93(2)	1.74(3)	2.6684(19)	175(2)

5.3.3 Dnba$^{(-)}$ + 3-aminopyridinium

Dnba$^{(-)}$ and 3apH formed a molecular complex which formed small brown block crystals. This molecular complex crystallised in the $P2_1/c$ system with the asymmetric unit consisting of 1 molecule of each 3apH, dnba$^{(-)}$ and water. A proton transfer occurred between the carboxylic acid of dnba$^{(-)}$ to the pyridinium of 3apH. The pyridinium of 3apH acts as a hydrogen bond donor to the carboxylate of dnba$^{(-)}$. Each hydrogen of the amino group of 3apH bonds to either water or the nitro groups of two adjacent dnba$^{(-)}$ molecules. Water acts as another hydrogen bond donor to the carboxylate of two dnba$^{(-)}$ molecule and thus acts as a bridge between the two. This structure has been reported previously by Wei [61].

Attempts to obtain an anhydrous crystalline form through either heating this hydrated form, using other anhydrous solvents when synthesizing the salts or using other crystallization methods have been unsuccessful.

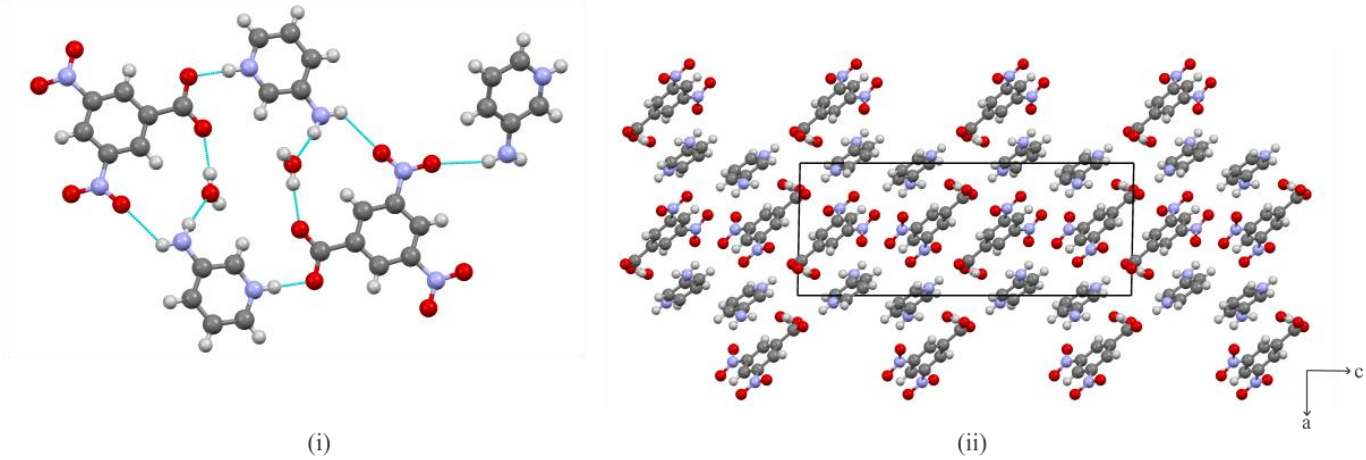

(i) (ii)

Fig. 5.3.3 The crystal structure of the dnba-3AP molecular complex showing (i) some of the possible hydrogen bond interactions and (ii) the packing of the crystal structure.

Table 5.3.3 Hydrogen bond table for $dnba^{(-)}$ + 3apH

D-H···A	d(D-H)	d(H···A)	d(D···A)	<(DHA)
N3-H3···O(2)	0.96(2)	1.65(2)	2.6136(15)	174(2)
N4-H4A···O(6) (i)	0.84(2)	2.49(2)	3.0470(17)	125(17)
N4-H4A···O5 (ii)	0.84(2)	2.44(2)	3.2206(18)	154(18)
N4-H4B···O1W (i)	0.90(2)	2.01(2)	2.9011(18)	168(17)
O1W-H1WA···O2 (iii)	0.85(3)	2.03(3)	2.8573(17)	167(2)
O(1W)-H(1WB)...O(1)	0.84(3)	1.97(3)	2.7991(16)	173(3)

(i) -x+2,-y+2,-z+1 (ii) x+1,-y+3/2,z-1/2 (iii) x,y+1,z

5.3.4. dnba + dimethylaminobenzophenone

DnbaH and dimethylaminobenzophenone (dmabp) formed a molecular complex and crystallised as fragile orange plates. This molecular complex crystallised in the $P2_1/n$ space group with the asymmetric unit consisting of 1 molecule of each dnbaH, dmabp and water. DnbaH, dmabp and water forms part of a dimer, where water acts as the primary hydrogen bond donor and acceptor. In this structure, water forms a bridge between dnba and dmabp by acting as a hydrogen bond acceptor from dnba and as a hydrogen bond donor to dmabp and another water molecule. These dimers form a 2D sheets which stack to form a layered structure.

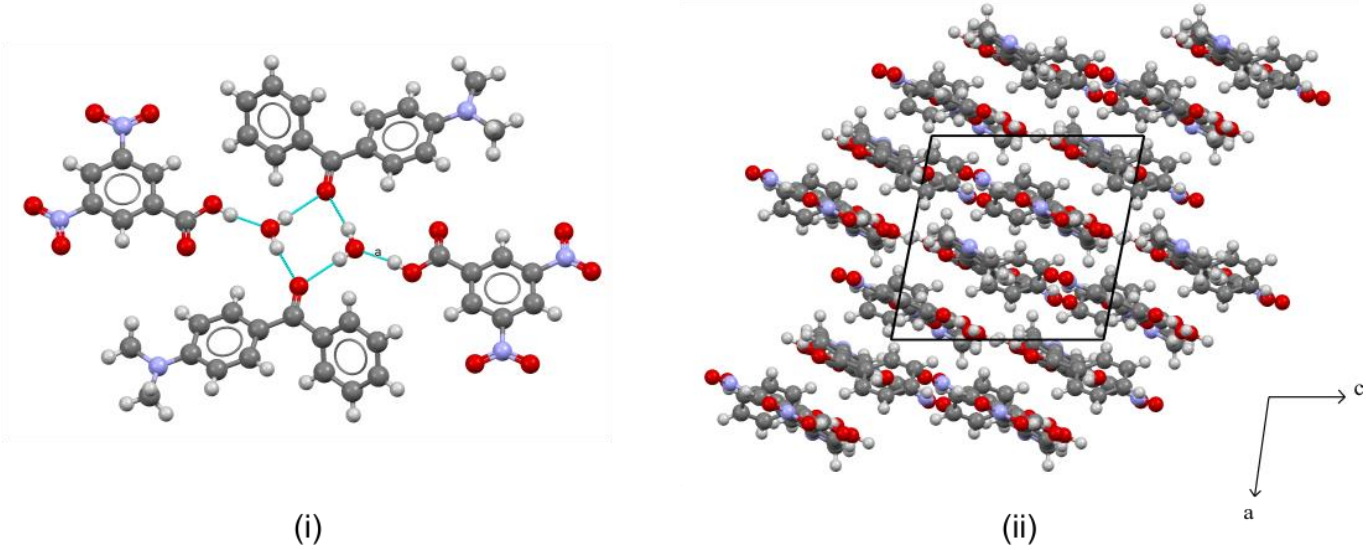

Fig. 5.3.4 The crystal structure of the dnbaH-dmabp molecular complex showing (i) the dimer formed by the "water bridge"and (ii) the layered type packing.

Table 5.3.4 Hydrogen bond table for the molecular complex of dnbaH-dmabp

D-H···A	d(D-H)	d(H···A)	d(D···A)	<(DHA)
O1W-H1WA···O7 (i)	0.92(6)	1.93(6)	2.842(5)	170(5)
O1W-H1WB···O7	0.77(6)	2.02(6)	2.789(5)	180(6)
O1-H2A···O1W	1.01(7)	1.57(6)	2.558(4)	164(6)
O1-H2A···O1W	1.01(7)	1.57(6)	2.558(4)	164(6)

(i) -x+1,-y+1,-z+2

5.3.5. dnba + flufenamic acid

DnbaH formed a co-crystal with fa, which crystallised as fragile orange plate crystals. The co-crystal crystallises in the *P*-1 space group with the asymmetric unit consisting of one molecule of each dnbaH and fa. Rotational disorder is present within the trifluoro group on the fa molecules. Hydrogen bonding exists between the carboxylic acids of both dnbaH and fa which give the $R_2^2(8)$ ring dimer, which can be observed in the Ortep diagram. These dimers stack together in a layered formation.

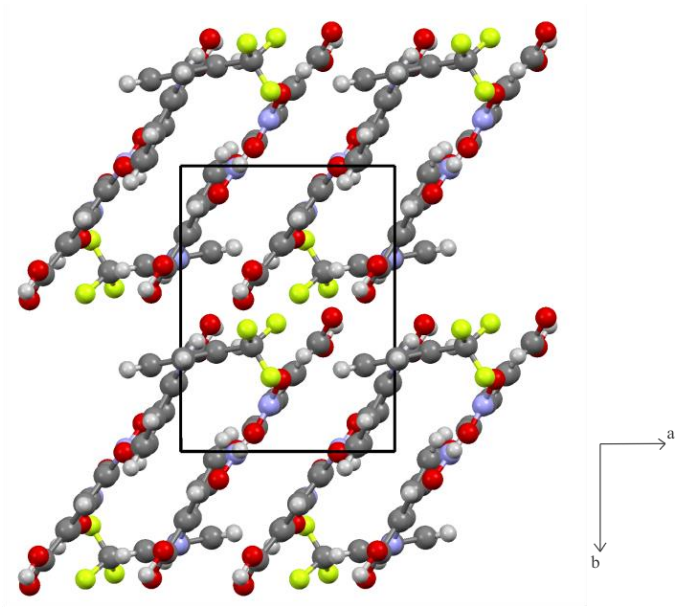

Fig. 5.3.5 Packing diagram of the dnbaH-fa co-crystal.

Table 5.3.5 Hydrogen bond table for the co-crystal of dnbaH-fa

D-H···A	d(D-H)	d(H···A)	d(D···A)	<(DHA)
O1-H1···O8	0.92(5)	1.72(5)	2.625(4)	167(5)
N3-H3···O8	0.82(4)	2.05(4)	2.683(4)	134(4)
O7-H7···O2	1.09(7)	1.56(7)	2.642(4)	167(6)

5.3.6. Dnba$^{(-)}$ + Pyridoxinium

Dnba$^{(-)}$ and pyd formed molecular salts, which crystallised as pale yellow prism crystals. The asymmetric unit consists of a 1:1 mol ratio of Dnba$^{(-)}$ to pyd, crystalizing in the $P2_1/n$ space group. A proton transfer occurred between the carboxylic acid of dnba and the pyridinium of pyd. Dnba(-) and pyd form several different hydrogen bonds that form a continuous 2D lattice, with these lattice stacking on top of each other via $\pi\cdots\pi$ stacking interactions.

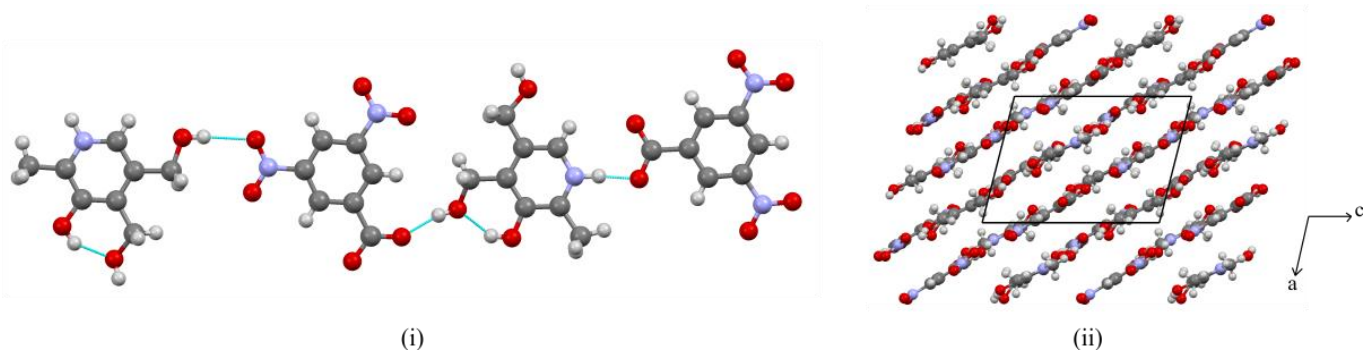

(i) (ii)

Fig. 5.3.6 The crystal structure of the dnba(-)-pyd molecular salt showing (i) the hydrogen bonding present and (ii) the packing consisting of the stacking of its various layers that is present.

Table 5.3.6 Hydrogen bond table for the molecular salt of dnba(-)-pyd

D-H···A	d(D-H)	d(H···A)	d(D···A)	<(DHA)
N3-H3···O1 (i)	0.98(2)	1.65(2)	2.6269(15)	174(2)
N3-H3···O2 (i)	0.98(2)	2.57(2)	3.2529(15)	126(2)
O9-H9···O4 (ii)	0.88(3)	2.15(3)	3.0239(17)	175(2)
O7-H7···O2	0.87(3)	1.76(3)	2.6019(15)	162(2)
O8-H8···O7	0.86(3)	1.80(3)	2.5685(17)	147(3)

(i) x-1/2,-y+1/2,z+1/2; (ii) x-1/2,-y+3/2,z+1/2

5.3.7. Dnba + Theophylline

DnbaH formed a co-crystal with thp, which crystallised as colourless blocks. The asymmetric unit consists of a 1:1 mol ratio of dnbaH to thp, crystalizing in the $C21/n$ space group. DnbaH forms a discrete hydrogen bond between the carboxylic acid O1-H1 to nitrogen N3 of thp, with a bond length of 1.01Å. This long bond length is indicative of the strong basicity of thp (pK_a=8.60 [62]), in which dnbaH is on the verge of a proton transfer occurring to thp. Thp forms part of a dimer held together by two molecules of THP forming a ring between N4-H8···O(8), with ring graph set of $R_2^2(10)$.

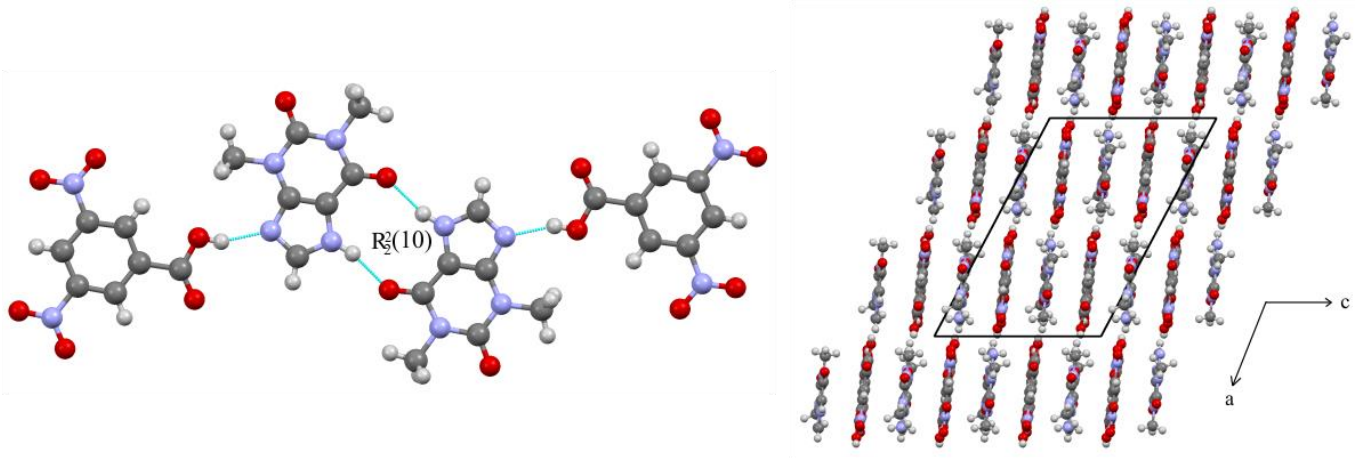

(i) (ii)

Fig. 5.3.7 The crystal structure of dnbaH-thp showing (i) the hydrogen bonded dimers with graph set of $R_2^2(10)$ and (ii) the packing of dnbaH-thp.

Table 5.3.7 Hydrogen bond table for the co-crystal of dnba-THP

D-H···A	d(D-H)	d(H···A)	d(D···A)	<(DHA)
N4-H4···O8 (i)	0.98(3)	1.76(3)	2.7264(16)	172(2)
O1-H1···N3	1.01(3)	1.66(3)	2.6264(15)	160(3)

(i) -x+3/2,-y+3/2,-z+1

5.3.8 Dnba + Thiourea

DnbaH formed a co-crystal with thiourea and crystallised as pale yellow blocks. This co-crystal crystallises in the $P2_1/c$ group with the asymmetric unit consisting of one molecule of each dnbaH and thiourea. In contrast to the previous co-crystals of the chlorobenzoic acids with urea, the dnbaH-thiourea co-crystal did not form a similar thioamide-carboxylic acid ring heterosynthon like the amide-carboxylic acid heterosynthons observed in the chlorobenzoic acid-urea co-crystals. Instead, dnbaH formed the carboxylic acid ring homosynthon instead, while thiourea formed a discrete hydrogen bond with one of the nitro groups instead. This leaves the nitro groups to readily accept the thiourea as a hydrogen bond pair acceptor. The dnba dimers form 1D columns, which stack together, with stack being linked by thiourea.

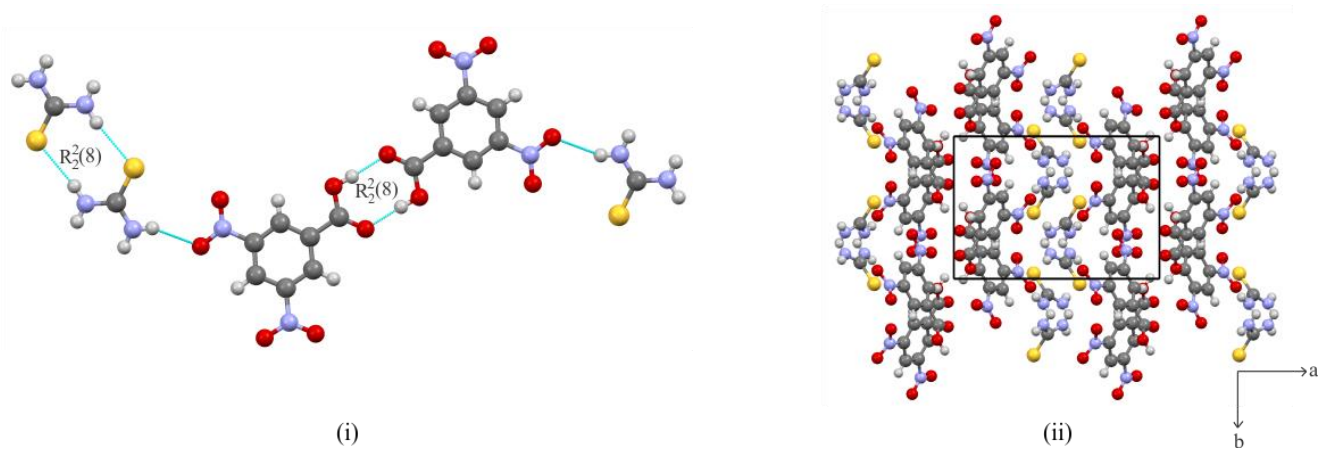

Fig. 5.3.8 The crystal structure of dnbaH-thiourea showing the (i) dnbaH dimers with thiourea forming discrete hydrogen bonding to the nitro groups and (ii) the 1D columns of dnbaH with channels of thiourea separating these columns.

Table 5.3.8 Hydrogen bond table for the co-crystal dnbaH-thiourea

D-H···A	**d(D-H)**	**d(H···A)**	**d(D···A)**	**<(DHA)**
N4-H4B···S1 (i)	0.89(2)	2.49(2)	3.3773(18)	173(2)
N3-H3A···O6	0.82(2)	2.39(2)	3.108(2)	146(2)
N4-H4A···S1 (ii)	0.85(2)	2.66(2)	3.4502(19)	157(2)
N3-H3B···S1 (ii)	0.89(2)	2.66(3)	3.470(2)	152(2)
O1-H1···O2 (iii)	0.88(3)	1.77(3)	2.6524(18)	176(3)
N4-H4B···S1 (i)	0.89(2)	2.49(2)	3.3773(18)	173(2)

(i) -x+1,-y+1,-z; (ii) -x+1,y+1/2,-z+1/2 (iii) -x+2,-y,-z+2

6. Comparison of nitrobenzoic acid Co-crystals and Salts

6.1 Introduction

One of the goals of crystal engineering is to develop materials with new or improved properties. In order to do so, insight into currently known materials is necessary. Therefore it would be important to make comparisons between structural similar compounds in order to gain some insight into the co-crystals and salts presented. Although a series of co-crystals/salts were attempted to be made, for example a series of aminopyridines for each of the nitrobenzoic acids, these co-crystals/salts did not form and precipitated out separately. However, where possible, a comparison can still be made by using the CSD to fill in "missing gaps", as well as comparing structurally similar co-formers that weren't considered for this work.

6.2 Comparison of aminopyridines in nitrobenzoic structures

The aminopyridines formed salts with each of the respective nitrobenzoic acids. The amine group acts a strong electron withdrawing group on the pyridine ring, which in turn makes the lone pair on the pyridine ring a stronger proton acceptor. In addition, the amino group acts a strong hydrogen bond donator, which forms hydrogen bonds with their respective hydrogen bond acceptors, which in the case of the nitrobenzoates, is the carboxylate group. The different positions of the amino group on pyridine would be expected to give different hydrogen bonding networks. For example, 2-aminopyridine can form a $R_2^2(8)$ type synthon as seen in Scheme 6.2.1. This distinguishes 2-aminoprydinium from the 3 and 4-aminopyridiums, which the latter cannot possibly form.

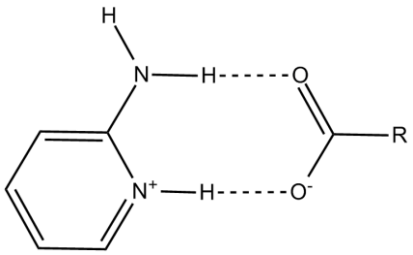

Scheme 6.2.1 The $R_2^2(8)$ that forms with 2-aminopyridinium and the respective nitrobenzoate.

For the purpose of the rest of this discussion, the following nitrobenzoate-aminopyridinium salts tabulated in Table 6.2.1 will be used. These also include aminopyridines with additional functional groups on the ring.

Table 6.2.1 List of aminopyridiniums and nitrobenzoates used for comparisons

Nitrobenzoate	Aminopyridinium	Reference (if not from this work)
4-nitrobenzoate	2-aminopyridium	[-62]
4-nitrobenzoate	4-aminopyridium	
4-nitrobenzoate	2-amino-4-methylpyridinium	[64]
4-nitrobenzoate	2-amino-5-bromopyridinium	
2-chloro-4-nitrobenzoate	2-aminopyridium	

2-chloro-4-nitrobenzoate	3-aminopyridium	
2-chloro-4-nitrobenzoate	4-aminopyridium	[42]
2-chloro-5-nitrobenzoate	4-aminopyridium	
3,5-dinitrobenzoate	3-aminopyridium*	

* This salt crystallises as a hydrate

6.2.1. Comparisons of nitrobenzoates with 2-aminopyridinium

For both 4nba(-) and 2c4n(-) a salt formed with 2-apH. The acidic proton from the carboxylic acid of the nitrobenzoic acids transferred to the nitrogen of the pyridine, forming the salt. Due to the position of the amino group, the synthon shown in Scheme 6.2.1 formed in each case. However, discrepancies between the different structures do indeed occur. For example, one difference between 4nba and 2c4n is the presence of the chlorine atom. One would expect that if the chlorine is not involved directly with the hydrogen bonding between the carboxylate and pyridinium then you would expect the same hydrogen bonding motifs to occur. However, this does not occur: the 2c4n(-)-2apH forms tetramers while the $4nba^{(-)}$-2apH forms long polymeric chains with fork-like interactions. The chlorines in 2c4n(-)-2apH do interact with each other via halogen bonding but not with the carboxylate-pyridinium interaction. This gives two completely different structures as opposed to two similar structures.

6.2.2 Comparisons of nitrobenzoates with 3-aminopyridinium and 4-aminopyridinium

It would be expected that salts containing nitrobenzoates with 3-aminopyridinium and 4-amino-pyridinium would give different results than 2-aminopyridinium. This is primarily due to the fact that synthon in Scheme 6.2.1 would not form. This should give salts involving 3-aminopyridinium and 4-amino-pyridinium more freedom of possible hydrogen bonding motifs. This is true for the pair of nitrobenzoates that did form salts with 3-aminopyridinium, for example $2c4n^{(-)}$-3apH formed tetramers while dnba(-)-3apH formed a hydrate complex. The structure of 4nba(-)-4apH for example, consists of 2 molecules of 4nba (one ionised, one neutral) that have a proton exchange occur between these two molecules in the presence of 4apH, which has not been observed in the other crystal structures. Even comparing other salts containing 3-aminopyridinium and 4-aminopyridinium there appears to be no distinct pattern for hydrogen bonding, giving rise to a great amount of diversity of differing hydrogen bonded networks.

6.3. Nitrobenzoic Acids and Urea/Thiourea co-crystals

2c4n and 2c5n both formed co-crystals with urea, while dnba formed a co-crystal with thiourea. For both 2c4n and 2c5n, the amide-carboxylic acid ring heterosynthon (Scheme 6.3.) formed. Although only three of the possible eight co-crystals with urea and thiourea formed, several co-crystals involving urea with other various benzoic acids have been reported in the literature. For this section, co-crystals involving urea and benzoic acids are compared to determine if there are any general trends or preferred synthons that form.

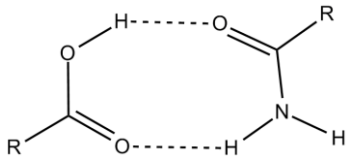

Scheme 6.3 The ring $R_2^2(8)$ synthon observed in co-crystal involving nitrobenzoic acid and urea.

Table 6.3 The co-crystals involving urea/thiourea with various nitrobenzoic acids listed with their ΔpK_a*'s*

Benzoic Acid	**Urea/Thiourea**	**Reference (if not from this work)**
2-chloro-4-nitrobenzoic acid	Urea	
2-chloro-5-nitrobenzoic acid	Urea	
3,5-Dinitrobenzoic Acid	Thiourea	
2-nitrobenzoic acid	Urea	[65]
3-nitrobenzoic acid	Urea	[65]
5-nitrosalicylic acid	Urea	[66]
3,5-dinitrosalicylic acid	Urea	[66]
4-aminobenzoic acid	Urea	[66]
Salicylic acid	Urea	[67]
3-methoxy-4-hydroxybenzoic acid (Vanillic Acid)	Urea	[68]

In each case, the benzoic acid formed a co-crystal with each urea and thiourea respectively. In most of the cases the carboxylic acid forms the heterosynthon observed in Scheme 6.3. In these cases the amide not involved with the amide-carboxylic acid heterosynthon can acts as an additional hydrogen bond donor, bonding to any additional hydrogen bond acceptors. However, this heterosynthon is not observed in all of the cases. For example, vanillic acid forms a ring homosynthon of two of the carboxylic molecules while urea forms hydrogen bonds with the hydroxyl and a discrete hydrogen bond to one of the oxygen atoms of the carboxylic acid. This is a similar type of hydrogen bond interaction that was observed for the dnbaH-thiourea co-crystal. Overall, there is no absolute type of hydrogen bond network that forms for benzoic acid-urea co-crystals.

6.4. Nitrobenzoic Acids and pyridoxinium salts

Pyd is a relatively strong organic base, with a pK_a of 9.63; pyd will favour the formation of a salt in most cases. It consists of three hydroxyl groups which could acts as potential hydrogen bond donors or hydrogen bond acceptors with the nitrogen acting as a fourth hydrogen bond donor in the case of the salt. The hydroxyl group on the 3' position forms a hydrogen bond to the hydroxyl on the 4' position, which effectively restricts the freedom of rotation of the 4' hydroxyl group. It was expected that for the benzoate

the carboxylate should form a hydrogen bond to the hydrogen of the pyridinium ring. The salts of pyd(-) with 2c4n(-), 2c5n(-) and dnba(-) are compared with each other and other benzoates

Table 6.4 Various nitrobenzoates used to compare the various pyridoxinium molecular salts

Benzoate	**Reference (if not from this work)**
2-chloro-4-nitrobenzoate	
2-chloro-5-nitrobenzoate	
3,5-dinitrobenzoates	
4-cyanobenzoate	[68]
4-aminobenzoate	[68]
4-nitrobenzoate	[68]

In each of these cases, the carboxylate is hydrogen bonding to the hydrogen of the pyridinium ring; as well the intramolecular hydrogen bond formed between the 3' and 4' hydroxyl groups. In addition, these hydroxyl groups tend to form hydrogen bonds to the carboxylate. The only differences that may occur may be is due to the additional different functional groups that occur on the benzoate of question. For example the nitro group acts as a hydrogen bond acceptor while the amino group as a hydrogen bond acceptor. This will cause different hydrogen bonded networks to occur. Overall, there is some form of a general trend that occurs between pyridoxinium and benzoic acids, although more examples in the literature may be required to confirm this.

7. Successful (and Failed Attempts) at Co-crystals and Salts

7.1 Introduction

Not all co-crystals or salts form according to plan. Despite the numerous successes and increasing number of co-crystals and salts being formed and published, the methods and means for predicting and forming said co-crystals and salts is still largely trial and error.

Therefore, for the purpose of this chapter analysis of each method for choosing appropriate co-formers for each nitrobenzoic acid is evaluated for its strengths and weaknesses. This includes an attempt to account for the reason why certain co-crystals or salts did not form, despite reasons stating otherwise.

7.2 Analysis of use of synthons

The planning and use of synthons have been beneficial to the formation of new co-crystals and salts. The particular focus on the carboxylic acid group of each of the nitrobenzoic acids, has led to finding suitable co-formers. For example, the pyridines formed co-crystals and salts with the synthon that appears in the top row of synthons in Scheme 1.2.2. Other synthons such as the hetrosynthon between the amide and carboxylic acid (Scheme 6.3.) also appeared. However, the nitro group of the nitrobenzoic acids across the co-crystals/salts did not feature much interaction. One plausible reason for this is that the hydrogen bond donors on some of the co-formers were involved with the carboxylic acid such that it would have been sterically unable to form suitable hydrogen bonds with the nitro group. Overall the synthons used led to successful co-crystals/salts.

7.3 Analysis of pK_a rule

The pK_a difference rule has been a useful tool in the prediction of co-crystal-salt formation. However, an analysis on whether it is accurate or reliable needs to be accessed in terms of this project. Below in Table 7.2 the co-crystals/molecular salts of the various nitrobenzoic acids with co-formers with ionisable salts are listed, along with their calculated pK_a's and the respective distances. Note that some co-formers were left out due to either the lack of ionisable sites, varying pK_a's (the pK_a of urea depends on the pH, for example) or no reliable data exists.

Table 7.2 Listing of the pK_a's of the nitrobenzoic acids with their co-formers that contain ionisable sites, along with their predicted and actual result used for this dissertation. pK_a values obtained are calculated from Scifinder database [62].

Nitrobenzoic acid	pK_a of Nitrobenzoic Acid	Co-former	pK_a of co-former	ΔpK_a	Predicted structure	Actual Result
4nba	3.42	4apH	9.26	5.84	Salt	Salt
4nba	3.42	imd	7.18	10.47	Salt	Salt
4nba	3.42	2A3OHP	5.15	1.73	Undetermined	Salt
4nba	2.22	2a5BrpH	2.73	0.51	Undetermined	Salt
2c4n	2.04	2ap	6.67	4.63	Salt	Salt
2c4n	2.04	3ap	6.16	4.12	Salt	Salt
2c4n	2.04	pyd	9.63	7.59	Salt	Salt

2c5n	2.22	3cnp	1.78	-0.44	Co-crystal	Co-crystal
2c5n	2.22	4ap	9.26	7.04	Salt	Salt
2c5n	2.22	Pyd	9.63	7.41	Salt	Salt
dnba	2.77	Pyd	9.63	6.86	Salt	Salt
dnba	2.77	2OAcp	3.00	0.23	Undetermined	Co-crystal
dnba	2.77	3cnp	1.78	-0.99	Co-crystal	Co-crystal
dnba	2.77	3ap	6.16	3.39	Salt	Salt
dnba	2.77	thp	8.60	5.83	Salt	Co-crystal

From the table above, the correlation between the predicted result and the actual result is rather accurate. Results where the ΔpK_a can be predicted (i.e. either below 0 or above 2-3) did give the predicted result. In the case where the result was in the intermediate region (ΔpK_a is between 0 and 3), no clear distinction could be made, and either resulted in a co-crystal or molecular salt. This indicates that the pK_a rule could be useful in the design of co-crystal and molecular salts, although it should not be relied on entirely since other factors such as thermal stability, kinetics, solvent etc. should still be considered, such as the case with the dnbaH-thp co-crystal.

7.4 Lack of co-crystals and/or salts

It should be noted that despite 60 possible co-crystals/salts that could form, only 21 have been synthesised. Despite several different approaches to selecting suitable co-formers for multi-component crystals, the formation of multi-components crystals is not guaranteed. Several different reasons for the lack of formation of multi-component exist, which could range from solubility to the choice of supramolecular synthons. For example, a study by Wahl et al. [69] explored the possibility of forming co-crystals consisting of a series of cyclotriphosphazenes derivatives. The cyclotriphosphazenes showed potential to either form strong supramolecular synthons and/or have awkward shapes to allow for co-crystal formation. However, despite a co-crystal screen of 300 experiments on 12 derivatives, only one co-crystal formed. Although no clear conclusion was given, several possible reasons were given: favour of homosyntons over their heterosynthon equivalents, favour of polymorph formation over co-crystal formation, size of co-formers vs. host molecule. This type of study shows that the search for multi-component crystals is not trivial as it may appear.

8. Thermal Studies

8.1 Differential Scanning Calorimetry

Differential scanning calorimetry (DSC) is a powerful tool used to determine phase transitions. This includes the temperature at which a phase transition occurs as well as the energy involved. DSC scans were done on the co-crystals and molecular salts. Samples were heated to temperatures between 250-350 °C, then cooled to -40 °C and heated back to 250-350 °C twice before being heated back to 25 °C, all at a heating/cooling rate of 10 °C. This was done to all samples to ensure that no solvent/co-formers were present in the sample. In almost all the scans, melting were followed by a decomposition of the crystal with no further significant events occurring, (Type I). However, some of the co-crystals and molecular salts showed cycles of melting and recrystallization, indicating a potential reversibility (Type II). Table 8 below summarises all the melting points and their associated energies.

The only exception to these cases was the molecular complex of dnba$^{(-)}$-3apH. In this case, two endothermic peaks were observed before the sample decomposed after the second endothermic peak. The first peak is associated with a potential dehydration. Under heating the sample in paratone oil via hot stage microscopy, bubbles were observed, indicating a potential dehydration. Eventually the sample melted and decomposed and no further significant heating events occurred. Attempts to obtain the potential anhydrous form were fruitless, since the crystals obtained after heating to the first peak (but before complete melting) diffracted poorly, and thus reliable data could not be collected.

From the melting points for the various co-crystals and molecular salts it can be concluded that the formation of co-crystals and molecular salts has led to the development of new properties. Indeed, the melting points of these co-crystals/salts are different with respect to the co-formers. For example, the melting point of 2a3opP and 4nbaH is between 168 – 172 °C and 237 °C respectively, while the melting range of the salt is 221-228 °C. This change in properties highlights the significance of crystal engineering of materials especially with respect to pharmaceuticals.

Table 8 Summary of the type of DSC curves and melting points/phase transitions of the co-crystals/molecular salts investigated in this dissertation.

Co-crystal/ Molecular Salt	DSC Curve Type (I/II)	Onset /°C	Peak /°C	Heat of Fusion ΔH_{fus} /J.g^{-1}
4nba(-) + imd	I	187.2	190.6	27.2
4nba(-) + 4ap	I	221.3	228.6	55.5
4nba(-) + 2a3hpH	I	218.9	227.9	138.2
4nbaH + Cinnamic Acid	I	178.8	182.9	45.8
4nba(-) + 2a5BrpH	I	173.0	176.4	78.6
2c4n(-) + 2apH	I	163.2	165.6	137.5
2c4n(-) + 3apH	I	161.9	166.5	34.0
2c4nH + cinnamic Acid	II	140.3	148.7	39.7
2c4n(-) + pyd	I	168.1	173.2	48.3
2c4nH + urea	I	105.5	107.6	277.0

2c4nH + fa	I	136.5	140.1	104.7
2c5nH + 3cnp	I	105.9	111.2	106.2
2c5n(-) + 4ap	I	161.3	167.1	114.1
2c5nH + urea	I	157.3	163.2	165.1
2c5n(-) + pyd	I	152.0	155.5	54.4
DnbaH + thp	II	194.2	203.9	128.5
Dnba(-) + pyd	I	161.6	168.5	70.4
DnbaH + 2OAcp	I	76.8	80.9	96.4
Dnba(-) + 3apH (1st peak, possible dehydration)	N/A	118.4	128.13	128.2
Dnba(-) + 3ap (2nd peak, melting/decomposition)	N/A	146.9	151.9	103.8
DnbaH + 3cnp	I	134.4	135.6	204.3
DnbaH + dmabp	I	86.8	93.0	91.8
DnbaH + fa	I	136.8	141.0	111.2
DnbaH + Thiourea	I	153.2	156.3	179.5

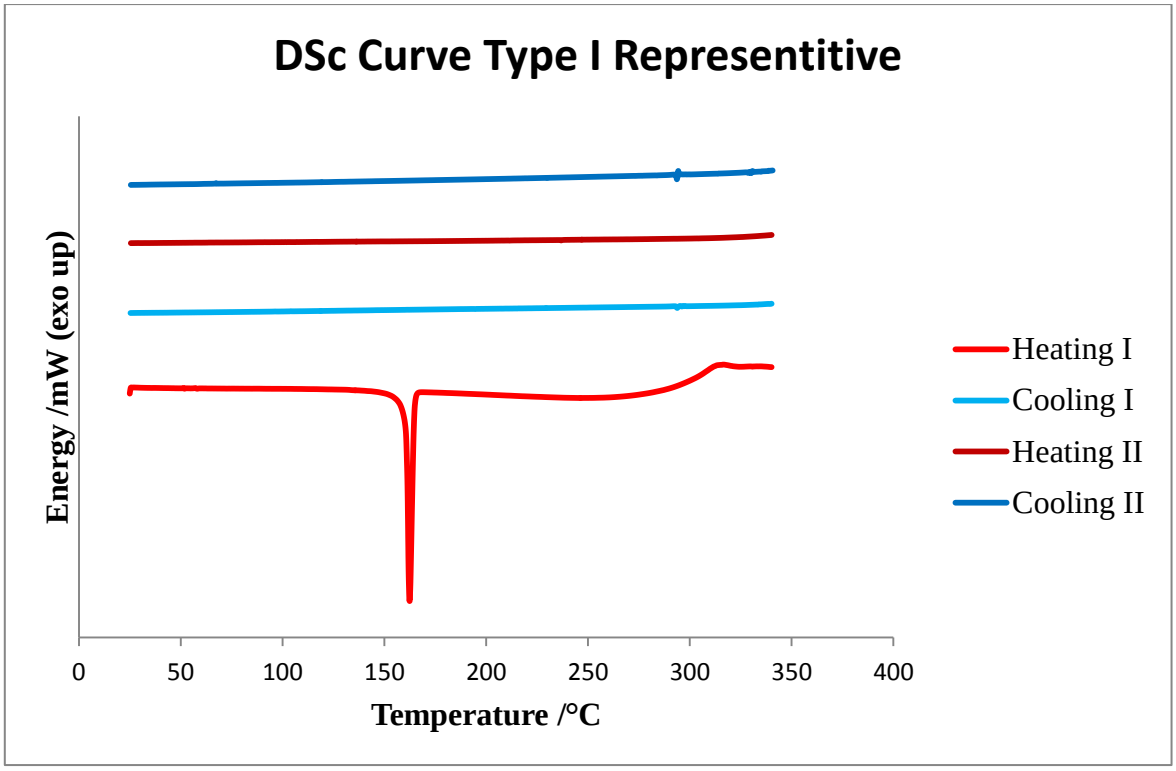

Figure 8.1.1 The representative curve for Type I behaviour observed among co-crystals/salts.

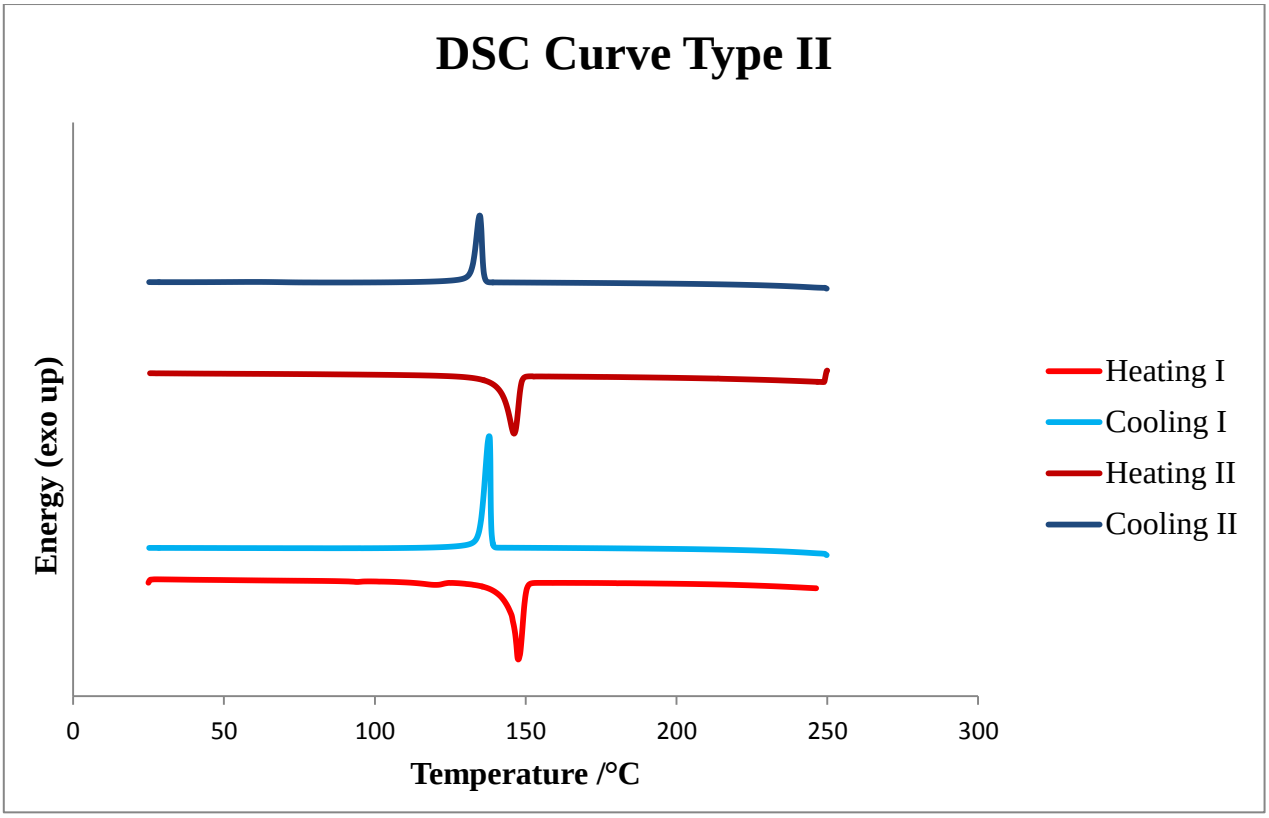

Figure 8.1.2 The representative curve for Type II behaviour observed among co-crystals/salts.

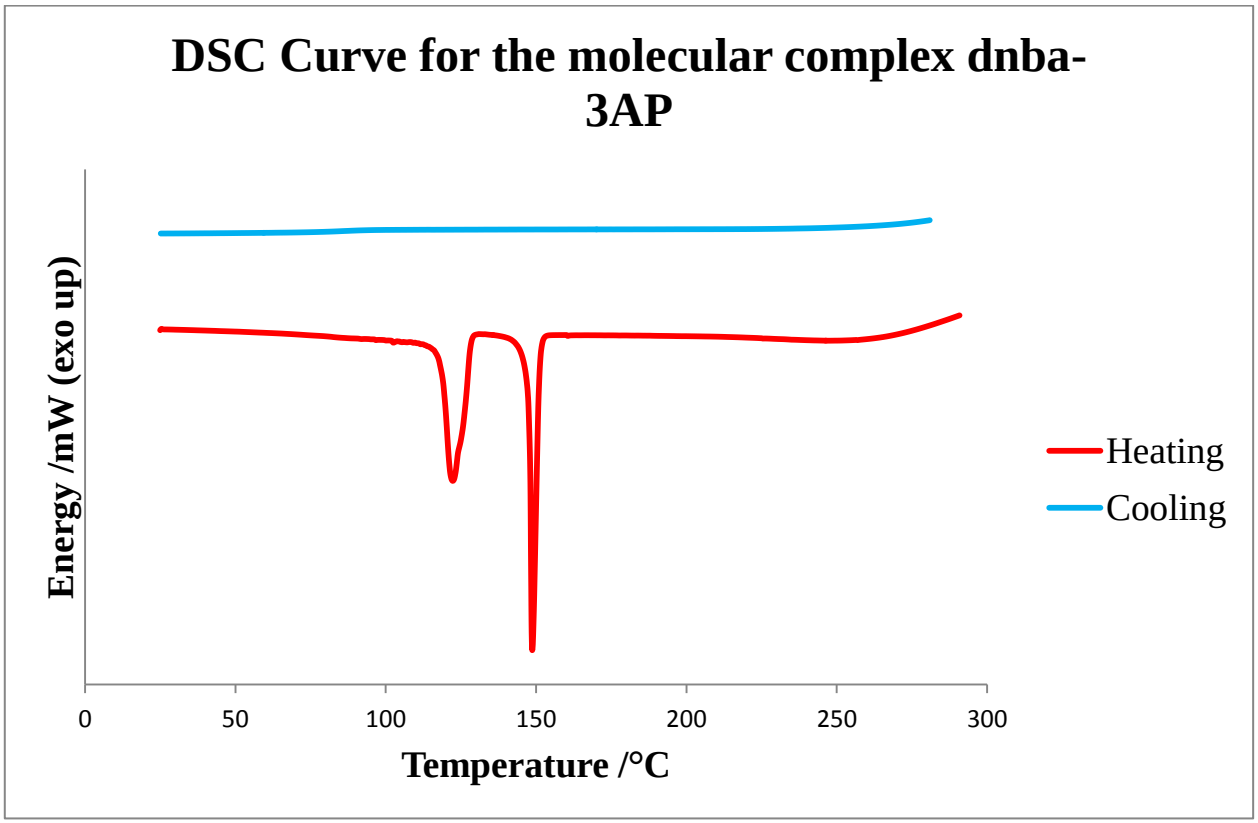

Figure 8.1.3 The DSC curve for dnba(-)-3apH

8.2 Thermal Gravimetric Analysis

A TGA curve for the molecular salt of dnba$^{(-)}$-3apH was obtained. Only the TGA for this salt was obtained since it is necessary to determine whether the 1st peak obtained was due to a possible dehydration or some other possible phase change. The TGA shows two significant thermal events – one occurring in the 118-128 °C range and one between the 130 – 400 °C range. The first thermal peak, which also corresponds to the 1st peak observed in the DSC curve, showed a weight loss of 5.75% after heating, which corresponds closely to the weight percent of water in the molecular salt. This implies that the molecular salt did undergo dehydration. The remaining weight loss is due to the decomposition of the remaining sample.

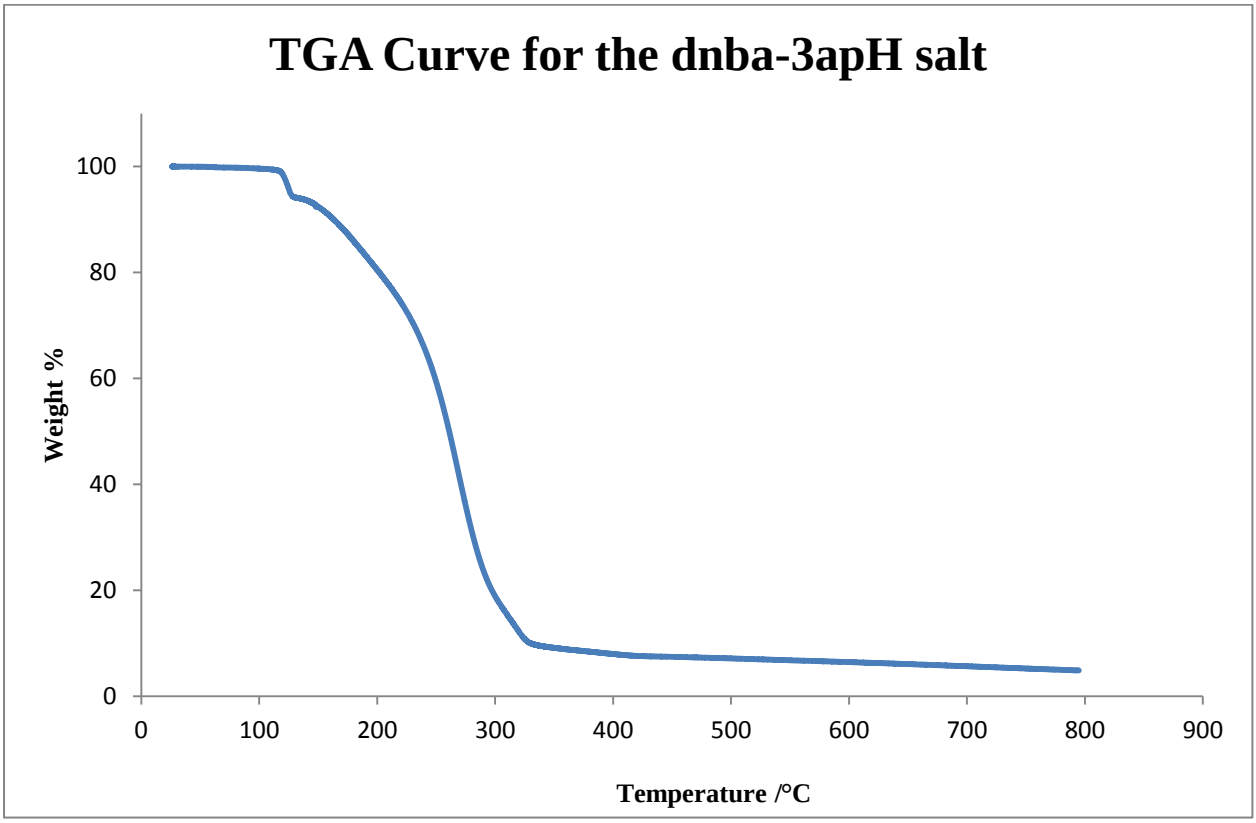

Figure 8.2 The TGA curve obtained for the molecular salt of the dnba$^{(-)}$-3apH. The starting mass of the sample used to obtain this particular curve was 9.566 mg.

9. Conclusion

9.1 Concluding Remarks

22 different co-crystals and molecular salts were synthesised, and their structures were determined by SC-XRD. DSC scans show these co-crystals/molecular salts have different properties in comparison to their co-formers. Although most of these crystal systems followed some of the predicted synthons, for example the 2c4nH and dnbaH with fa, which formed the expected ring carboxylic acid synthon (presented in Fig. 1.2.1). Some of the crystal systems showed different interactions and/or included additional molecules (i.e. hydrates). For example, in the dnbaH + dmabp complex it was expected that the dnbaH molecule to hydrogen bond discretely towards the oxygen of the dmabp but instead the water bridge formed. Overall the nitrobenzoic acids show great potential in the design and synthesis of new co-crystals and salts, which can be used to circumvent problematic properties of both old and new drugs.

9.2 Future Work

One of the goals of crystal engineering is to improve the physical properties of existing solids. In this study only one property was studied, the melting point. Other properties such as solubility were mentioned in this work, but these properties were not investigated into. Therefore it would be useful to explore these properties in other work, as this will prove the usefulness of crystal engineering with respect to improving the physical properties of pharmaceutical drugs with poor physical properties.

In addition it would prove to be useful to investigate forming multicomponent crystals using other compounds. These compounds could be part of the same class of compounds, for example mefenamic acid and tolfenamic acid are structurally similar to flufenamic acid, and could potentially form co-crystals in a similar way. In addition, it would prove useful to investigate forming multi-component crystals with other drugs that possess structural features that are similar to the ones shown in this work. This would show the versatility of using these nitrobenzoic in search of new multi-component crystals.

10. References

[1] https://www.pharmaceutical-technology.com/features/worlds-biggest-pharmaceutical-companies-2018/, Date of Access: 15 April 2019

[2] Patrick G.L., *An Introduction to Medicinal Chemistry*; Oxford University Press: United Kingdom, 2013

[3] B. Moulton, M.J. Zaworotko, *Chem. Rev.*2001 , **101**, 1629-1658.

[4] Arunan E., Desiraju G., Klein R.A. , Sadlej J., Scheiner S.,Alkorta I., Clary D.C., Crabtree R.H., Dannenberg J.J., Hobza Prgaard H.G., Legon A.C., Mennucci B., Nesbitt D.J., *Pure Appl. Chem.*, 2011, **83**, 1637–1641

[5] Steiner T., *Angew. Chem. Int. Ed.*, 2002, **41**, 48-7.

[6] Aakeröy C.B., Seddon K.R., *Chem. Soc. Rev.*, 1993, **22**, 397-407

[7] Fuller W., *J. Phys. Chem.*, 1959, **63**, 1705–1717

[8] Etter M.C., MacDonald J.C., Berstein J., *Acta Cryst.* 1990, **B46,** 256-262

[9] J. Lehn, *Angew Chem. Int Ed.,* 1988, **27,** 89-112.

[10] G.R. Desiraju, *Angew Chem. Int Ed*, 1995, **34**, 2311-2327

[11] Desiraju G.R., *Nature*, 2002, **1**, 77-79

[12] Mangin D., Puel F., Veesler S., Organic Process Research & Development, 2009, **13**, 1241–1253

[13] B.S. Sekhon, *Ars Pharm*, 2009, **50**, 99-117

[14] S.K. Nechipadappu, V. Tekuri, D. R. Trivedi, *Journal of Pharmaceutical Sciences*, **106** 2017, 1384-1390

[15] Rossini E., Netz R.R. , Knapp E., *J.Chem. Theory Comput*. 2016, **12**, 3360−3369

[16] A.J. Cruz-Cabeza, *CrystEngComm*, 2012, **14**, 6362–6365

[17] Lemmerer A., Govindraju S., Johnston M., Motloung X., Savig K.L., *Cryst Eng Comm*, 2015, **17** , 3591–3595

[18] F.H. Allen, C.A. Baalham, J. P. M. Lommerse, P. R. Raithby, E. Sparr, *Acta Cryst.* 1997, **B53**, 1017-1024

[19] Bruker, *SAINT+, version 6.02 (including XPREP), Bruker AXS Inc., Madison, WI, USA*, 1999. A.J. Cruz-Cabeza, *CrystEngComm*, 2012, **14**, 6362–6365

[20] G. M. Sheldrick, *SHELX, release 97-2 (includes SHELXS and SHELXL), University of Göttingen*, 1997.

[21] L. Farrugia, *Journal of Applied Crystallography*, 1997, **30**, 565.

[22] Mercury: visualization and analysis of crystal structures, C. F. Macrae, P. R. Edgington, P. McCabe, E. Pidcock, G. P. Shields, R. Taylor, M. Towler, J. van de Streek, *J. Appl. Cryst.*, 2006, **39**, 453-457

[23] S. Shakoor, T. Ahsan, K. Jabeen, M. Raza, R. Hasan, *The Int. J. of Tuberculosis and Lung Disease*,2010, **12**, 1644–1646

[24] The Cambridge Structural Database, C. R. Groom, I. J. Bruno, M. P. Lightfoot and S. C. Ward, *Acta Cryst*. 2016, B72, 171-179

[25] Diniz L.F., Souza M.S., Carvalho Jr. P.S., da Silva C.C.P., D'Vries R.F., Ellena J, *Journal of Molecular Structure*, 2018, **1153**, 58-68

[26] Hemamalini M., Loh W., Quah C.K., Fun H., *Chemistry Central Journal*, 2014, **8**:31

[27] Jina S., Zhua Q.,Weia S.,Wang D., *Journal of Molecular Structure*, 2013, **1049**, 132–148

[28] Aakeröy C.B., Beatty A.M., Helfrich B.A., Nieuwenhuyzen M., Crystal Growth & Design, 2003, **3**, 159-165

[29] Tan T., Han J., Pang M., Song H, Ma Y., Meng J., *Crystal Growth & Design*, 2006, **6**, 1186-1193

[30] Vadivelan G., Murugesan V., Saravanabhavan M., Sekar M., Optik, 2017, **140**, 571–578

[31] Balasubraman K., Fun H., *ActaCryst.*, 2009. **E65**, o1511–o1512

[32] Smith G., Wermuth U.D., *ActaCryst.*, 2012, **E68**, o1649–o1650

[33] Pawel Grobelny, A. Mukherjee, G.R. Desiraju, CrystEngComm, 2011, **13**, 4358-4364

[34] C.K. Quah, S.R. Jebasa, H. Fun, *ActaCryst. E*. 2008, **64**, o1878–o1879

[35] D Kinchinqton, T Ng, N. Mathews, M. Tisdale, D. Devine, W.O. Ayuko, *Antiviral Chemistry & Chemotherapy*, 1997, **8**, 121-130

[36] I. Barsky, J. Bernstein, P. W. Stephens, K. H. Stone, *New J.Chem.*, 2008, **32**, 1747–1753

[37] Lemmerer A., *CrystEngComm*, 2012,**14**, 2465–2478

[38] Ishida H., Rahmanand B., Kashino S., *Acta Cryst.*, 2001, **E57**, o744-o745

[39] Pandey A., Verma C., Singh B., Ebenso E.E., *J. of Molecular Structure*, 2018, **1155**, 110-122

[40] Ishida H., Fukunaga T., Kashino S., *Acta Cryst.*, 2002, **E58**, o1083-o1084

[41] Ishida H., Fukunaga T., Kashino S. Acta Cryst., 2002,. **E58**, o1085-o1087

[42] Sugiyama T., Menga J., Matsuura T., Acta Cryst., 2002, **C58**, o242-o246

[43] Ishida H., Fukunaga T., Acta Cryst., 2004, **E60**, o1664-o1665

[44] Aitipamula S., Wong A.B.H., Chowaand P.S., Tan R.B.H., *CrystEngComm*, 2012, **14**, 8515–8524

[45] Mani R., Rietveld I.B., Nicolaï B., Varadharajan K., Louhi-Kultanen M., Narasimhan S., *Chemical Physics*, 2015, **458**, 52–61

[46] Gotoh K., Ishida H., ActaCryst., 2009, **C65**, o534–o538

[47] Tan T., *J. of Molecular Structure*, 2007, **840**, 6–13

[48] Ishida H., Rahman B., Kashino S., *Acta Cryst.*, 2001, **C57**, 1450-1453

[49] Sugiyamaa T., Menga J., Matsuura T., *J. of Molecular Structure*, **611**, 2002, 53-64

[50] M. Oruganti, S.K. Nechipadappu, P. A. Khade, D. R. Trivedi, *ACS Omega*, 2017, **2**, 7146-7162

[51] P. Prince, F.R. Fronczek, R. D. Gandou, *Acta Cryst.*, 1991, **C47**, 895-898

[52] Jerzykiewicz L.B., Malarski Z., Sobczyk L., Lis T., Grech E., *J. of Molecular Structure*,1998, **440**, 175-185

[53] Ding X., Cui L., Li Y., Wang S., Huang W., *NewJ.Chem*.,2012,**36**, 1884–1890

[54] Jina S., Wang D., *J. of Molecular Structure*, 2013, **1037**, 242–255

[55] Girisha M., Yathirajan H.S., Jasinskiband J.P., Glidewell C., *ActaCryst.*, **C72**, 612–618

[56] Bott R.C., Smith G., Wermuth U.D., Dwyer N.C., Aust. J. Chem., 2000, **53**, 767–777

[57] Moragues-Bartolome A.M., Jones W., Cruz-Cabeza A.J., *CrystEngComm*, 2012,**14**, 2552–2559

[58] Sathya K., Dhamodharan P., Dhandapani M., *J. of Molecular Structure*, 2017, **1130**, 414-424

[59] Lynch D.E., Smith G., Byriel K.A., Kennard C.H.L., *Aust. J. Chem.*, 1994, **47**, 1789-1798

[60] Subashini A., Muthiah P.T., Bocelliband G., Cantoni A., *ActaCryst.*, 2007,. **E63**, o4408–o4409

[61] L. Wei, *Acta Cryst.*, 2007. E63, o4174

[62] SciFinder, *https://scifinder.cas.org/scifinder/view/scifinder/scifinderExplore.jsf*, Date of Access: 19-22 September 2018

[63] Jebas S.R., Balasubramanian T., *ActaCryst.*, 2006, **E62**, o2209–o2211

[64] Hemamalini M., Fun H., ActaCryst., 2010, **E66**, o335

[65] Wicker J.G.P., Crowley L.M., Robshaw O., Little E.J., Stokes S.P., Cooperaand R.I., Lawrence S.E., CrystEngComm, 2017, **19**, 5336

[66] Smith G., Baldry K.E., Byriel K.A., Kennard C.H.L., *Aust. J. Chem.*, 1997, **50**, 727-736

[67] Emsley J., Reza N.M., Kuroda R., J. of Crystallographic and Spectroscopic Research, 1986, **16**, 57-69

[68] Ganduri R., Cherukuvada S., Row T.N.G., *Cryst. Growth Des.*, 2015, **15**, 3474−3480

[69] Wahl H., Haynes D.A., le Roex T., S. Afr. J. Chem., 2016, **69**, 35–43

Appendix

4-Nitrobenzoic Acid PXRD patterns

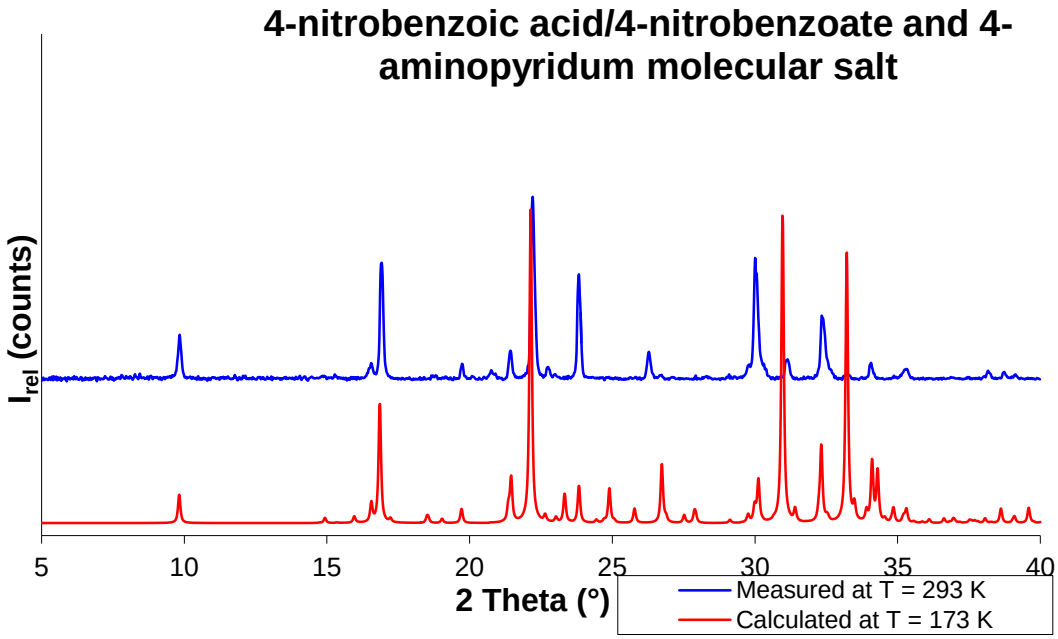

Figure A1 Calculated and measured PXRD Pattern for 4nbaH/4nba$^{(-)}$-4apH molecular salt

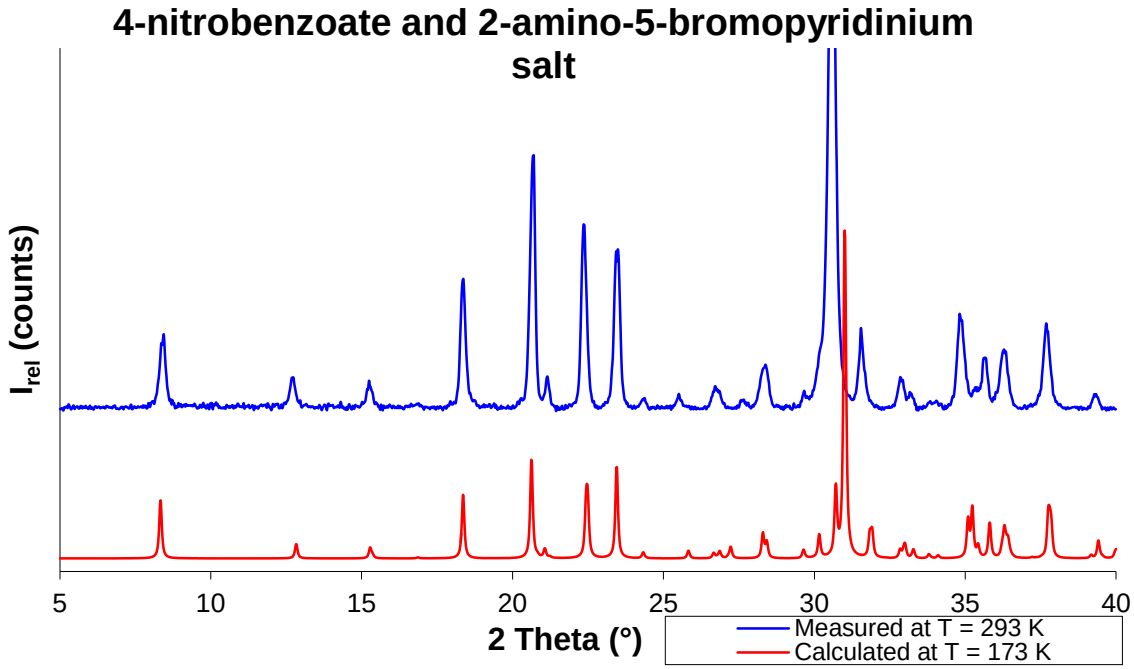

Figure A2 Calculated and measured PXRD Pattern for 4nba$^{(-)}$-2a5BrpH molecular salt

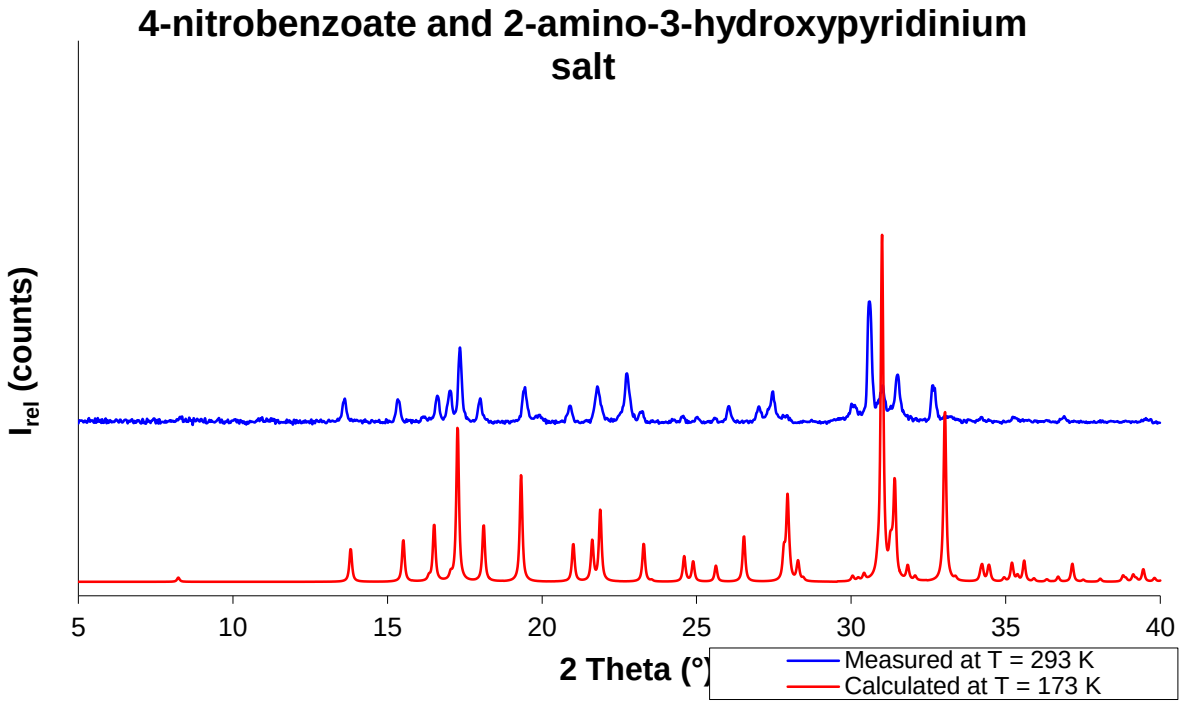

Figure A3 Calculated and measured PXRD Pattern for $4nba^{(-)}$-2a3hpH molecular salt

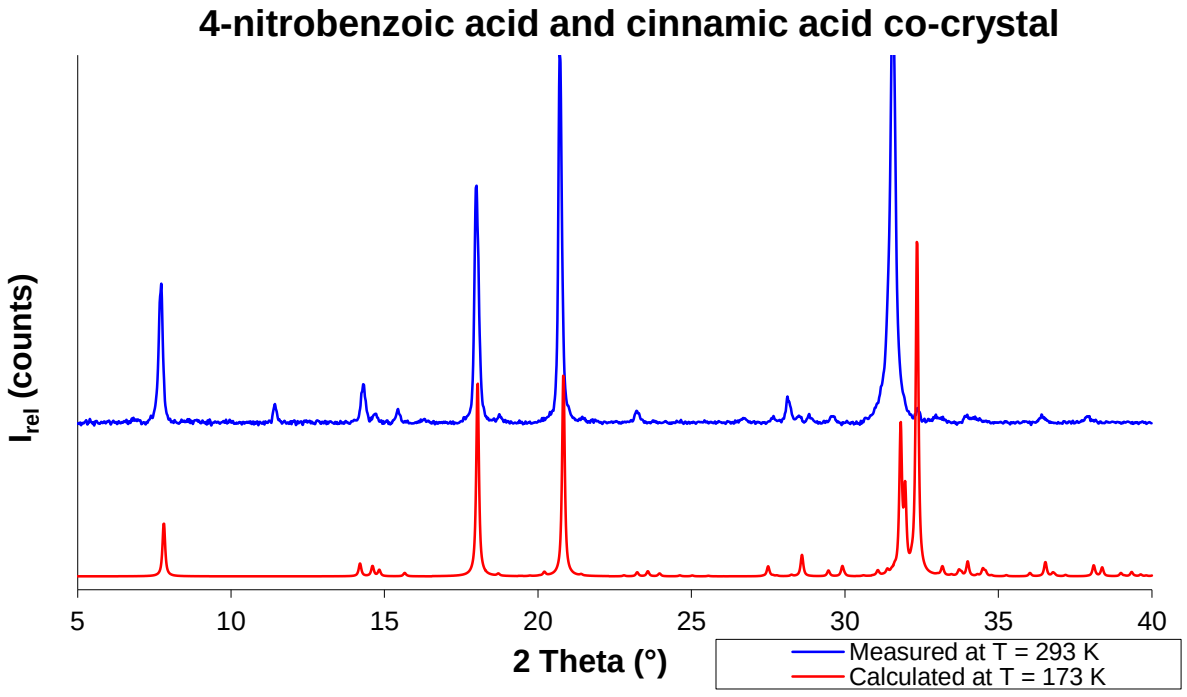

Figure A4 Calculated and measured PXRD Pattern for 4nbaH-cinnamic acid co-crystal

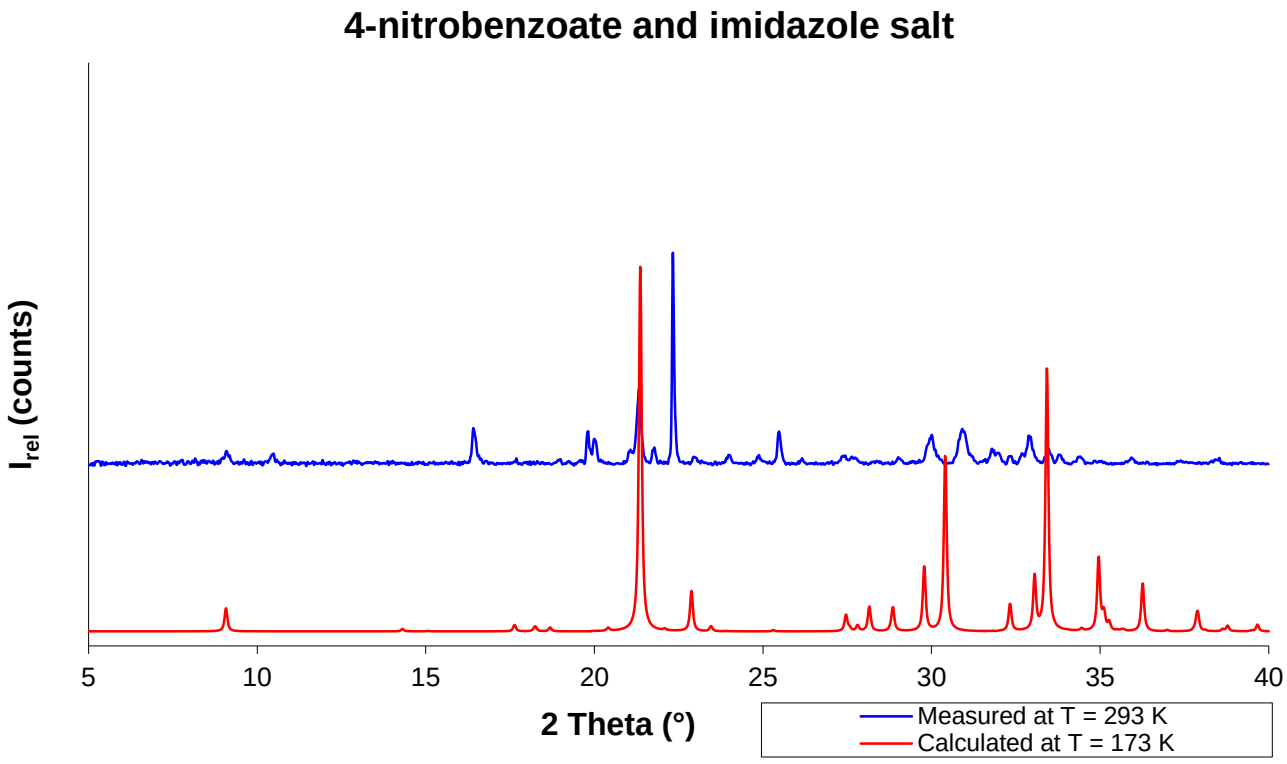

Figure A5 Calculated and measured PXRD Pattern for 4nba$^{(-)}$-imd molecular salt. The extra peaks (most noticeably between 10-20° range) are due to impurities.

2-chloro-4-Nitrobenzoic Acid PXRD patterns

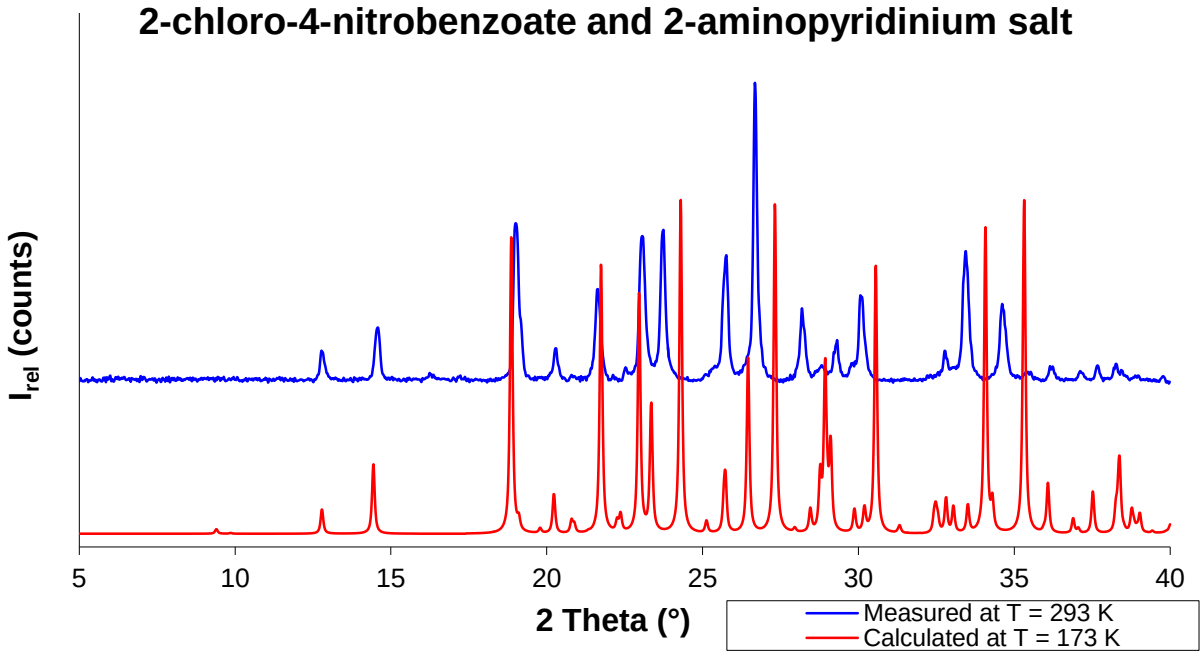

Figure A6 Calculated and measured PXRD Pattern for 2c4n$^{(-)}$-2apH molecular salt

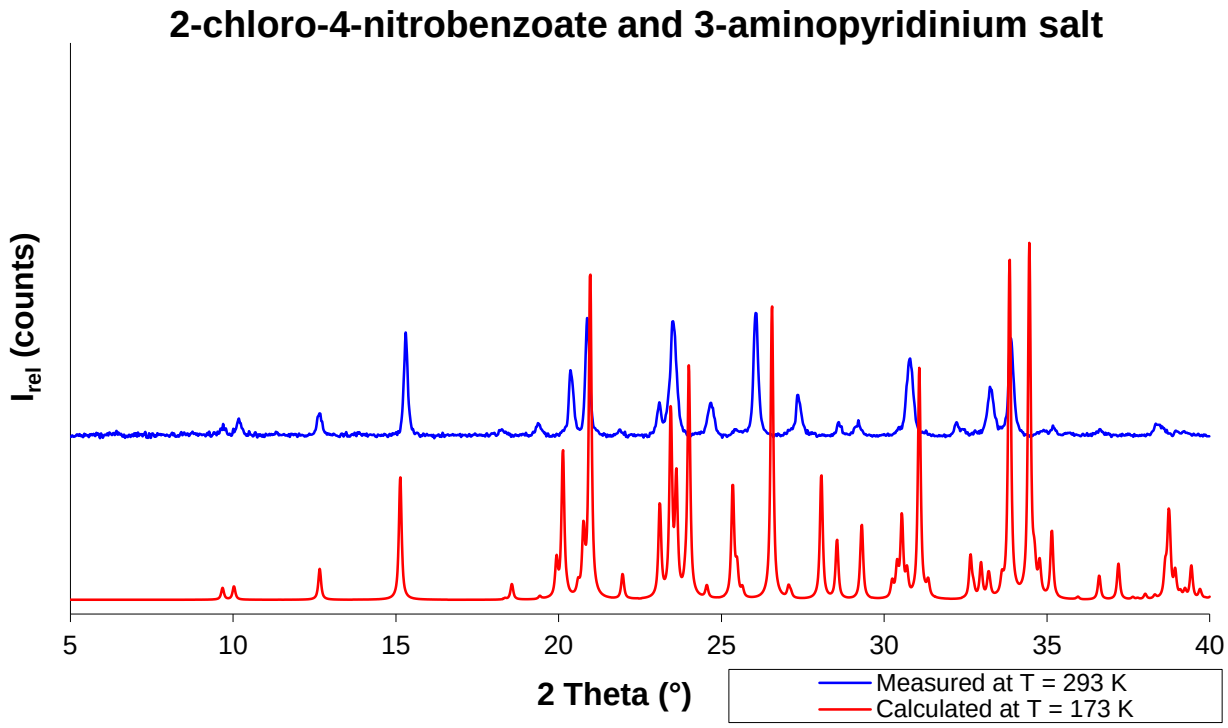

Figure A7 Calculated and measured PXRD Pattern for 2c4n$^{(-)}$-3apH molecular salt

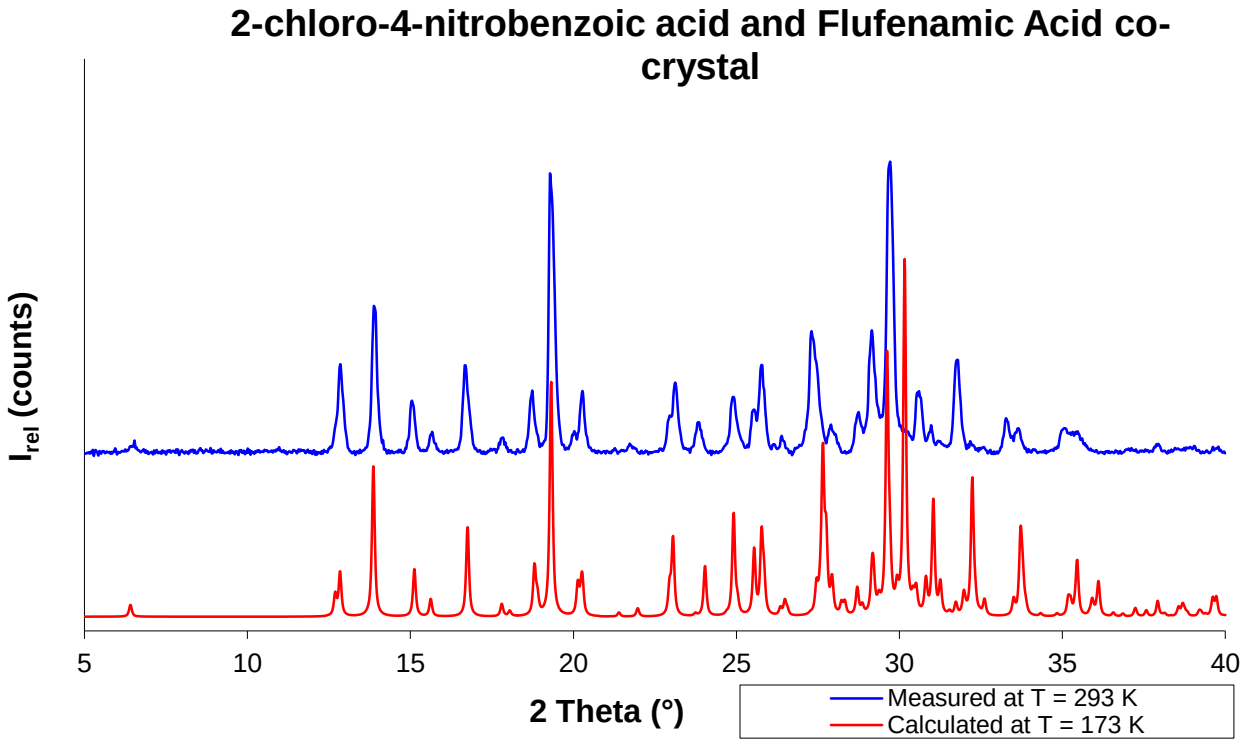

Figure A8 Calculated and measured PXRD Pattern for 2c4nH-fa acid co-crystal

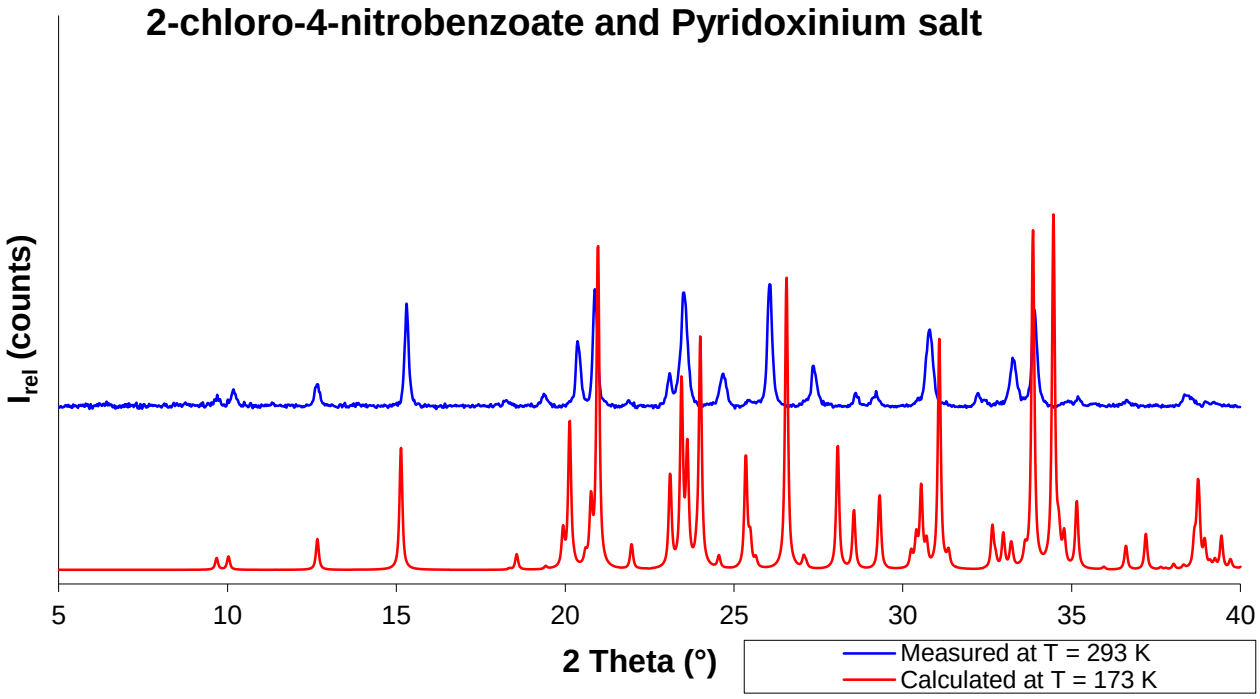

Figure A9 Calculated and measured PXRD Pattern for 2c4n$^{(-)}$-pyd molecular salt

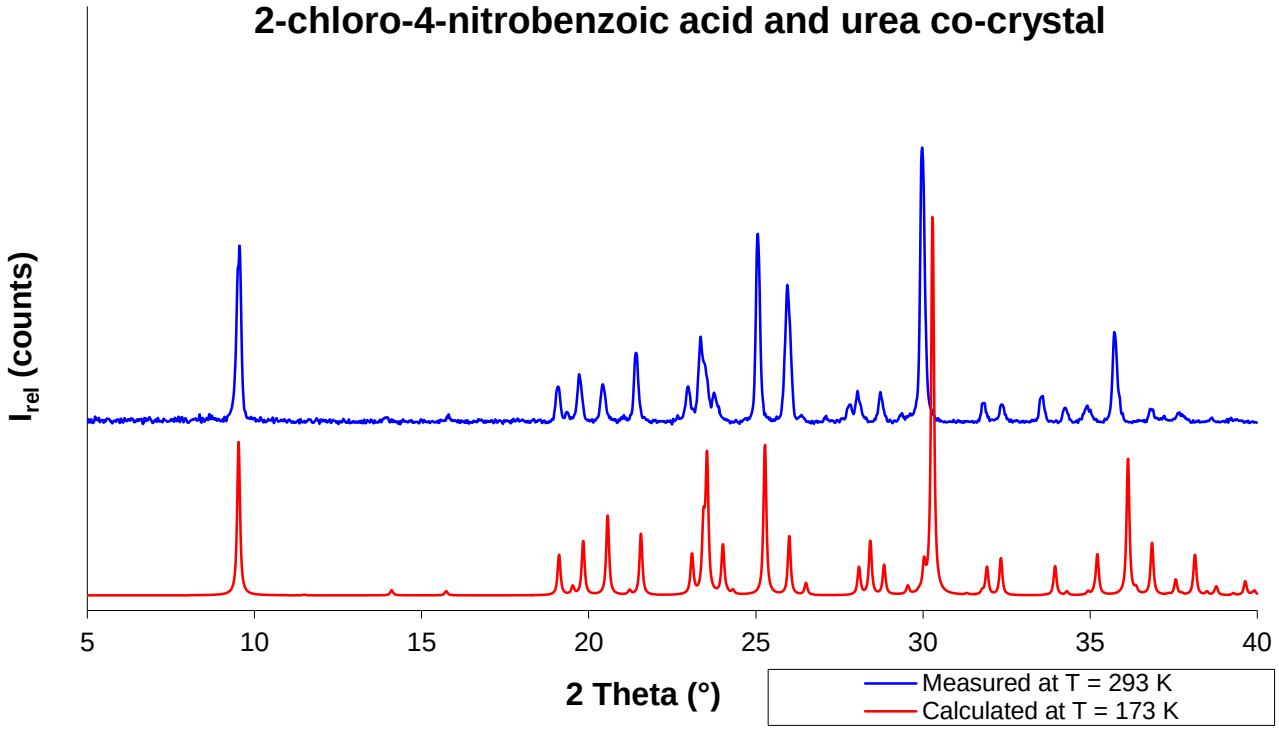

Figure A10 Calculated and measured PXRD Pattern for 2c4nH-urea acid co-crystal

2-chloro-5-Nitrobenzoic Acid PXRD patterns

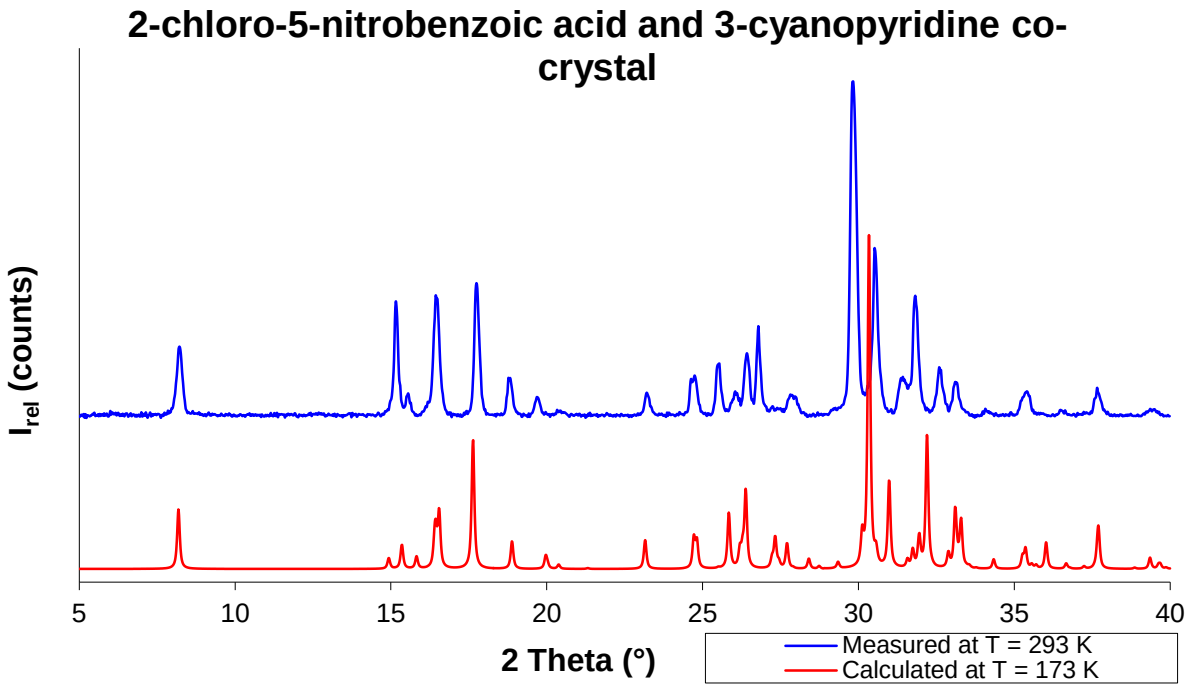

Figure A11 Calculated and measured PXRD Pattern for 2c5nH-3cp co-crystal

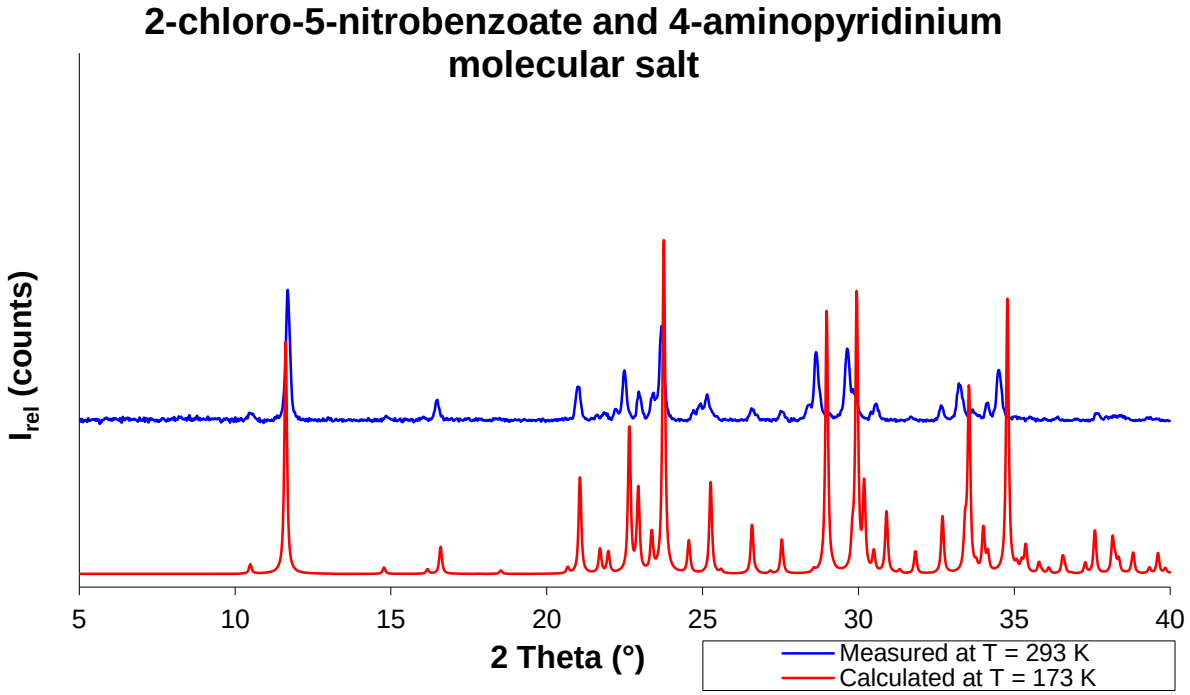

Figure A12 Calculated and measured PXRD Pattern for 2c5n$^{(-)}$-4apH molecular salt

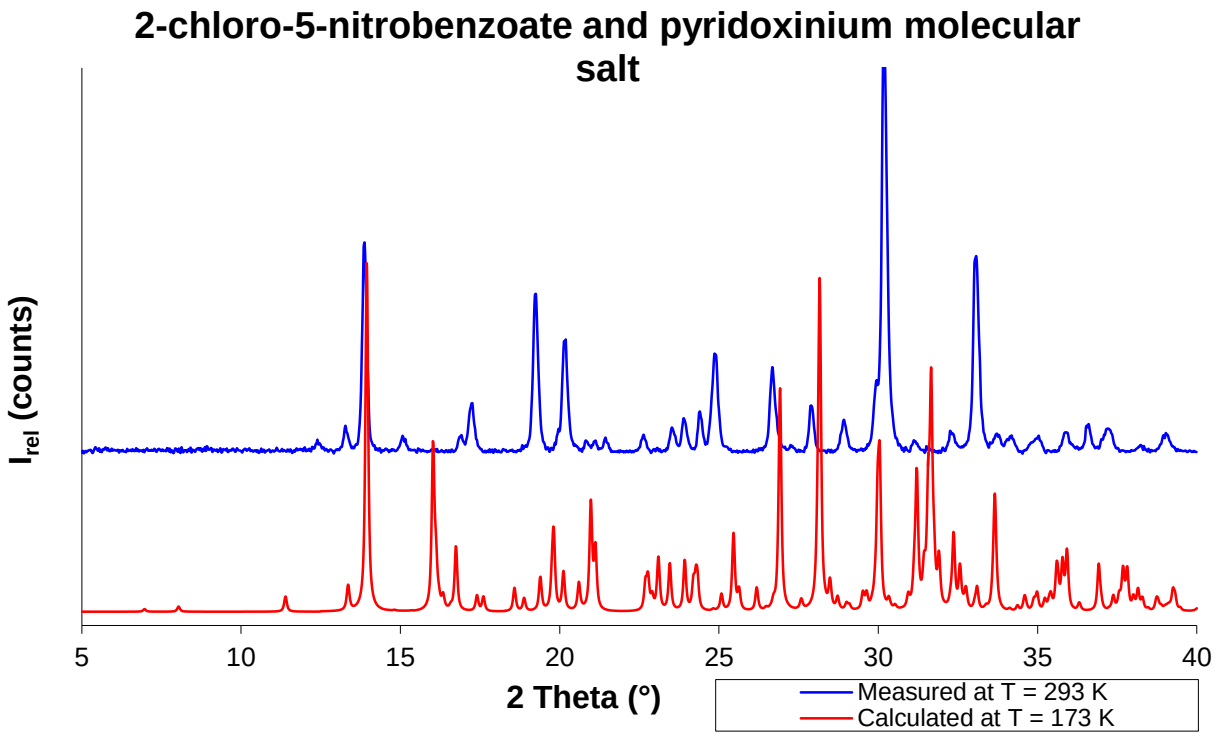

Figure A13 Calculated and measured PXRD Pattern for 2c5n$^{(-)}$-pyd molecular salt

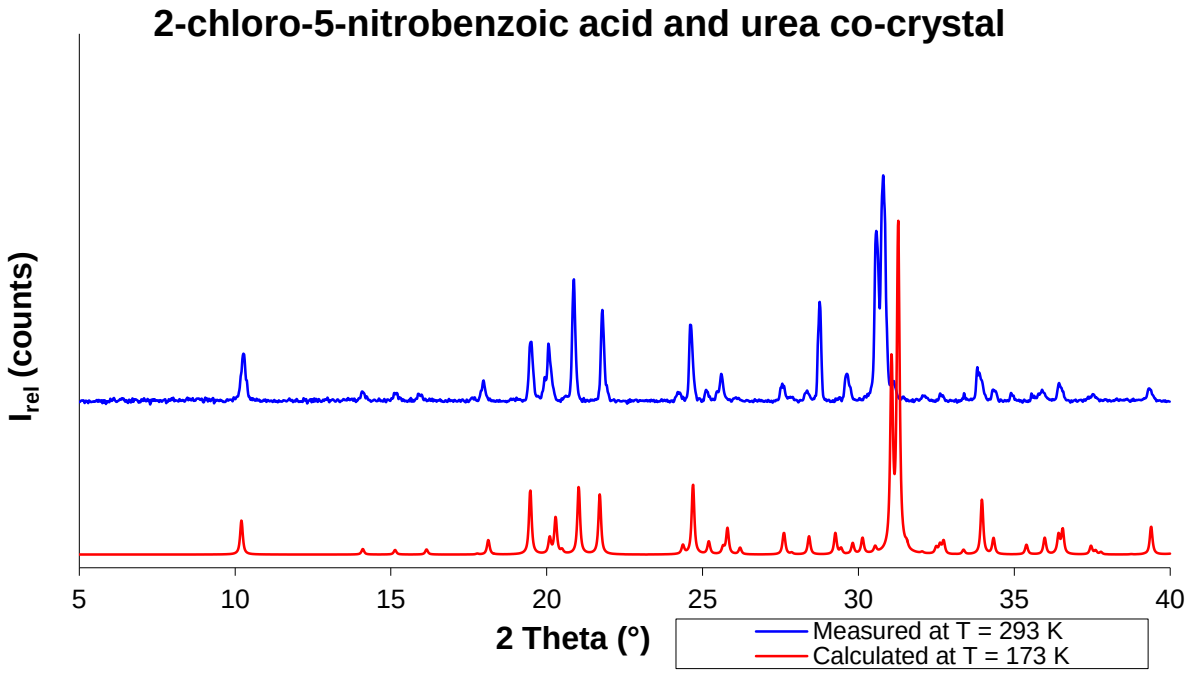

Figure A14 Calculated and measured PXRD Pattern for 2c5n-urea co-crystal

3,5-Dinitrobenzoic Acid PXRD results

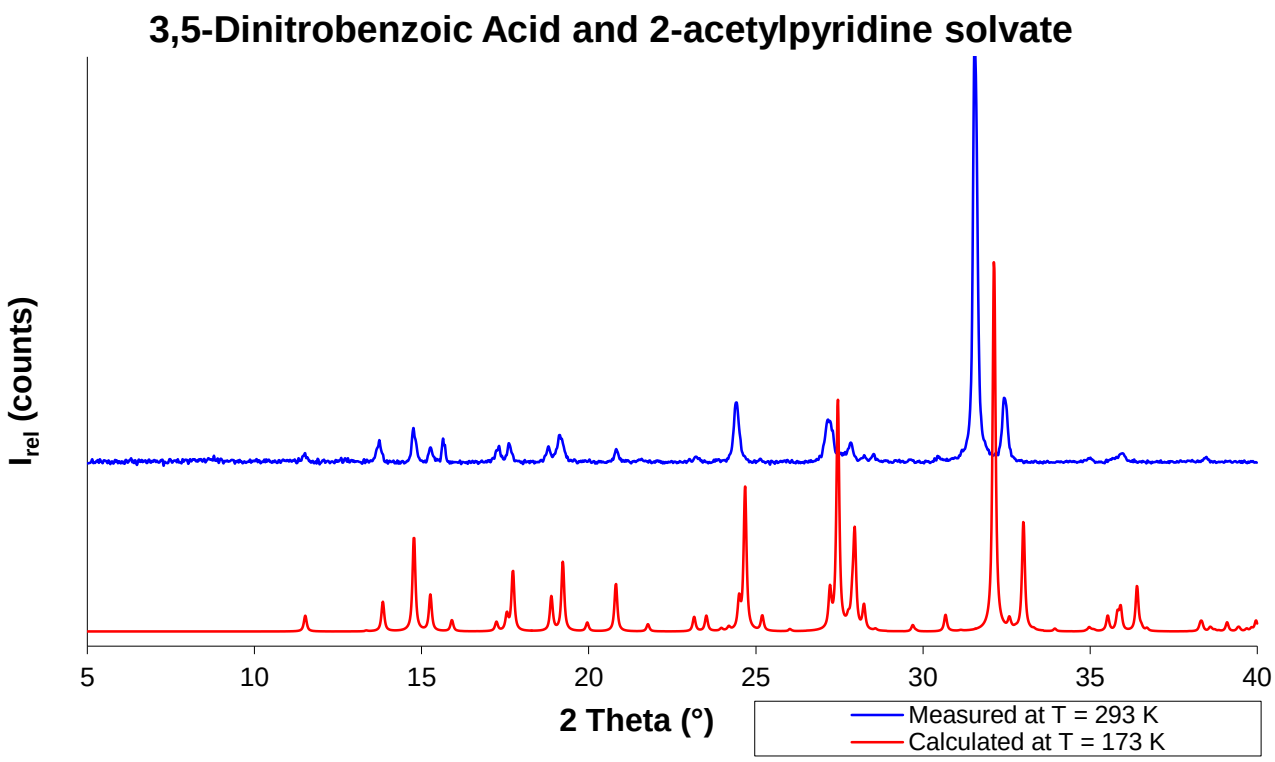

Figure A15 Calculated and measured PXRD Pattern for dnbaH-2OAcP solvate

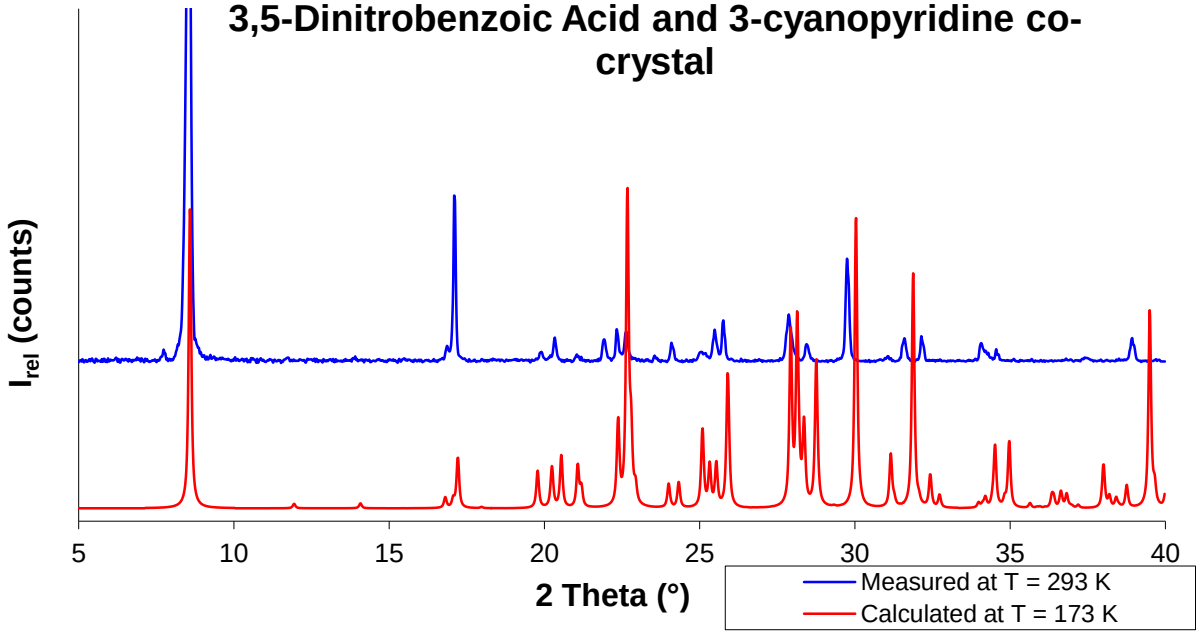

Figure A16 Calculated and measured PXRD Pattern for dnbaH-3cp co-crystal

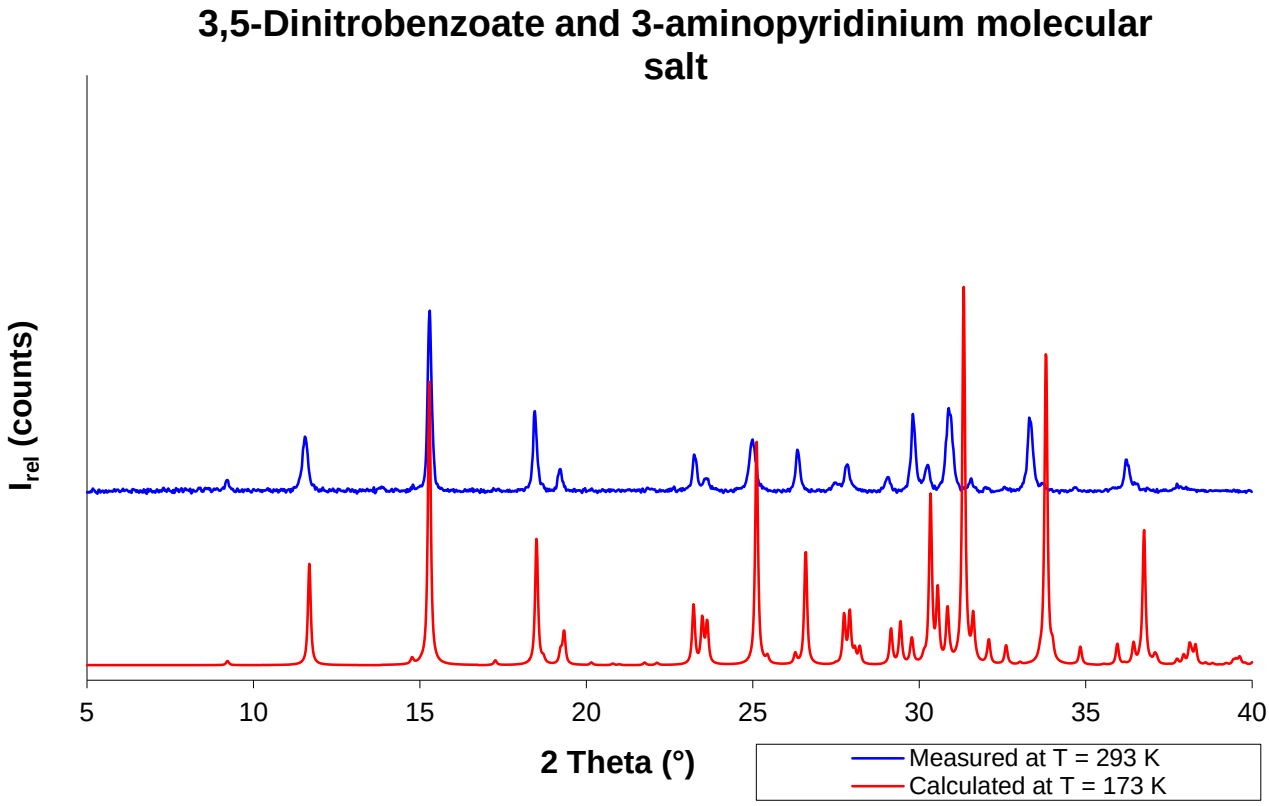

Figure A17 Calculated and measured PXRD pattern for dnba$^{(-)}$-3ap molecular salt

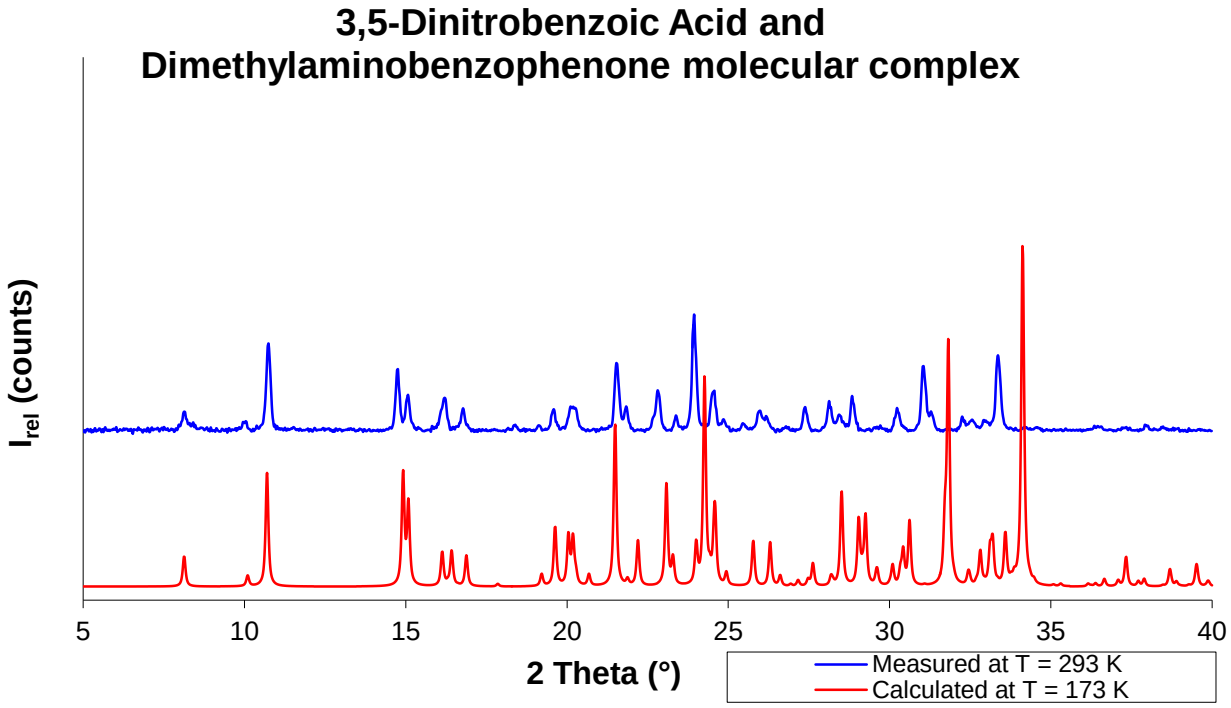

Figure A18 Calculated and measured PXRD Pattern for dnbaH-dmabp co-crystal

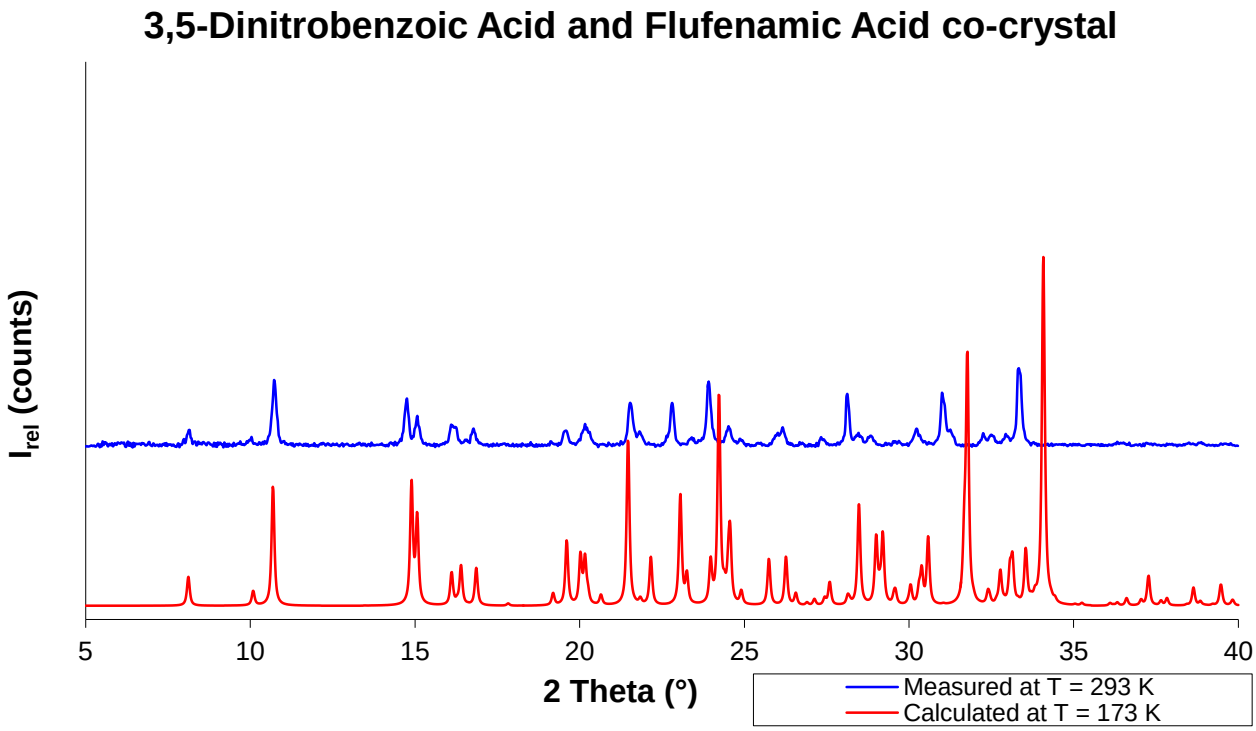

Figure A19 Calculated and measured PXRD Pattern for dnbaH-fa co-crystal

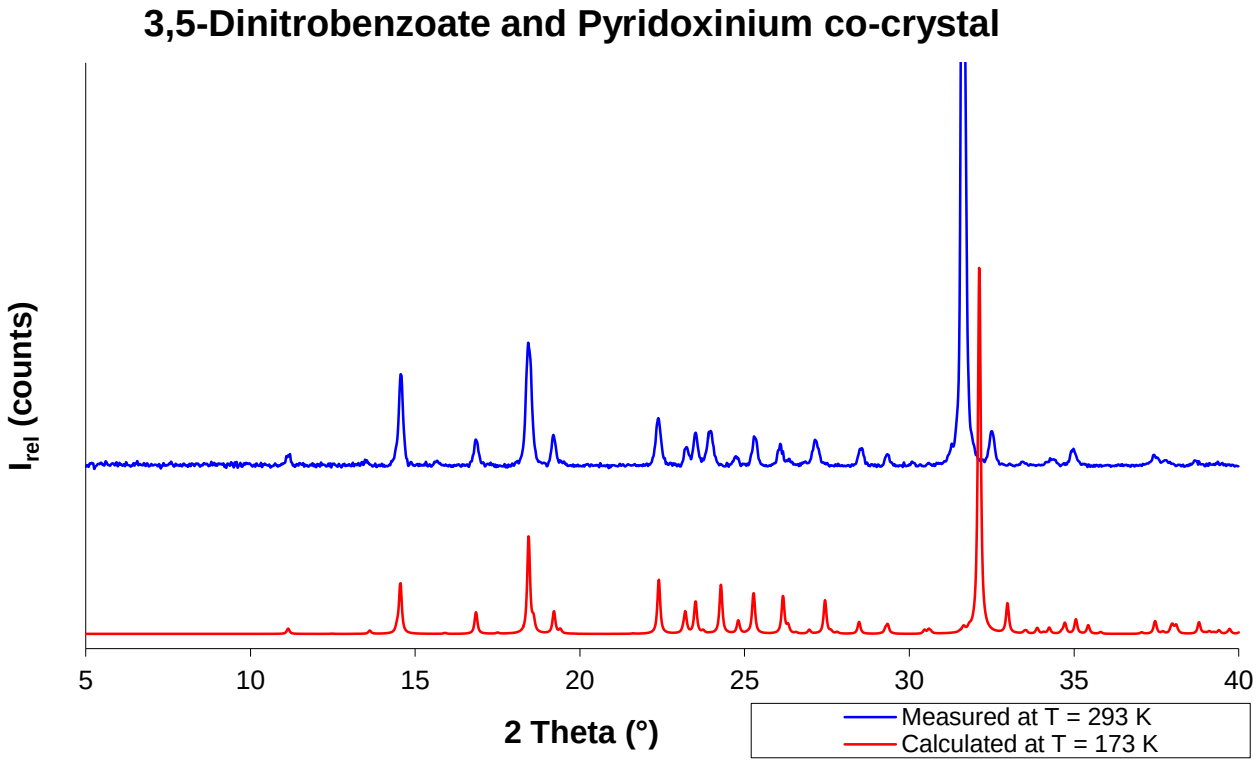

Figure A20 Calculated and measured PXRD Pattern for dnba$^{(-)}$-pyd molecular salt

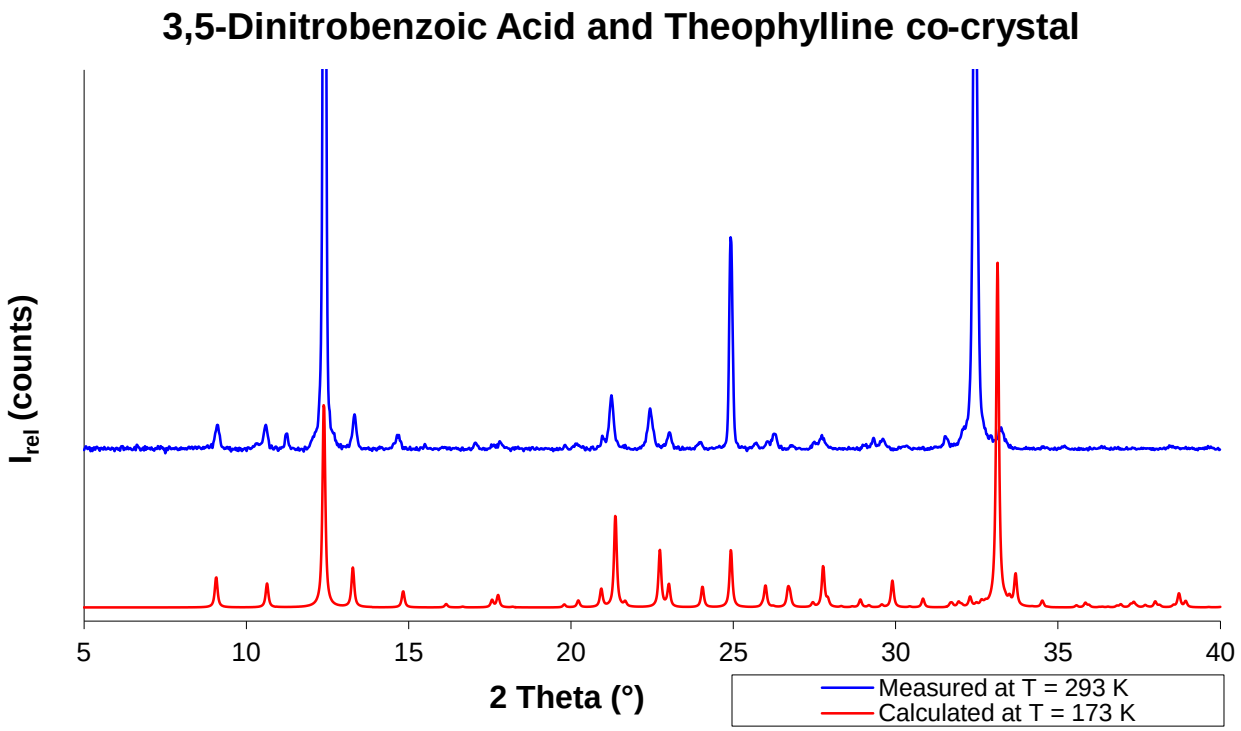

Figure A21 Calculated and measured PXRD Pattern for dnbaH-thp co-crystal

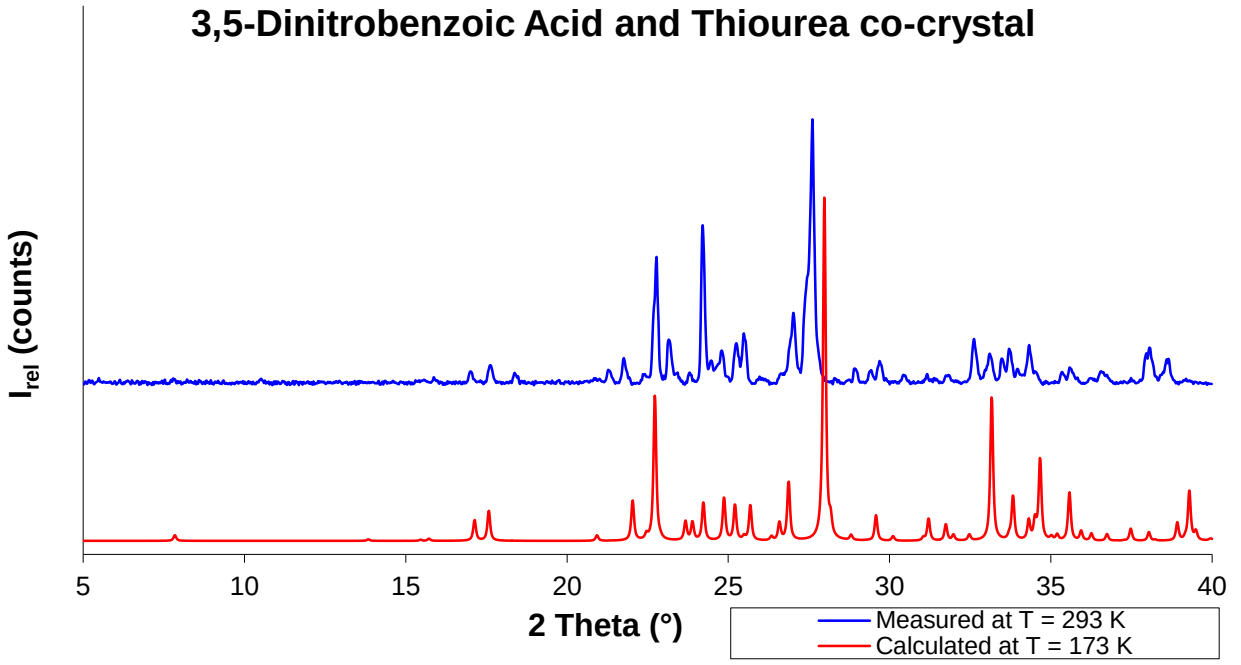

Figure A22 Calculated and measured PXRD Pattern for dnbaH-urea co-crystal